DISSERTATION

ACUTE AND REPETITIVE INHALATIONAL ORGANIC DUST EXPOSURE MODULATES IMMUNE RESPONSE MITIGATION BY OMEGA-3 FATTY ACIDS AND SUSCEPTIBILITY TO SECONDARY RESPIRATORY BACTERIAL INFECTION

Submitted by:

Logan S. Dean

Graduate Degree Program in Cell and Molecular Biology

In partial fulfillment of the requirements

For the Degree of Doctor of Philosophy

Colorado State University

Fort Collins, Colorado

Summer 2025

Doctoral Committee:

Advisor: Lucas Argueso
Co-Advisor: Tara Nordgren

Mercedes Gonzalez-Juarrero
Karen Dobos
Jessica Prenni
Sarah Clark

ABSTRACT

ACUTE AND REPETITIVE INHALATIONAL ORGANIC DUST EXPOSURE MODULATES IMMUNE RESPONSE MITIGATION BY OMEGA-3 FATTY ACIDS AND SUSCEPTIBILITY TO SECONDARY RESPIRATORY BACTERIAL INFECTION

Inhalational organic dust exposure (ODE), both acute and repetitive, is inflammatory and highly neutrophilic. Prolonged ODE is clinically linked to an increased risk of asthma and COPD development, to both workers in the livestock and agricultural industries, as well as individuals who live in proximity to such operations. As such, a greater understanding of the immune response to ODE, increased focus on therapeutic strategies, and understanding of translational insights into comorbid infections is necessary. This work provides key insights into a pivotal process implicated in furthering inflammation, neutrophil extracellular trap (NET) formation in acute dust exposure. Furthermore, insights into the chronic inflammatory environment crafted by repetitive ODE are investigated and compared to a mouse model of balanced omega-3 fatty acids, key resolution promoting parent molecules. Finally, this work utilizes a mouse model of repetitive ODE to investigate if the inflammatory environment promotes susceptibility to the common respiratory bacterium, *Streptococcus pneumoniae*. Collectively, this work provides key insights into immune cell population alterations in murine models of acute and repetitive ODE. I demonstrate that NET formation is increased in acute ODE in a subset of mature and lung-resident neutrophil populations, that repetitive ODE in a mouse model of balanced omega-3 fatty acids preferentially recruits monocyte populations in a sex dependent manner to the airway and

lung tissue, and that repetitive ODE is protective against secondary *S. pneumoniae* infection and mortality through the induction of effector and highly cytotoxic lymphocyte populations.

AKNOWLEDGEMENTS

Holy Fuck. My first thought is that I have too many people to thank, which is a clear sign that I have completed this experience correctly. Writing this section is a moment of reflection on the work, grit, and people that have supported this journey to PhD.

My first thanks are to Tara Nordgren, who has mentored and shaped my scientific and personal development over these last 3 years. She has set the bar for standing up to unjust practices and has fostered my independence and grown me as a scientist. I would also like to thank my wonderful, supportive, wise, and fun committee members (Mercedes, Karen, Jessica, Sarah, and Lucas) for their guidance, encouragement, and many words of wisdom.

Many thanks to the CMB program, specifically the support from Carol, Lucas, and Tai. Many thanks to the humor of Mercedes Cooper. To the undergraduates that I had the pleasure of mentoring, there is no amount of gratitude I can express towards the work you have done and the many laughs we've shared. My hope is that you grow in your endeavors and surpass my own scientific achievements one day.

To my lab mates, I have appreciated your comradery and support. Working with wonderful people shouldn't be called work, but I will always take the paycheck. To the many friends and colleagues that this time has brought, endless thanks for the kind words, hot gossip, and cheeky conversations that enhance the ordinary day. To Marcella Henao-Tamayo and Chris Gentile,

your willingness in providing a laboratory home when no one else would has made a lasting impact on my time here at CSU and will never be forgotten

To Juwon Park, this entire PhD thing was enabled by your willingness to take a chance on me. Your mentorship, support, guidance, wisdom, laughs, and candor have been instrumental in shaping my scientific prowess and I will continue to pay that forward. To the friends outside of the academic bubble, I thank you for refreshing conversations, lots of hours of sunshine and volleyball, and for reminding me about the life that is to be lived outside of the laboratory.

To my family, I have no adequate words. You have supported my dreams, picked me up during failures, and celebrated my wins. Even if you don't get what I do, you support me anyways and I will continue to fly, never forgetting my roots as a lowly turkey.

To my wife, Ana. Our entire relationship, I have been in school, and you have earned every bit of those degrees as I have through your endless support, love, and many laughs. It is surreal to look back at all that we have accomplished together, and I am so excited for our next adventure together. Cheers to being Dr. Deans!!

TABLE OF CONTENTS

Chapter 1

The Respiratory System

Physiology & Function

By surface area, the respiratory tract of the human body makes up the largest surface area of the human body exposed to the environment, the lungs alone spreading an impressive 70 m^2 (1). Comprised of an upper and lower respiratory tract **(Figure 1.1A)**, this system is the primary means of gas exchange required for normal cellular respiration, as well the means of entrance for a host of microbial, organic, inorganic, and gaseous insults. These insults must survive, evade, and penetrate this complex passageway to cause damage, the defenders of which are numerous and relentless **(Figure 1.1B)**.

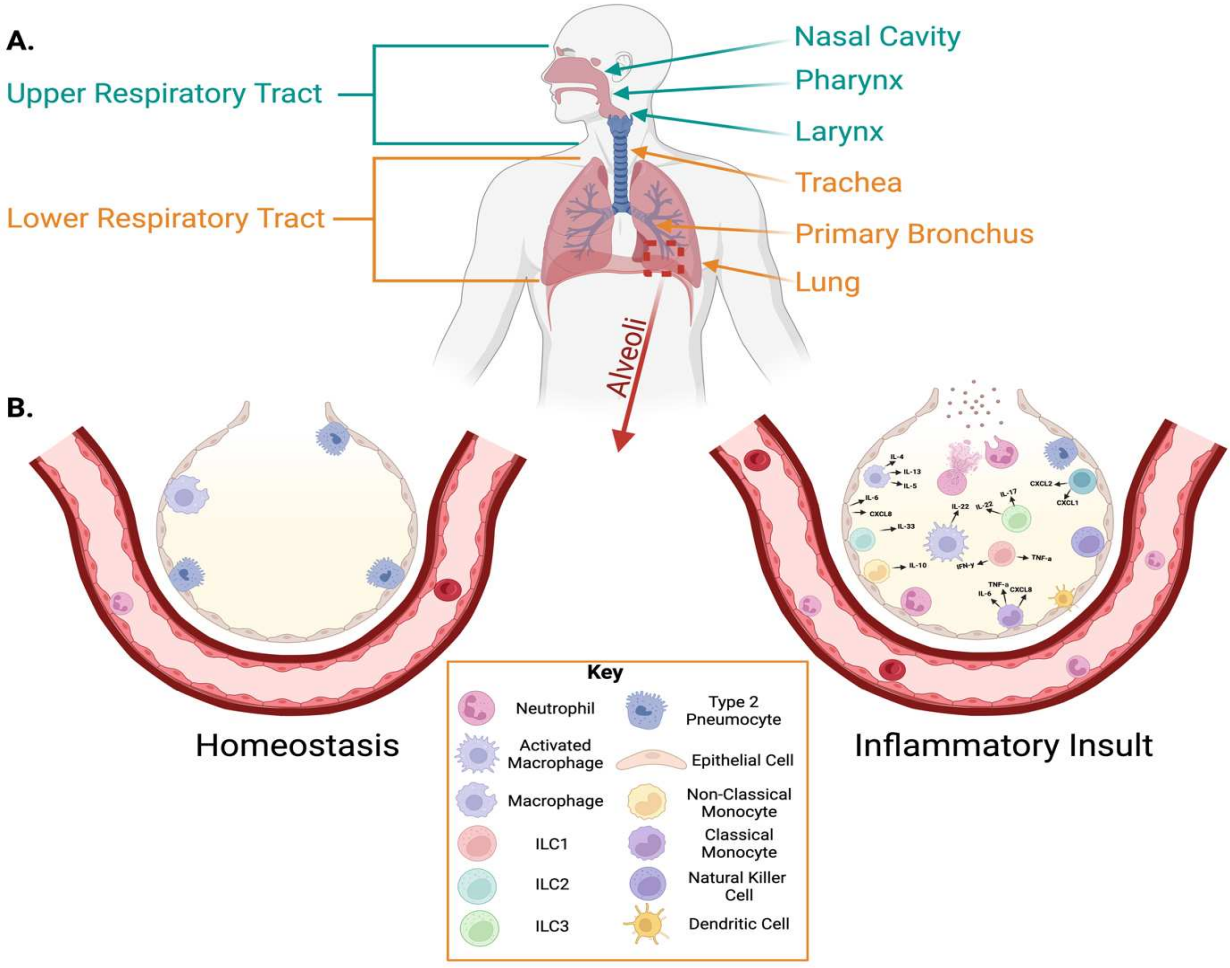

Figure 1.1 The human respiratory tract is broken up into upper and lower portions **(A)**. The lower respiratory tract houses the alveoli, responsible for gas exchange. At homeostasis, the alveolar space remains relatively clear of immune cells, the inverse of when an inflammatory insult occurs **(B)**.

Defense

Within the upper respiratory tract, defense mechanisms rely on the combination of innate, epithelial, and adaptive responses (2,3). The innate and epithelial arm of defense relies on ciliated epithelial cell, basal cells, club cells, and mucus secreting goblet cells for defense mechanisms (4). Nasal-associated lymphoid tissue (NALT) and induced bronchus-associated lymphoid tissue (iBALT) are specialized structures found in the upper and lower respiratory tract, respectively, that represent the adaptive arm of defense (5,6). Mucin produced by goblet and club cells, such as MUC5AC and MUC5B are one of the primary defense mechanisms found on upper airway epithelial cells, and in conjunction with antimicrobial peptides (AMP) and secretory IgA (sIgA), block or impair microbial adherence and virulence factors (7,8). Upon sensing of damage associate patterns (DAMPS) via toll like receptors (TLR) or cytokine receptors, airway epithelial cells increase AMP production and release IL-1β and TNF, attracting canonical immune cells to the site (9). Intriguingly, airway epithelial cells have been demonstrated to perform phagocytic functions, suggesting alternative forms of defense are likely present, yet undefined, in our airway's most common cell type (10).

Within the lower respiratory tract, goblet cell proportions decrease, and alveolar type 1 (AT1) and alveolar type 2 (AT2) cells are found. AT1 cells are primarily responsible for structural maintenance and gas exchange, while AT2 cells secrete pulmonary surfactants that reduce surface tension and serve as progenitor cells during repair and resolution processes (11,12).

At homeostasis, alveolar macrophages (Aφ) survey the alveolar compartments at a ratio of 1 Aφ:3 alveoli, maintaining themselves via self-replenishment or monocyte recruitment and differentiation (13,14). This homeostatic environment maintained via Aφ- mediated clearance of debris and apoptotic cells is due to release of IL-10, membrane-tethered TGF-β, and CD200 signaling from airway epithelial cells to Aφ (15). During an acute insult, such as microbial infection or toxic inhalation, the full weight of the immune system is brought to bear against the invasion, mediated by primary cytokine release. These cytokines, including IL-1α, IL-β, IFN-α, IFN-β, IFN-λ, IL-8, IL-23, IL-33, TNF, all play crucial roles in the initial alert and recruitment of immune cell types in an invader-specific manner (16). Within hours, the first cells to arrive are neutrophils, the body's most common leukocyte. Migrating to the area of inflammation via chemotactic gradients formed by CXCL8 (IL-8 in humans) and homing to the lung via CXCL12, these jacks-of-all-trades immune cell make up the first wave of most immune response-generating stimuli. Effector functions such as phagocytosis, reactive oxygen species (ROS) production, degranulation, cytokine/chemokine release, and neutrophil extracellular trap (NET) formation all play essential roles in neutrophil's ability to respond to inflammatory stimuli (17). These NETS can occur in both lytic and non-lytic forms, varied by the stimuli required for induction (**Figure 1.2**). Neutrophil and alveolar macrophage synergy facilitates further recruitment of lymphocytes, T cells and B cells, should an inflammatory insult not resolve within 1-5 days of initial onset (18). The movement and effector functions of many of these recruited cells are mediated via release of second-order cytokines such as IFN-γ, IL-4, IL-5, IL-9, IL-10, IL-13, IL-17, IL-22, TGF-β, and amphiregulin (19). These cytokines alter the "flavor" and bias of the immune response, skewing towards Th1- or Th2-based phenotypes (20) .

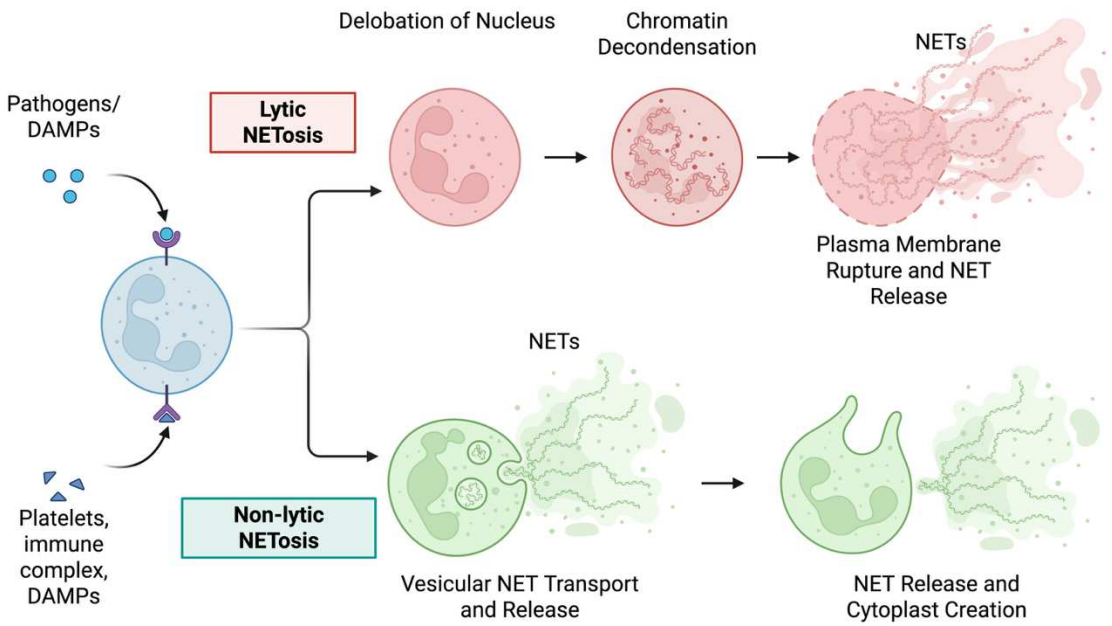

Figure 1.2. Neutrophil extracellular trap (NET) formation is differentially induced by varied stimuli and conditions. Lytic NETosis results in NET formation and a non-viable neutrophil. Non-lytic (vital) NETosis results in NET formation and viable cytoplast generation.

The resolution of inflammation begins with neutrophil apoptosis and phagocyte (macrophage/monocyte) clearance of debris. NK cells aid in this process, triggering cellular death of recruited lymphocytes (21). Neutrophils cease the production of potent inflammatory molecules, such as leukotriene B4 (LTB4), and convert to release of bioactive lipid molecules that decrease neutrophil recruitment, increase epithelial barrier integrity, and activate downstream phagocytic and apoptotic functions in macrophages and neutrophils (22). Efferocytosis of interstitial macrophages, recruited monocytes, dendritic cells, and alveolar macrophages are responsible for the bulk of phagocytosis-based cleanup of damage and cellular debris (23). Non-professional phagocytes, such as type-2 alveolar (MLE-12) and bronchial (BEAS-2B) epithelial cells have also been demonstrated to play phagocytic roles during this resolution response (10,24). Neutralization of released neutrophil elastase (NE) and sequestration of TGF-β aid in the regulation of epithelial barrier repair and replacement of damaged cells

through transit across the basement membrane (25). Re-formation of extracellular matrix spaces occurs primarily through fibroblast and myofibroblast recruitment, activation, and release of proteinaceous extracellular matrix production (26,27). The goal of inflammatory resolution within the lung is to re-establish respiratory gas exchange, epithelial barrier integrity, and return to homeostatic conditions, on the cellular and molecular level, until the next insult arises.

Disease

Despite extensive defense mechanisms, respiratory disease accounts for the third-leading cause of death globally, with the primary contributor to mortality being that of chronic obstructive pulmonary disease (COPD) (28). Smoking, past or present, remains the leading cause of COPD development and mechanistic understandings of this phenomenon are well described (29–33), but additional risk factors such as alpha-1 antitrypsin disorder or repeated microbial infections have been linked to COPD development (**Figure 1.3**) (29–33). Despite this knowledge, treatment strategies are only able to slow COPD progression, rather than reverse damage (34). The hallmark of COPD is a loss of lung function, characterized histologically by a loss of alveolar structures and space and reduction in bronchiole branching (35). Clinically, this disease presents with progressive dyspnea, enhanced with physical activity-based exertions (36). Subclinical detection of COPD development remains challenging, and it has been demonstrated that over 80% of small airways must be occluded for a noticeable impairment of breathing to occur, making early detection improbable (37).

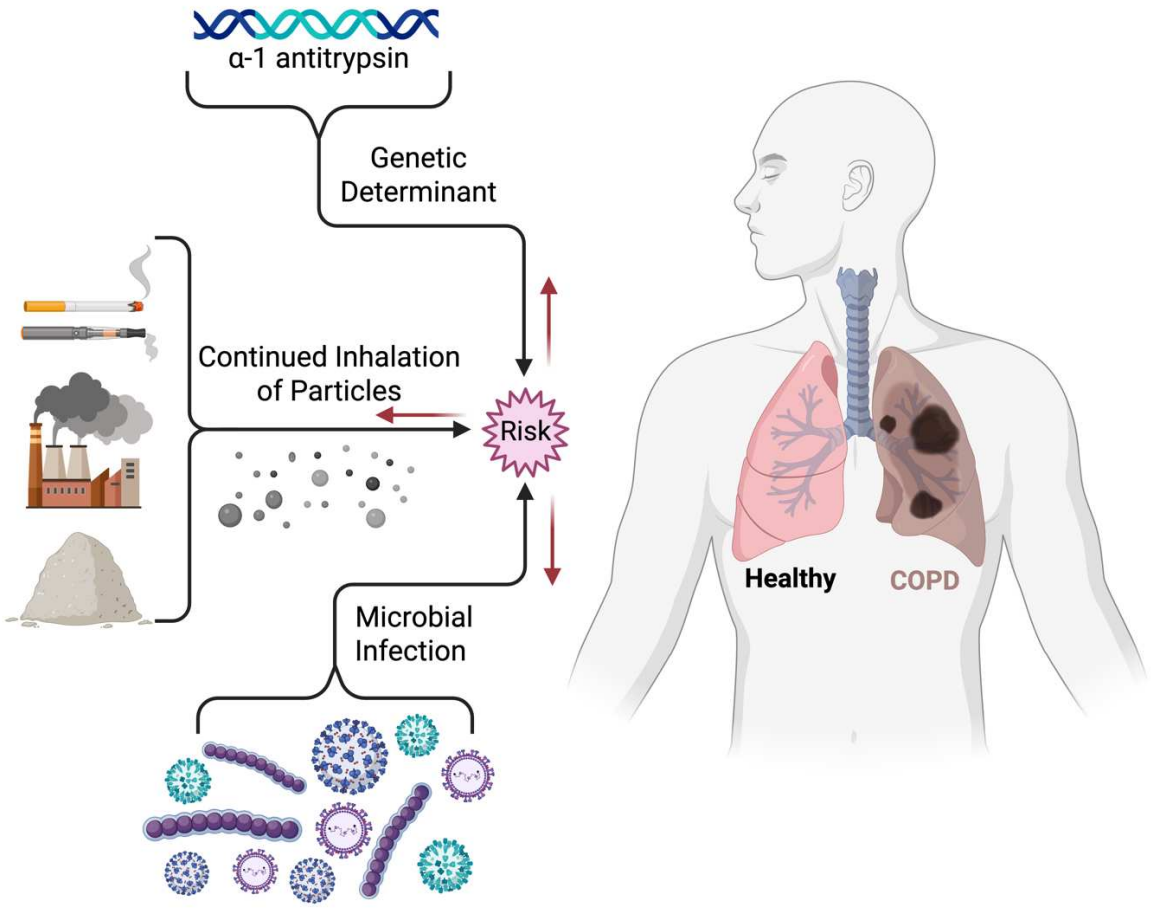

Figure 1.3. Genetic, exposure, and infection status all predispose an individual to COPD development. These same pre-disposing factors also serve as risk factors that exacerbate and worsen COPD disease once developed.

In terms of immunopathology, COPD is the result of a dysregulated inflammation-resolution loop, leading to over-remodeling and a chronically inflamed phenotype. Alveolar macrophage populations have been found increased, correlating with increased GOLD scores. Interestingly, these macrophages do not demonstrate a particular phenotypic skewing (e.g. M1 vs M2) (38). Moderate and prolonged neutrophilia is classically seen in sputum and bronchoalveolar lavage fluid (BALF) samples obtained from patients diagnosed with COPD (39). Intriguingly, increased levels of myeloperoxidase and MIP-1α, a neutrophil chemotactic agent, is consistently demonstrated, suggesting a role for continued release of inflammatory-stimulating proteins as a

potential mechanism for the inflammatory environment characteristic of COPD (40). Increased populations of lymphocytes ($CD4^+$/$CD8^+$ T cells, and B cells), the formation of lymphoid aggregations, and increase presence of neutrophils and macrophages have been demonstrated to correlate with increased COPD severity (41). IL-17 and IL-22 levels increase according to COPD status, with the intriguing finding that the cellular source of these cytokines appears to be endothelial in nature, not lymphocyte produced (42). Intriguingly, B cell aggregations in structures resembling iBALT suggest a role for activated, but polyclonal, B cell populations maintained via the inflammatory environment (43–45). Traditionally, a minor role for eosinophils and mast cells has been described in COPD, but increasing evidence suggests a potentially unexplored role for these canonically allergen-induced cells in COPD immunopathology (46–48).

As it stands, the primary focus of therapeutic strategies has centered on reducing the mechanical consequence of COPD: bronchoconstriction. Short-acting bronchodilators and inhaled muscarinic antagonists synergistically relieve constriction of airways, while the addition of an inhaled corticosteroid for eosinophilic-heavy COPD is included in a patient-depended manner (49). Behavioral interventions such as smoking cessation or respiratory therapy, or prolonged supplemental oxygen are alternative non-pharmacologic strategies in response to increased COPD severity (50). Currently, a defined mechanism to prevent COPD development remains elusive, hindering strategies that mitigate the inflammatory cause that leads to COPD development.

Secondary Infection and COPD

COPD pre-disposes patients to an increased risk of infection with viral and bacterial invaders (51). Current understanding of pathology implicates the chronic inflammatory environment and dysregulated immune responses as a primary factor responsible for infection susceptibility (52) . Common respiratory infections that would normally be cleared in a few days, such as RSV, SARS-CoV-2, influenza A virus (IAV), and *Streptococcus pneumoniae* (*S. pneumoniae*) all become problematic and exacerbate COPD symptomologies, requiring hospitalization and supportive care in severe cases (53). Within the clinical setting, *S. pneumoniae* accounts for 60% of these hospitalizations due to exacerbation of COPD symptoms, making this bacterium one of great concern to patients managing their diagnosis (54–56).

Streptococcus pneumoniae is a Gram-positive, facultative anaerobe, α-hemolytic bacteria commonly found in the human upper respiratory tract (57). Sequencing efforts of *S. pneumonia'*s 2 Mb genome have provided invaluable insight into the encoded proteins necessary for success as a pathogen and revealed that approximately 75% of the genome is conserved across all clinically known isolates (58). The capsular polysaccharide (CPS) is the primary delineating structure utilized to differentiate subtypes, and each CPS type is associated with differential phenotypic and disease-specific responses (59–62). Asymptomatic carriage of *S. pneumoniae* is quite common in children under the age of 5 years old, with rates as high as 90% (63). An altered immune state, such as immunocompromised status, increased age, or comorbid conditions such as diabetes, heart, or lung disease all predispose individuals to infection (64). In addition, severe viral infections, primarily with IAV, enhances *S. pneumoniae* infection, the role for which has been defined as disruption of mucociliary clearance, suppression of IFN-γ, and promotion of an altered immunologic state (65–67).

Defense against *S. pneumoniae* requires antigen-specific IL-17$^+$ CD4$^+$ T cells, with the induction of IL-17 promoting a strong neutrophilic response necessary for infection clearance (68). Intriguingly, in a clinical trial of human infection, a previously undefined role for CD8$^+$ T cells, specifically mucosal associated invariant (MAIT) CD8$^+$ T cells in reducing *S. pneumoniae* infection and carriage has been demonstrated (69). Initial defense systems against *S. pneumoniae* in the lower respiratory tract require alveolar macrophages phagocytosis and direct cytotoxicity (70–72). Clearance of apoptotic alveolar macrophages and replenishment of macrophage populations by recruited CCR2$^+$ monocytes is required for *S. pneumoniae* clearance (73). IL-10 has been found to play an instrumental role in dampening over-exuberant responses to *S. pneumoniae* infection, and cellular sources like NK cells remain under active investigation (74,75). An antibody-mediated role for protection is well described, but other soluble mediators, such as complement are equally important in pneumococcal defense, with waning immunoglobulin levels a hallmark of older adults who develop pneumococcal disease (76–78)

Vaccination and Therapeutics for S. pneumoniae

A vaccine against common disease-causing *S. pneumonia* strains was developed in the 1980's, but lack of inducible and lasting T cell immunity prompted reformulation that included an inactivated diphtheria toxin conjugate to enhance long-term efficacy (79). Two vaccines are currently in use clinically, a protein conjugate and CPS based vaccine, formulated against 23 serotypes (80). These vaccines are recommended for those under the age of 5 and over the age of 50 to reduce chance of pneumococcal-associated mortality (81). CPS-based vaccines have reduced efficacy against non-formulation targets, necessitating alternative vaccination strategies

(82). Protein- and whole cell-based formulations are serotype-independent and avoid cost and batch effects associated with the currently approved regimen (83). Collectively, the current approved vaccine regimens for *S. pneumoniae* infection are efficacious but can be improved to target non-vaccine strains as they arise and to approve effectiveness and safety in immunocompromised individuals (84).

Particulate Matter Exposure

A rising number of cases of COPD have a more insidious origin; environmental particulate matter exposure (85–87). Particulate matter (PM) is composed of coarse (10 um to 2.5 um), fine (2.5 um-1 um), and ultrafine (<1 um) particulates which differ by deposition pattern throughout the respiratory system (88). Coarse deposition is primarily in upper bronchi, fine PM makes its way to the alveolar space, and ultrafine is known to cross the epithelial barrier within the alveolar space and make its way systemically through the blood stream (89). Given the variety of PM exposures, ranging from organics such as pollen, mold spores, and dusts, to inorganic combusted particles, metals, or dusts, the immune response and reaction to sustained exposure varies (90). Furthermore, PM exposures naturally occur in a variety of occupations ranging from construction and dentistry to agriculture or metalworking (91). The Environmental Protection Agency (EPA) has set guidelines for PM exposure a limit of 12 $\mu g/m^3$ of annual average $PM_{2.5}$, and 35 $\mu g/m^3$ daily, however studies have demonstrated increases in morbidity and mortality at even these “acceptable” levels of PM exposure (92,93).

Organic Dust Exposure

Organic dust exposure (ODE) is a type of PM exposure impacting laborers on livestock or agricultural operations but with secondary impacts on communities and residential areas near or around such facilities (94–97). The organic dust itself is composed of multiple components of viral, bacterial, and fungal origin, in concert with trace metals and minerals, as well as soil elements (98–100). Clinical findings of increased respiratory disease incidence associated with agriculture work and the formal definition of organic dust toxic syndrome (ODTS) in the late 80's/early 90's kickstarted investigation into the cellular mechanisms responsible for disease development (101–103). Later work has demonstrated that prolonged ODE is a contributor to chronic respiratory disease, ultimately ending in the development of COPD, oftentimes earlier in life and with greater severity than non-agricultural worker counterparts (104–109).

Immunologically, the response to ODE has been studied in acute (single exposure followed by sample collection 5 hours post instillation), repetitive (1-3 weeks), or chronic (3^+ months) timepoints *in vitro* and *in vivo* through murine models.

In vitro- Acute Exposure

Regarding epithelial cell responses to ODE, initial *in vitro* studies using BEAS-2B human airway epithelial cells revealed that ODE stimulated potent release of IL-8, IL-6, and via the protein kinase C (PKC) activation, with further studies demonstrating increased ICAM-1 expression, necessary for extravasation of recruited immune cells (110,111). Ciliary beating, crucial to mucociliary clearance, was also found decreased following exposure to DE, as well as migratory behavior as assessed via scratch assays (112,113). Similar exposures on lung-resident mesenchymal stem cells revealed similar release of pro-inflammatory cytokines (IL-6, TNF, IL-

8), matrix metalloproteinase 2 (MMP-2) and MMP-9 and wound healing mediators fibroblast growth factor 10 (FGF-10), amphiregulin, and resolvin-D1 (114). Exposure of primary murine and human fibroblasts to DE stimulates release of pro-inflammatory cytokines (IL-6, CXCL1, and IL-8) and decreases release of pro-resolution mediators amphiregulin (115). Collectively, these data suggest a role for the airway epithelium and fibroblasts in the production of pro-inflammatory mediators during ODE, while also demonstrating an impairment of homeostatic functions pivotal to airway maintenance and repair processes.

Recruited phagocytic immune cells have also been found to reduce their functionality and behavior in response to DE. A single treatment of DE in the human monocytic cell line THP-1 demonstrated a DE-induced increase in TNF, IL-8, IL-6, and IL-10, while re-stimulation with dust extract (DE) found increases only in IL-8 and IL-10 (116). In the murine monocyte cell line RAW 264.7, stimulation with DE resulted in increased release of CCL9, the production of which was readily decreased in knockdown of PKC-δ via siRNA targeting (117). Intriguingly, boiling of DE to inactive heat-labile components was effective in reducing the induced CCL-9 production, however this same approach was not efficient in reducing THP-1 cells' secretion of IL-6, TNF, IL-8, and IL-10 (116,117). DE has also been demonstrated to decrease monocyte-derived dendritic cell phenotype and function, with decreased differentiation into dendritic cells observed in monocytes after DE, as well as a lack of maturation, phagocytosis, and T-cell stimulation capability (118). Collectively, *in vitro* data suggest that ODE enhances pro-inflammatory cytokine release and decreases overall functionality of phagocytic and antigen presenting cells.

In vivo Model Development

In vivo exposure to DE has primarily relied on the inbred C57BL/6 mouse, naturally skewing the response towards a Th1-biased immune response, consistent with findings of the Th1/Th17 biased response to ODE (119). A relevant model of exposures of organic dusts at levels found in environmental levels has been trialed with the hanging of murine cages in swine confinement facilities (120,121). Unfortunately, these investigations only minimally replicated the airway hyperresponsiveness seen in humans but demonstrated low levels of inflammatory cytokines and immune cells found in clinical lavage, even after a month of exposure. As a result, a laboratory reproducible method that recapitulates the immune response was developed via intranasal instillations of DE (122).

In vivo- Acute Exposure

An acute exposure to 12.5% DE demonstrates airway hyperresponsiveness, increased alveolar cellularity, and a significant increase in immune cells (neutrophils, macrophages, and lymphocytes) (122,123). Increased neutrophil extracellular trap formation from neutrophils was also observed (123). Soluble mediators observed *in vitro* (TNF and IL-6) were confirmed *in vivo*, with additional findings of increased levels of KC, MIP-2, CXCL1, CXCL2, Amphiregulin, and MPO in bronchoalveolar lavage fluid (BALF) post ODE (122,123).

In vivo- Repetitive Exposure

Repetitive installations within *in vivo* models have advanced our understanding of the molecular and cellular processes the contribute to the chronic inflammatory environment necessary for COPD development in human subjects (96,124). Initial studies utilizing the repetitive form of

ODE focused on 1- and 2-week timepoints, and demonstrated a significant increase in neutrophils, macrophages, and lymphocytes via cytocentrifugation, as well as the development of induced iBALT (122). KC, TNF, IL-6, and MIP-2 all remain elevated at this timepoint compared to control animals (122). Induction of neutrophil and macrophage recruitment to the airway in a 3-week ODE model (the current standard after 2012) revealed profound increases in macrophage populations, with increases in co-stimulatory molecule (CD80 and CD86), but not MHC-2, expression (125). Intriguingly, reduction of macrophage populations via clodronate liposomes resulted in a subsequent preferential recruitment of neutrophils, as well as increased histopathologic scores, demonstrating a protective role for macrophages in ODE response (125). At 3 weeks of ODE, CD4+ T cells, especially those that secrete IL-17, accumulate and knockout of αβTCR $CD4^+$ cells drastically reduces iBALT development and cellular recruitment within alveolar spaces (119). Furthermore, reduction of B cells via $BCR^{-/-}$ mice in response to repetitive ODE revealed reduced levels of TNF, CXCL1, CXCL2, and IL-6 (126). A reduction in interstitial macrophages within the lung tissue and increase in memory B cells both in BALF and lung tissue was reported, coinciding with elevated IgG and IgE levels observed in serum (126). Complete loss of iBALT structure was noted, as well as a decrease in bronchiole inflammation, likely suggesting a B cell/iBALT role in cellular recruitment near airways (126).

Investigation into the recovery phases following repetitive (3-weeks) of ODE reveals significant reduction of airway neutrophils by 1 week, airway lymphocytes by 2 weeks, and a maintenance of macrophage populations by 4 weeks (127). Within the lung tissue, neutrophils and exudative macrophages remained elevated until week 3 and week 2, respectively, while $CD4^+$ and $CD8^+$ T cells remained elevated until 3 weeks of recovery (127). At 1 week recovery in a knockout of

scavenger receptor A (CD204), an increase in neutrophils, $CD4^+$, and $CD8^+$ T cells was characteristic at the recovery timepoint compared to WT, suggesting a necessity for CD204 in sensing and modulation of initial and recovery processes to repetitive ODE (128). In an 8-day repetitive ODE scheme, 3 days of intranasal IL-10 at 10 ng/ml was sufficient to reduce neutrophils in BALF, as well as decrease iBALT formation (129). For both previous studies, only male mice were utilized, potentially in acknowledgement of typical demographic makeups of swine farm workers (130). Collectively, recovery studies on ODE suggest prolonged alteration (up to a month or more) of recruited immune cell population, specifically in the lung tissue, necessitating a greater understanding of how homeostatic return can be optimized.

Omega-3 Fatty Acids: Health and Disease

Omega-3 fatty acids (n-3 FA) are polyunsaturated fatty acids (PUFAs) essential to cellular and organismal health (131). Primarily obtained through dietary consumption, foods high in n-3 FA like fatty fish and flax seeds are recommended, but not normally consumed in the common western diet (132,133). Supplementation of n-3 FA in the form of capsules utilizing fish or algal sources has become a method of obtaining recommended levels not available through diet (134,135). The growing body of research identifying the health benefits of n-3 FA focus on alpha-linoleic, docosahexaenoic, and eicosapentaenoic acids (ALA, DHA, EPA, respectively) (136). Dietary consumption is necessary for obtaining n-3 FAs as the human body does not possess cellular machinery necessary to synthesize fatty acids longer than 9 carbons, which grant ALA, DHA, and EPA their status as both an essential and long-chain fatty acid (137,138). N-3 FA bioaccumulate and are absorbed with 95% efficiency, initially distributing to the human body

via the lymphatic system and secondarily into primary circulation (139–141). Multiple uses for n-3 FAs have been described; functional in the formation and integrity of cell membranes, use in metabolism as free fatty acids, and as the basis for signaling molecules, termed eicosanoids (docosanoids for those derived from DHA), that are primary mediators of initial inflammatory signaling (leukotrienes and prostaglandins, specifically) (142–144) (**Figure 1.4**). *De novo* synthesis of n-3 and n-6 PUFAs is hampered by a lack of mammalian Δ-12 and Δ-15 fatty acid desaturase, requiring dietary intake for maintaining healthy levels of these essential fatty acids (145). Specifically, an n-6:n-3 FA ratio of 1:1 is ideal, which stands in stark comparison to the common western diet which is typically comprised of a ratio nearing 20:1 (146). This ratio imbalance is increasingly appreciated as problematic due to the innate competition of n-6 and n-3 PUFAs to their downstream metabolites via the same enzymes (112) (111). As such, imbalances of parent molecules to lead to bottlenecking and imbalanced downstream metabolite production (147–150).

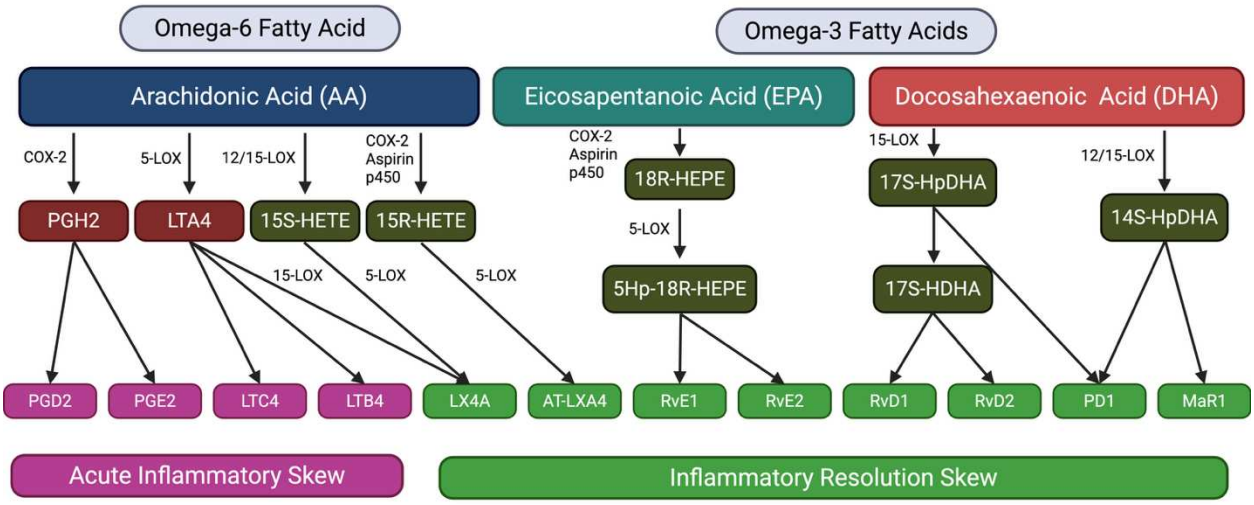

Figure 1.4. Select lipid mediators derived from arachidonic, eicosapentaenoic, and docosahexaenoic acid. Enzymes required for conversion or labeled next to appropriate reaction arrows. *Adapted from Serhan and Petasis, 2011.*

Known clinical conditions of n-3 FA deficits have been demonstrated in the form of neurodevelopmental deficits and/or visible dermatologic conditions; rough and/or scaly skin, and dermatitis(151,152). Unfortunately, research to date, although establishing that decreases are associated with diminished health, has failed to establish wherein deficits create clinically relevant and diagnosable presentations (153). Research on the benefits of n-3 FA have centered on DHA and EPA, and demonstrate benefits in cardiovascular, neurologic, ocular, mental, and developmental health (154–162). Results suggest that a diet with balanced levels of n-3FAs contributes to better health outcomes (i.e. less progressive disease, decreased incidence of disease) (163). Establishing causality for n-3 FA levels remains a challenge, so no official guidelines for n-3 FA levels have been established (164).

Specialized Pro-resolving Lipid Mediators

Specialized Pro-resolving lipid Mediators (SPM) are a group of fatty acid-derived molecules initially discovered in inflammatory exudates (pus) with potent immunomodulatory activities (165,166). The parent molecules of SPM, n-6 and n-3 PUFAs are converted to SPM via cytochrome p450 (cyp450), cyclooxygenase 2 (COX-2), arachidonate 2-lipoxygenase (ALOX-2), ALOX-12, and ALOX-15 enzymes (167–169) from parent molecules arachidonic acid (AA), DHA, and EPA (170). The downstream metabolite of AA, lipoxins, have been described in two forms, LXA4 and LXB4. DHA is metabolized into the six D-series resolvins (RvD1-RvD6), protectins (PD1), and maresins (MaR1). EPA is metabolized into four E-series resolvins, RvE1-RvE4 (171). SPM are produced by immune cells, epithelial cells, platelets, or in some cases, a combination of two types of cells, such as that performed in lipoxin synthesis with neutrophils

and platelets (172–174). SPM exert their actions through agonism of their cognate g-protein coupled receptors (**Table 1.1**) (175–178).

Table 1.1. Example SPM and identified cognate receptors, if present.

SPM	Receptor
LXA4	ALX/FPR2
LXB4	*Not Identified
RvD1	ALX/FPR2, GPR32/DRV1, GPR101
RvD2	GPR18/DRV2, GPR101
RvD3	ALX/FPR2, GPR32/DRV1, GPR101
RvD4	ALX/FPR2, GPR101
RvD5	GPR32/DRV1, GPR101
RvD6	GPR101
RvE1	LTB4R/BLT1, CMKLR1/ChemR23/ERV1
RvE2	LTB4, BLT1
RvE3	*Not Identified
RvE4	*Not Identified
PD1	GPR37
MaR1	LGR6

SPM and Innate Immunity

SPM have shown diverse impacts on a variety of immune and non-immune cells (179–183). LXA4 has been shown to increase epithelial and endothelial cell proliferation after injury, inhibit IL-6 and IL-8 release, and reduce the production of ROS in response to damage (184–186). RvD2 has been shown to reduce neutrophil migration through the production of endothelial cell nitric oxide, decreasing extravasation and septic inflammation (187). RvD3 has shown potent

activity in restoring epithelial barrier integrity in a model of acute lung injury (ALI) caused by hydrochloric acid exposure (188).

The impact of SPM on neutrophil phenotype and effector function has been extensively studied, as this cell type was key to SPM discovery. LXA4 alone has been demonstrated to reduce neutrophil chemotaxis, neutrophil-epithelial interactions and extravasation, and decreased superoxide production (189–194). Intriguingly, LXB4-treated neutrophils exhibit the same effector function and phenotype, despite a lack of an identifiable receptor (189,191,193). Other SPM have similar effects on neutrophil behavior, but additional impacts such as upregulation of CCR5, and reduction of IFN-γ and TNF have also been reported (195,196). Compared to neutrophils, monocytes are inversely impacted by treatment with LXA4 and LXB4, demonstrating increased migration and cellular adhesion following treatment (197). Macrophages treated with LXA4 exhibit increased phagocytosis of apoptotic neutrophils, while RvD1, RvD2, MaR1, PD1 and RvE1 similarly increase phagocytosis of allergens, bacteria, and apoptotic cells (198–202). Induction of an M2 phenotype in macrophages is possible with treatment of RvE1 and RvD1 (187,203).

NK cells and ILC2 treated with SPM demonstrate decreases in cytotoxicity/inducing apoptosis and reduced levels of IL-13, but increased levels of amphiregulin release, respectively (204–207). Treatment of dendritic cells with RvD1 decreases MHC-2 expression (208). After treatment with LXB4, mast cells reduce their granulation capacity, while treatment of eosinophils with LXA4 or LXB4 decreases chemotaxis (209–212). Collectively, SPM enhance

phagocytic capacities, decrease granule release, and decrease recruitment of innate granulocytes and phagocytes, all supporters of the resolution response.

SPM in Adaptive Immunity

As SPM's primary roles involved increasing the pace at which resolution occurs, it is no surprise that adaptive immune cells respond to SPM treatment by changing their effector functions. Inhibition of 5-ALOX and 12/15-ALOX profoundly reduces the pro and pre-B cell development in the bone marrow, ultimately reducing peripheral B cell populations (213). Induction of B cell migration via LXA4 protected mice from sepsis via B-cell produced GM-CSF and subsequent macrophage population enhancement (214). Via upregulation of COX-2, LXB4 enhanced IgG production from B cells, as well as promoted B cells to differentiate into memory B cells (215,216). Reduction of IgE production in B cells has been noted in B cells treated with SPM (217). These impacts seem primarily context dependent but skewed towards mitigation of immune responses through suppression of non-specific immunoglobulins and increases in specificity of known encountered antigens through IgGs.

T lymphocytes are similarly impacted by SPM, and deletion of ALOX-15 in T regulatory cells results in impaired functionality, a phenotype rescuable by exogenous RvD3 treatment (218). Using purified T cells from mice with DHA-supplemented diets, it was demonstrated the T cells increased their proliferation and decreased their production of Th2 cytokines such as IL-2 and IL-4 (219). Upregulation in CCR5, a key receptor for targeted apoptosis, is found following treatment of T cells with LXA4 or RvD1 (220). In a model of acute lung injury, treatment with

MaR1 reduced inflammation via increased Treg production through the FoxP3 transcription factor (221).

SPM in Organic Dust Exposure

Within the acute and chronic inflammatory environment created by ODE, a particular interest in the use n-3 fatty acids and SPM has arisen to reduce ODE-induced inflammatory profiles (222). DHA treatment given before ODE was found to reduce inflammatory cytokine production *in vitro* and *in vivo* and reduce recruited neutrophils within BALF (223). Similarly, pretreatment of mice with DHA metabolite MaR1 before a single or repetitive (15) dose(ing) of ODE significantly reduced neutrophil infiltration as well as levels of CXCL1, IL-6, and TNF, without altering histopathologic features of ODE (224). *In vitro*, DHA treatment post ODE enhances epithelial growth and recovery via amphiregulin induction (225). Dietary interventions that incorporate optimal DHA levels in a mouse model of ODE led to increased recruitment of macrophages and enhanced levels of BALF MCP-1 (123). DHA diet in a separate investigation reduced cellularity and pro-inflammatory cytokine release by 1 week of recovery (226). The use of transgenic mice (Fat-1) that contain a desaturase enzyme to modulate a balanced n-6:n-3 FA ratio in ODE demonstrated a sex-dependent reduction in iBALT formation (227–229). Collectively, n-3 balance or supplementation, via dietary or genetic means, alters the inflammatory profile induced by ODE.

Study Rationale and Aims

The immune response to inhaled PM, such as ODE, presents a unique immunopathologic paradigm that necessitates a greater understanding of the immune cell players responsible for

acute and repetitive exposure response. Given the demonstrated neutrophilic response, a deeper understanding of the phenotype and functionality (ie NET formation) of these neutrophils is warranted. Furthermore, the efficacy of n-3 FA and their down-stream metabolites at modulating immune response present a unique opportunity for therapeutic intervention, however a deeper understanding of the cell populations altered by n-6:n-3 FA balance precludes such investigations. Furthermore, in what manner the inflammatory environment of ODE alters susceptibility to common pathogens, such as *Streptococcus pneumoniae* remain un-investigated. We have developed 3 aims to investigate these processes.

Specific Aim 1: Develop a flow cytometry method for NET-forming neutrophil identification and tracking following acute dust exposure. *Hypothesis: Acute dust exposure will increase neutrophil and NET-forming neutrophil populations.*

Specific Aim 2: Deeply phenotype the response and resolution promoted by increased n-3 fatty acids following repetitive ODE. *Hypothesis: N-3 fatty acid balanced mice will recruit immune cells that are skewed towards resolution, and lead to swifter reduction of inflammatory cells and tissue pathology.*

Specific Aim 3: Determine the immune response induced by repetitive ODE followed by infection with *Streptococcus pneumoniae. Hypothesis: Repetitive ODE will predispose mice to a greater infectious burden and mortality rate with infection of S. pneumoniae.*

These described aims will enhance understanding of the impact of acute ODE on neutrophil phenotype and NET formation, additionally providing an improved flow cytometry method for analyzing NET formation. In advancing the field of immunopathologic understanding of repetitive ODE, our investigation will reveal key innate immune cell populations differentially present at homeostasis and recruited and in response to balanced n-3 FA levels. Furthermore, our investigations will provide insight into how the inflammatory environment of repetitive ODE alters susceptibility to a secondary respiratory infection with *S. pneumoniae*. Collectively, these investigations will enhance our understanding of the immune cell landscape governing response to acute and repetitive ODE, providing invaluable insight into how these players are secondarily altered via n-3 FA or secondary infection.

References

1. Fröhlich E, Mercuri A, Wu S, Salar-Behzadi S. Measurements of Deposition, Lung Surface Area and Lung Fluid for Simulation of Inhaled Compounds. *Front Pharmacol* (2016) 7:181. doi: 10.3389/fphar.2016.00181
2. Csencsits KL, Jutila MA, Pascual DW. Nasal-Associated Lymphoid Tissue: Phenotypic and Functional Evidence for the Primary Role of Peripheral Node Addressin in Naive Lymphocyte Adhesion to High Endothelial Venules in a Mucosal Site. *The Journal of Immunology* (1999) 163:1382–1389. doi: 10.4049/jimmunol.163.3.1382
3. Gopallawa I, Dehinwal R, Bhatia V, Gujar V, Chirmule N. A four-part guide to lung immunology: Invasion, inflammation, immunity, and intervention. *Front Immunol* (2023) 14:1119564. doi: 10.3389/fimmu.2023.1119564
4. Hewitt RJ, Lloyd CM. Regulation of immune responses by the airway epithelial cell landscape. *Nat Rev Immunol* (2021) 21:347–362. doi: 10.1038/s41577-020-00477-9
5. Silva-Sanchez A, Randall TD. "Role of iBALT in Respiratory Immunity.," (2019). p. 21–43 doi: 10.1007/82_2019_191
6. Pizzolla A, Wang Z, Groom JR, Kedzierska K, Brooks AG, Reading PC, Wakim LM. Nasal-associated lymphoid tissues (NALTs) support the recall but not priming of influenza virus-specific cytotoxic T cells. *Proceedings of the National Academy of Sciences* (2017) 114:5225–5230. doi: 10.1073/pnas.1620194114
7. Fahy J V, Dickey BF. Airway mucus function and dysfunction. *N Engl J Med* (2010) 363:2233–47. doi: 10.1056/NEJMra0910061
8. Corthésy B. Multi-faceted functions of secretory IgA at mucosal surfaces. *Front Immunol* (2013) 4:185. doi: 10.3389/fimmu.2013.00185
9. Cowland JB, Muta T, Borregaard N. IL-1β-Specific Up-Regulation of Neutrophil Gelatinase-Associated Lipocalin Is Controlled by IκB-ζ. *The Journal of Immunology* (2006) 176:5559–5566. doi: 10.4049/jimmunol.176.9.5559
10. Juncadella IJ, Kadl A, Sharma AK, Shim YM, Hochreiter-Hufford A, Borish L, Ravichandran KS. Apoptotic cell clearance by bronchial epithelial cells critically influences airway inflammation. *Nature* (2013) 493:547–551. doi: 10.1038/nature11714
11. Knudsen L, Ochs M. The micromechanics of lung alveoli: structure and function of surfactant and tissue components. *Histochem Cell Biol* (2018) 150:661–676. doi: 10.1007/s00418-018-1747-9
12. Olajuyin AM, Zhang X, Ji H-L. Alveolar type 2 progenitor cells for lung injury repair. *Cell Death Discov* (2019) 5:63. doi: 10.1038/s41420-019-0147-9
13. Bhattacharya J, Westphalen K. Macrophage-epithelial interactions in pulmonary alveoli. *Semin Immunopathol* (2016) 38:461–469. doi: 10.1007/s00281-016-0569-x
14. Hu G, Christman JW. Editorial: Alveolar Macrophages in Lung Inflammation and Resolution. *Front Immunol* (2019) 10: doi: 10.3389/fimmu.2019.02275
15. Hussell T, Bell TJ. Alveolar macrophages: plasticity in a tissue-specific context. *Nat Rev Immunol* (2014) 14:81–93. doi: 10.1038/nri3600
16. Fajgenbaum DC, June CH. Cytokine Storm. *New England Journal of Medicine* (2020) 383:2255–2273. doi: 10.1056/NEJMra2026131
17. Liu J, Pang Z, Wang G, Guan X, Fang K, Wang Z, Wang F. Advanced Role of Neutrophils in Common Respiratory Diseases. *J Immunol Res* (2017) 2017:6710278. doi: 10.1155/2017/6710278

18. Mettelman RC, Allen EK, Thomas PG. Mucosal immune responses to infection and vaccination in the respiratory tract. *Immunity* (2022) 55:749–780. doi: 10.1016/j.immuni.2022.04.013
19. Iwasaki A, Foxman EF, Molony RD. Early local immune defences in the respiratory tract. *Nat Rev Immunol* (2017) 17:7–20. doi: 10.1038/nri.2016.117
20. Wan Y, Bramson J. Role of Dendritic Cell-Derived Cytokines in Immune Regulation. *Curr Pharm Des* (2001) 7:977–992. doi: 10.2174/1381612013397627
21. Levy BD, Serhan CN. Resolution of Acute Inflammation in the Lung. *Annu Rev Physiol* (2014) 76:467–492. doi: 10.1146/annurev-physiol-021113-170408
22. Kerr JFR, Wyllie AH, Currie AR. Apoptosis: A Basic Biological Phenomenon with Wideranging Implications in Tissue Kinetics. *Br J Cancer* (1972) 26:239–257. doi: 10.1038/bjc.1972.33
23. Grabiec AM, Hussell T. The role of airway macrophages in apoptotic cell clearance following acute and chronic lung inflammation. *Semin Immunopathol* (2016) 38:409–423. doi: 10.1007/s00281-016-0555-3
24. Yun JH, Henson PM, Tuder RM. Phagocytic clearance of apoptotic cells: role in lung disease. *Expert Rev Respir Med* (2008) 2:753–765. doi: 10.1586/17476348.2.6.753
25. Lucas A, Yasa J, Lucas M. Regeneration and repair in the healing lung. *Clin Transl Immunology* (2020) 9:e1152. doi: 10.1002/cti2.1152
26. Quesnel C, Nardelli L, Piednoir P, Leçon V, Marchal-Somme J, Lasocki S, Bouadma L, Philip I, Soler P, Crestani B, et al. Alveolar fibroblasts in acute lung injury: biological behaviour and clinical relevance. *European Respiratory Journal* (2010) 35:1312–1321. doi: 10.1183/09031936.00074709
27. Ghonim MA, Boyd DF, Flerlage T, Thomas PG. Pulmonary inflammation and fibroblast immunoregulation: from bench to bedside. *J Clin Invest* (2023) 133: doi: 10.1172/JCI170499
28. Momtazmanesh S, Moghaddam SS, Ghamari S-H, Rad EM, Rezaei N, Shobeiri P, Aali A, Abbasi-Kangevari M, Abbasi-Kangevari Z, Abdelmasseh M, et al. Global burden of chronic respiratory diseases and risk factors, 1990–2019: an update from the Global Burden of Disease Study 2019. *EClinicalMedicine* (2023) 59:101936. doi: 10.1016/j.eclinm.2023.101936
29. Song Q, Chen P, Liu X-M. The role of cigarette smoke-induced pulmonary vascular endothelial cell apoptosis in COPD. *Respir Res* (2021) 22:39. doi: 10.1186/s12931-021-01630-1
30. Yoshida T, Tuder RM. Pathobiology of Cigarette Smoke-Induced Chronic Obstructive Pulmonary Disease. *Physiol Rev* (2007) 87:1047–1082. doi: 10.1152/physrev.00048.2006
31. Kotlyarov S. The Role of Smoking in the Mechanisms of Development of Chronic Obstructive Pulmonary Disease and Atherosclerosis. *Int J Mol Sci* (2023) 24: doi: 10.3390/ijms24108725
32. Toumpanakis D, Usmani OS. Small airways disease in patients with alpha-1 antitrypsin deficiency. *Respir Med* (2023) 211:107222. doi: 10.1016/j.rmed.2023.107222
33. Leung JM, Tiew PY, Mac Aogáin M, Budden KF, Yong VFL, Thomas SS, Pethe K, Hansbro PM, Chotirmall SH. The role of acute and chronic respiratory colonization and infections in the pathogenesis of COPD. *Respirology* (2017) 22:634–650. doi: 10.1111/resp.13032
34. Barnes PJ, Burney PGJ, Silverman EK, Celli BR, Vestbo J, Wedzicha JA, Wouters EFM. Chronic obstructive pulmonary disease. *Nat Rev Dis Primers* (2015) 1:15076. doi: 10.1038/nrdp.2015.76

35. Molfino NA, Jeffery PK. Chronic obstructive pulmonary disease: Histopathology, inflammation and potential therapies. *Pulm Pharmacol Ther* (2007) 20:462–472. doi: 10.1016/j.pupt.2006.04.003
36. Barnes PJ, Celli BR. Systemic manifestations and comorbidities of COPD. *European Respiratory Journal* (2009) 33:1165–1185. doi: 10.1183/09031936.00128008
37. Hogg JC, Chu F, Utokaparch S, Woods R, Elliott WM, Buzatu L, Cherniack RM, Rogers RM, Sciurba FC, Coxson HO, et al. The Nature of Small-Airway Obstruction in Chronic Obstructive Pulmonary Disease. *New England Journal of Medicine* (2004) 350:2645–2653. doi: 10.1056/NEJMoa032158
38. Hiemstra PS. Altered Macrophage Function in Chronic Obstructive Pulmonary Disease. *Ann Am Thorac Soc* (2013) 10:S180–S185. doi: 10.1513/AnnalsATS.201305-123AW
39. Barnes PJ. Cellular and Molecular Mechanisms of Chronic Obstructive Pulmonary Disease. *Clin Chest Med* (2014) 35:71–86. doi: 10.1016/j.ccm.2013.10.004
40. Singh D. Chronic Obstructive Pulmonary Disease, Neutrophils and Bacterial Infection: A Complex Web Involving IL-17 and IL-22 Unravels. *EBioMedicine* (2015) 2:1580–1. doi: 10.1016/j.ebiom.2015.10.021
41. Hogg JC. Pathophysiology of airflow limitation in chronic obstructive pulmonary disease. *The Lancet* (2004) 364:709–721. doi: 10.1016/S0140-6736(04)16900-6
42. Di Stefano A, Caramori G, Gnemmi I, Contoli M, Vicari C, Capelli A, Magno F, D'Anna SE, Zanini A, Brun P, et al. T helper type 17-related cytokine expression is increased in the bronchial mucosa of stable chronic obstructive pulmonary disease patients. *Clin Exp Immunol* (2009) 157:316–324. doi: 10.1111/j.1365-2249.2009.03965.x
43. Brusselle GG, Demoor T, Bracke KR, Brandsma C-A, Timens W. Lymphoid follicles in (very) severe COPD: beneficial or harmful? *European Respiratory Journal* (2009) 34:219–230. doi: 10.1183/09031936.00150208
44. van der Strate BWA, Postma DS, Brandsma C-A, Melgert BN, Luinge MA, Geerlings M, Hylkema MN, van den Berg A, Timens W, Kerstjens HAM. Cigarette Smoke–induced Emphysema. *Am J Respir Crit Care Med* (2006) 173:751–758. doi: 10.1164/rccm.200504-594OC
45. Olloquequi J, Ferrer J, Montes JF, Rodríguez E, Montero MA, García-Valero J. Differential lymphocyte infiltration in small airways and lung parenchyma in COPD patients. *Respir Med* (2010) 104:1310–1318. doi: 10.1016/j.rmed.2010.03.002
46. Higham A, Dungwa J, Pham T, McCrae C, Singh D. Increased mast cell activation in eosinophilic chronic obstructive pulmonary disease. *Clin Transl Immunology* (2022) 11: doi: 10.1002/cti2.1417
47. Higham A, Beech A, Singh D. The relevance of eosinophils in chronic obstructive pulmonary disease: inflammation, microbiome, and clinical outcomes. *J Leukoc Biol* (2024) 116:927–946. doi: 10.1093/jleuko/qiae153
48. Roque A, Taborda-Barata L, Cruz ÁA, Viegi G, Maricoto T. COPD treatment – a conceptual review based on critical endpoints. *Pulmonology* (2023) 29:410–420. doi: 10.1016/j.pulmoe.2023.02.015
49. Yawn BP, Mintz ML, Doherty DE. GOLD in Practice: Chronic Obstructive Pulmonary Disease Treatment and Management in the Primary Care Setting. *Int J Chron Obstruct Pulmon Dis* (2021) 16:289–299. doi: 10.2147/COPD.S222664
50. Yawn BP. Is "GOLD" standard for the management of COPD in clinical practice? *Drugs Context* (2012) 2012:212243. doi: 10.7573/dic.212243

51. Linden D, Guo-Parke H, Coyle P V., Fairley D, McAuley DF, Taggart CC, Kidney J. Respiratory viral infection: a potential "missing link" in the pathogenesis of COPD. *European Respiratory Review* (2019) 28:180063. doi: 10.1183/16000617.0063-2018
52. Frickmann H, Jungblut S, Hirche TO, Groß U, Kuhns M, Zautner AE. The influence of virus infections on the course of COPD. *Eur J Microbiol Immunol (Bp)* (2012) 2:176–85. doi: 10.1556/EuJMI.2.2012.3.2
53. Wedzicha JA. Role of Viruses in Exacerbations of Chronic Obstructive Pulmonary Disease. *Proc Am Thorac Soc* (2004) 1:115–120. doi: 10.1513/pats.2306030
54. Gou X, Zhang Q, More S, Bamunuarachchi G, Liang Y, Haider Khan F, Maranville R, Zuniga E, Wang C, Liu L. Repeated Exposure to Streptococcus pneumoniae Exacerbates Chronic Obstructive Pulmonary Disease. *Am J Pathol* (2019) 189:1711–1720. doi: 10.1016/j.ajpath.2019.05.012
55. Mantero M, Aliberti S, Azzari C, Moriondo M, Nieddu F, Blasi F, Di Pasquale M. Role of Streptococcus pneumoniae infection in chronic obstructive pulmonary disease patients in Italy. *Ther Adv Respir Dis* (2017) 11:403–407. doi: 10.1177/1753465817728479
56. Pichavant M, Sharan R, Le Rouzic O, Olivier C, Hennegrave F, Rémy G, Pérez-Cruz M, Koné B, Gosset P, Just N, et al. IL-22 Defect During Streptococcus pneumoniae Infection Triggers Exacerbation of Chronic Obstructive Pulmonary Disease. *EBioMedicine* (2015) 2:1686–1696. doi: 10.1016/j.ebiom.2015.09.040
57. Narciso AR, Dookie R, Nannapaneni P, Normark S, Henriques-Normark B. Streptococcus pneumoniae epidemiology, pathogenesis and control. *Nat Rev Microbiol* (2024) doi: 10.1038/s41579-024-01116-z
58. Donati C, Hiller NL, Tettelin H, Muzzi A, Croucher NJ, Angiuoli S V, Oggioni M, Dunning Hotopp JC, Hu FZ, Riley DR, et al. Structure and dynamics of the pan-genome of Streptococcus pneumoniae and closely related species. *Genome Biol* (2010) 11:R107. doi: 10.1186/gb-2010-11-10-r107
59. Sandgren A, Sjöström K, Olsson-Liljequist B, Christensson B, Samuelsson A, Kronvall G, Henriques Normark B. Effect of Clonal and Serotype-Specific Properties on the Invasive Capacity of *Streptococcus pneumoniae*. *J Infect Dis* (2004) 189:785–796. doi: 10.1086/381686
60. Brueggemann AB, Peto TEA, Crook DW, Butler JC, Kristinsson KG, Spratt BG. Temporal and Geographic Stability of the Serogroup-Specific Invasive Disease Potential of *Streptococcus pneumoniae* in Children. *J Infect Dis* (2004) 190:1203–1211. doi: 10.1086/423820
61. Sjostrom K, Spindler C, Ortqvist A, Kalin M, Sandgren A, Kuhlmann-Berenzon S, Normark BH. Clonal and Capsular Types Decide Whether Pneumococci Will Act as a Primary or Opportunistic Pathogen. *Clinical Infectious Diseases* (2006) 42:451–459. doi: 10.1086/499242
62. Pimenta F, Moiane B, Gertz RE, Chochua S, Snippes Vagnone PM, Lynfield R, Sigaúque B, Carvalho M da G, Beall B. New Pneumococcal Serotype 15D. *J Clin Microbiol* (2021) 59: doi: 10.1128/JCM.00329-21
63. Tvedskov ESF, Hovmand N, Benfield T, Tinggaard M. Pneumococcal carriage among children in low and lower-middle-income countries: A systematic review. *International Journal of Infectious Diseases* (2022) 115:1–7. doi: 10.1016/j.ijid.2021.11.021
64. Naucler P, Galanis I, Petropoulos A, Granath F, Morfeldt E, Örtqvist Å, Henriques-Normark, B. Chronic Disease and Immunosuppression Increase the Risk for Nonvaccine Serotype Pneumococcal Disease: A Nationwide Population-based Study. *Clinical Infectious Diseases* (2022) 74:1338–1349. doi: 10.1093/cid/ciab651

65. Mina MJ, Klugman KP. The role of influenza in the severity and transmission of respiratory bacterial disease. *Lancet Respir Med* (2014) 2:750–763. doi: 10.1016/S2213-2600(14)70131-6
66. Sun K, Metzger DW. Inhibition of pulmonary antibacterial defense by interferon-γ during recovery from influenza infection. *Nat Med* (2008) 14:558–564. doi: 10.1038/nm1765
67. Nakamura S, Davis KM, Weiser JN. Synergistic stimulation of type I interferons during influenza virus coinfection promotes Streptococcus pneumoniae colonization in mice. *Journal of Clinical Investigation* (2011) 121:3657–3665. doi: 10.1172/JCI57762
68. Zhang Z, Clarke TB, Weiser JN. Cellular effectors mediating Th17-dependent clearance of pneumococcal colonization in mice. *Journal of Clinical Investigation* (2009) doi: 10.1172/JCI36731
69. Jochems SP, de Ruiter K, Solórzano C, Voskamp A, Mitsi E, Nikolaou E, Carniel BF, Pojar S, German EL, Reiné J, et al. Innate and adaptive nasal mucosal immune responses following experimental human pneumococcal colonization. *Journal of Clinical Investigation* (2019) 129:4523–4538. doi: 10.1172/JCI128865
70. Aberdein JD, Cole J, Bewley MA, Marriott HM, Dockrell DH. Alveolar macrophages in pulmonary host defence – the unrecognized role of apoptosis as a mechanism of intracellular bacterial killing. *Clin Exp Immunol* (2013) 174:193–202. doi: 10.1111/cei.12170
71. Sun K, Gan Y, Metzger DW. Analysis of Murine Genetic Predisposition to Pneumococcal Infection Reveals a Critical Role of Alveolar Macrophages in Maintaining the Sterility of the Lower Respiratory Tract. *Infect Immun* (2011) 79:1842–1847. doi: 10.1128/IAI.01143-10
72. Verma AK, Bansal S, Bauer C, Muralidharan A, Sun K. Influenza Infection Induces Alveolar Macrophage Dysfunction and Thereby Enables Noninvasive *Streptococcus pneumoniae* to Cause Deadly Pneumonia. *The Journal of Immunology* (2020) 205:1601–1607. doi: 10.4049/jimmunol.2000094
73. Winter C, Herbold W, Maus R, Länger F, Briles DE, Paton JC, Welte T, Maus UA. Important Role for CC Chemokine Ligand 2-Dependent Lung Mononuclear Phagocyte Recruitment to Inhibit Sepsis in Mice Infected with *Streptococcus pneumoniae*. *The Journal of Immunology* (2009) 182:4931–4937. doi: 10.4049/jimmunol.0804096
74. Peñaloza HF, Nieto PA, Muñoz-Durango N, Salazar-Echegarai FJ, Torres J, Parga MJ, Alvarez-Lobos M, Riedel CA, Kalergis AM, Bueno SM. Interleukin-10 plays a key role in the modulation of neutrophils recruitment and lung inflammation during infection by *Streptococcus pneumoniae*. *Immunology* (2015) 146:100–112. doi: 10.1111/imm.12486
75. Clark SE, Schmidt RL, Aguilera ER, Lenz LL. IL-10-producing NK cells exacerbate sublethal Streptococcus pneumoniae infection in the lung. *Translational Research* (2020) 226:70–82. doi: 10.1016/j.trsl.2020.07.001
76. Vissers M, van de Garde MDB, He SWJ, Brandsen M, Hendriksen R, Nicolaie MA, van der Maas L, Meiring HD, van Els CACM, van Beek J, et al. Quantity and Quality of Naturally Acquired Antibody Immunity to the Pneumococcal Proteome Throughout Life. *J Infect Dis* (2024) 230:1466–1475. doi: 10.1093/infdis/jiae255
77. He SWJ, Voß F, Nicolaie MA, Brummelman J, van de Garde MDB, Bijvank E, Poelen M, Wijmenga-Monsuur AJ, Wyllie AL, Trzciński K, et al. Serological Profiling of Pneumococcal Proteins Reveals Unique Patterns of Acquisition, Maintenance, and Waning of Antibodies Throughout Life. *J Infect Dis* (2024) 230:e1299–e1310. doi: 10.1093/infdis/jiae216
78. Gil E, Noursadeghi M, Brown JS. Streptococcus pneumoniae interactions with the complement system. *Front Cell Infect Microbiol* (2022) 12: doi: 10.3389/fcimb.2022.929483

79. Nakafero G, Grainge MJ, Card T, Mallen CD, Nguyen Van-Tam JS, Abhishek A. Effectiveness of pneumococcal vaccination in adults with common immune-mediated inflammatory diseases in the UK: a case–control study. *Lancet Rheumatol* (2024) 6:e615–e624. doi: 10.1016/S2665-9913(24)00128-0
80. Wang Y, Li J, Wang Y, Gu W, Zhu F. Effectiveness and practical uses of 23-valent pneumococcal polysaccharide vaccine in healthy and special populations. *Hum Vaccin Immunother* (2018) 14:1003–1012. doi: 10.1080/21645515.2017.1409316
81. Daniels CC, Rogers PD, Shelton CM. A Review of Pneumococcal Vaccines: Current Polysaccharide Vaccine Recommendations and Future Protein Antigens. *J Pediatr Pharmacol Ther* (2016) 21:27–35. doi: 10.5863/1551-6776-21.1.27
82. Savulescu C, Krizova P, Lepoutre A, Mereckiene J, Vestrheim DF, Ciruela P, Ordobas M, Guevara M, McDonald E, Morfeldt E, et al. Effect of high-valency pneumococcal conjugate vaccines on invasive pneumococcal disease in children in SpIDnet countries: an observational multicentre study. *Lancet Respir Med* (2017) 5:648–656. doi: 10.1016/S2213-2600(17)30110-8
83. Converso TR, Assoni L, André GO, Darrieux M, Leite LCC. The long search for a serotype independent pneumococcal vaccine. *Expert Rev Vaccines* (2020) 19:57–70. doi: 10.1080/14760584.2020.1711055
84. Micoli F, Romano MR, Carboni F, Adamo R, Berti F. Strengths and weaknesses of pneumococcal conjugate vaccines. *Glycoconj J* (2023) 40:135–148. doi: 10.1007/s10719-023-10100-3
85. Lu W, Aarsand R, Schotte K, Han J, Lebedeva E, Tsoy E, Maglakelidze N, Soriano JB, Bill W, Halpin DMG, et al. Tobacco and COPD: presenting the World Health Organization (WHO) Tobacco Knowledge Summary. *Respir Res* (2024) 25:338. doi: 10.1186/s12931-024-02961-5
86. Zhao J, Li M, Wang Z, Chen J, Zhao J, Xu Y, Wei X, Wang J, Xie J. Role of PM2.5 in the development and progression of COPD and its mechanisms. *Respir Res* (2019) 20:120. doi: 10.1186/s12931-019-1081-3
87. Wang Q, Liu S. The Effects and Pathogenesis of PM2.5 and Its Components on Chronic Obstructive Pulmonary Disease. *Int J Chron Obstruct Pulmon Dis* (2023) Volume 18:493–506. doi: 10.2147/COPD.S402122
88. Mukherjee A, Agrawal M. "A Global Perspective of Fine Particulate Matter Pollution and Its Health Effects.," (2017). p. 5–51 doi: 10.1007/398_2017_3
89. Croft DP, Zhang W, Lin S, Thurston SW, Hopke PK, van Wijngaarden E, Squizzato S, Masiol M, Utell MJ, Rich DQ. Associations between Source-Specific Particulate Matter and Respiratory Infections in New York State Adults. *Environ Sci Technol* (2020) 54:975–984. doi: 10.1021/acs.est.9b04295
90. Kim K-H, Kabir E, Kabir S. A review on the human health impact of airborne particulate matter. *Environ Int* (2015) 74:136–143. doi: 10.1016/j.envint.2014.10.005
91. Fang SC, Cassidy A, Christiani DC. A systematic review of occupational exposure to particulate matter and cardiovascular disease. *Int J Environ Res Public Health* (2010) 7:1773–806. doi: 10.3390/ijerph7041773
92. Shi L, Zanobetti A, Kloog I, Coull BA, Koutrakis P, Melly SJ, Schwartz JD. Low-Concentration PM2.5 and Mortality: Estimating Acute and Chronic Effects in a Population-Based Study. *Environ Health Perspect* (2016) 124:46–52. doi: 10.1289/ehp.1409111
93. Kloog I, Ridgway B, Koutrakis P, Coull BA, Schwartz JD. Long- and short-term exposure to PM2.5 and mortality: using novel exposure models. *Epidemiology* (2013) 24:555–61. doi: 10.1097/EDE.0b013e318294beaa

94. Poole JA, Zamora-Sifuentes JL, De las Vecillas L, Quirce S. Respiratory Diseases Associated With Organic Dust Exposure. *J Allergy Clin Immunol Pract* (2024) 12:1960–1971. doi: 10.1016/j.jaip.2024.02.022
95. Christiani DC. Organic dust exposure and chronic airway disease. *Am J Respir Crit Care Med* (1996) 154:833–4. doi: 10.1164/ajrccm.154.4.8887570
96. Nordgren TM, Charavaryamath C. Agriculture Occupational Exposures and Factors Affecting Health Effects. *Curr Allergy Asthma Rep* (2018) 18:65. doi: 10.1007/s11882-018-0820-8
97. Nordgren TM, Bailey KL. Pulmonary health effects of agriculture. *Curr Opin Pulm Med* (2016) 22:144–149. doi: 10.1097/MCP.0000000000000247
98. Poole JA, Dooley GP, Saito R, Burrell AM, Bailey KL, Romberger DJ, Mehaffy J, Reynolds SJ. Muramic Acid, Endotoxin, 3-Hydroxy Fatty Acids, and Ergosterol Content Explain Monocyte and Epithelial Cell Inflammatory Responses to Agricultural Dusts. *J Toxicol Environ Health A* (2010) 73:684–700. doi: 10.1080/15287390903578539
99. Boissy RJ, Romberger DJ, Roughead WA, Weissenburger-Moser L, Poole JA, LeVan TD. Shotgun pyrosequencing metagenomic analyses of dusts from swine confinement and grain facilities. *PLoS One* (2014) 9: doi: 10.1371/journal.pone.0095578
100. Poole JA, Wyatt TA, Von Essen SG, Hervert J, Parks C, Mathisen T, Romberger DJ. Repeat organic dust exposure–induced monocyte inflammation is associated with protein kinase C activity. *Journal of Allergy and Clinical Immunology* (2007) 120:366–373. doi: 10.1016/j.jaci.2007.04.033
101. Von Essen SG, Robbins RA, Thompson AB, Ertl RF, Linder J, Rennard S. Mechanisms of Neutrophil Recruitment to the Lung by Grain Dust Exposure. *American Review of Respiratory Disease* (1988) 138:921–927. doi: 10.1164/ajrccm/138.4.921
102. Gurney JW, Unger JM, Dorby CA, Mitby JK, Von Essen SG. Agricultural disorders of the lung. *RadioGraphics* (1991) 11:625–634. doi: 10.1148/radiographics.11.4.1887117
103. Spurzem JR, Romberger DJ, Von Essen SG. Agricultural lung disease. *Clin Chest Med* (2002) 23:795–810. doi: 10.1016/S0272-5231(02)00024-2
104. Andersen CI, Von Essen SG, Smith LM, Spencer J, Jolie R, Donham KJ. Respiratory symptoms and airway obstruction in swine veterinarians: a persistent problem. *Am J Ind Med* (2004) 46:386–92. doi: 10.1002/ajim.20080
105. Von Essen SG, Auvermann BW. Health effects from breathing air near CAFOs for feeder cattle or hogs. *J Agromedicine* (2005) 10:55–64. doi: 10.1300/J096v10n04_08
106. Bailey KL, Meza JL, Smith LM, Von Essen SG, Romberger DJ. Agricultural exposures in patients with COPD in health systems serving rural areas. *J Agromedicine* (2007) 12:71–6. doi: 10.1300/J096v12n02_10
107. von Essen SG, Banks DE. Life-long exposures on the farm, respiratory symptoms, and lung function decline. *Chest* (2009) 136:662–663. doi: 10.1378/chest.09-0944
108. O'Connor AM, Auvermann B, Bickett-Weddle D, Kirkhorn S, Sargeant JM, Ramirez A, Von Essen SG. The association between proximity to animal feeding operations and community health: a systematic review. *PLoS One* (2010) 5:e9530. doi: 10.1371/journal.pone.0009530
109. Harting JR, Gleason A, Romberger DJ, Von Essen SG, Qiu F, Alexis N, Poole JA. Chronic obstructive pulmonary disease patients have greater systemic responsiveness to ex vivo stimulation with swine dust extract and its components versus healthy volunteers. *J Toxicol Environ Health A* (2012) 75:1456–70. doi: 10.1080/15287394.2012.722186

110. Romberger DJ, Bodlak V, Von Essen SG, Mathisen T, Wyatt TA. Hog barn dust extract stimulates IL-8 and IL-6 release in human bronchial epithelial cells via PKC activation. *J Appl Physiol* (2002) 93:289–296. doi: 10.1152/japplphysiol.00815.2001
111. Mathisen T, Von Essen SG, Wyatt TA, Romberger DJ. Hog barn dust extract augments lymphocyte adhesion to human airway epithelial cells. *J Appl Physiol (1985)* (2004) 96:1738–44. doi: 10.1152/japplphysiol.00384.2003
112. Wyatt TA, Sisson JH, Von Essen SG, Poole JA, Romberger DJ. Exposure to hog barn dust alters airway epithelial ciliary beating. *Eur Respir J* (2008) 31:1249–55. doi: 10.1183/09031936.00015007
113. Slager RE, Allen-Gipson DS, Sammut A, Heires A, DeVasure J, Von Essen S, Romberger DJ, Wyatt TA. Hog barn dust slows airway epithelial cell migration in vitro through a PKCα-dependent mechanism. *American Journal of Physiology-Lung Cellular and Molecular Physiology* (2007) 293:L1469–L1474. doi: 10.1152/ajplung.00274.2007
114. Nordgren TM, Bailey KL, Heires AJ, Katafiasz D, Romberger DJ. Effects of Agricultural Organic Dusts on Human Lung-Resident Mesenchymal Stem (Stromal) Cell Function. *Toxicological Sciences* (2018) 162:635–644. doi: 10.1093/toxsci/kfx286
115. Poole JA, Nordgren TM, Heires AJ, Nelson AJ, Katafiasz D, Bailey KL, Romberger DJ. Amphiregulin modulates murine lung recovery and fibroblast function following exposure to agriculture organic dust. *Am J Physiol Lung Cell Mol Physiol* (2020) 318:L180–L191. doi: 10.1152/ajplung.00039.2019
116. Poole JA, Wyatt TA, Von Essen SG, Hervert J, Parks C, Mathisen T, Romberger DJ. Repeat organic dust exposure–induced monocyte inflammation is associated with protein kinase C activity. *Journal of Allergy and Clinical Immunology* (2007) 120:366–373. doi: 10.1016/j.jaci.2007.04.033
117. Schneberger D, DeVasure JM, Bailey KL, Romberger DJ, Wyatt TA. Swine barn dust stimulates CCL9 expression in mouse monocytes through PKC-delta activation. *Environ Dis* (2020) 5:93–99. doi: 10.4103/ed.ed_16_20
118. Poole JA, Thiele GM, Alexis NE, Burrell AM, Parks C, Romberger DJ. Organic dust exposure alters monocyte-derived dendritic cell differentiation and maturation. *American Journal of Physiology-Lung Cellular and Molecular Physiology* (2009) 297:L767–L776. doi: 10.1152/ajplung.00107.2009
119. Poole JA, Gleason AM, Bauer C, West WW, Alexis N, Reynolds SJ, Romberger DJ, Kielian T. αβ T cells and a mixed Th1/Th17 response are important in organic dust-induced airway disease. *Annals of Allergy, Asthma & Immunology* (2012) 109:266-273.e2. doi: 10.1016/j.anai.2012.06.015
120. Charavaryamath C, Juneau V, Suri SS, Janardhan KS, Townsend H, Singh B. ROLE OF TOLL-LIKE RECEPTOR 4 IN LUNG INFLAMMATION FOLLOWING EXPOSURE TO SWINE BARN AIR. *Exp Lung Res* (2008) 34:19–35. doi: 10.1080/01902140701807779
121. Charavaryamath C, Janardhan KS, Townsend HG, Willson P, Singh B. Multiple exposures to swine barn air induce lung inflammation and airway hyper-responsiveness. *Respir Res* (2005) 6:50. doi: 10.1186/1465-9921-6-50
122. Poole JA, Wyatt TA, Oldenburg PJ, Elliott MK, West WW, Sisson JH, Von Essen SG, Romberger DJ. Intranasal organic dust exposure-induced airway adaptation response marked by persistent lung inflammation and pathology in mice. *American Journal of Physiology-Lung Cellular and Molecular Physiology* (2009) 296:L1085–L1095. doi: 10.1152/ajplung.90622.2008

123. Dominguez EC, Heires AJ, Pavlik J, Larsen TD, Guardado S, Sisson JH, Baack ML, Romberger DJ, Nordgren TM. A High Docosahexaenoic Acid Diet Alters the Lung Inflammatory Response to Acute Dust Exposure. *Nutrients* (2020) 12: doi: 10.3390/nu12082334
124. Poole JA, Romberger DJ. Immunological and inflammatory responses to organic dust in agriculture. *Curr Opin Allergy Clin Immunol* (2012) 12:126–132. doi: 10.1097/ACI.0b013e3283511d0e
125. Poole JA, Gleason AM, Bauer C, West WW, Alexis N, van Rooijen N, Reynolds SJ, Romberger DJ, Kielian TL. CD11c(+)/CD11b(+) cells are critical for organic dust-elicited murine lung inflammation. *Am J Respir Cell Mol Biol* (2012) 47:652–9. doi: 10.1165/rcmb.2012-0095OC
126. Poole JA, Mikuls TR, Duryee MJ, Warren KJ, Wyatt TA, Nelson AJ, Romberger DJ, West WW, Thiele GM. A role for B cells in organic dust induced lung inflammation. *Respir Res* (2017) 18:214. doi: 10.1186/s12931-017-0703-x
127. Warren K, Wyatt T, Romberger D, Ailts I, West W, Nelson A, Nordgren T, Staab E, Heires A, Poole J. Post-Injury and Resolution Response to Repetitive Inhalation Exposure to Agricultural Organic Dust in Mice. *Safety* (2017) 3:10. doi: 10.3390/safety3010010
128. Poole JA, Anderson L, Gleason AM, West WW, Romberger DJ, Wyatt TA. Pattern recognition scavenger receptor A/CD204 regulates airway inflammatory homeostasis following organic dust extract exposures. *J Immunotoxicol* (2015) 12:64–73. doi: 10.3109/1547691X.2014.882449
129. Wyatt TA, Nemecek M, Chandra D, DeVasure JM, Nelson AJ, Romberger DJ, Poole JA. Organic dust-induced lung injury and repair: Bi-directional regulation by TNFα and IL-10. *J Immunotoxicol* (2020) 17:153–162. doi: 10.1080/1547691X.2020.1776428
130. Biswas A, Harbin S, Irvin E, Johnston H, Begum M, Tiong M, Apedaile D, Koehoorn M, Smith P. Sex and Gender Differences in Occupational Hazard Exposures: a Scoping Review of the Recent Literature. *Curr Environ Health Rep* (2021) 8:267–280. doi: 10.1007/s40572-021-00330-8
131. Gabbs M, Leng S, Devassy JG, Monirujjaman M, Aukema HM. Advances in Our Understanding of Oxylipins Derived from Dietary PUFAs. *Advances in Nutrition* (2015) 6:513–540. doi: 10.3945/an.114.007732
132. Gebauer SK, Psota TL, Harris WS, Kris-Etherton PM. n−3 Fatty acid dietary recommendations and food sources to achieve essentiality and cardiovascular benefits. *Am J Clin Nutr* (2006) 83:1526S-1535S. doi: 10.1093/ajcn/83.6.1526S
133. Simopoulos AP. The importance of the ratio of omega-6/omega-3 essential fatty acids. *Biomedicine & Pharmacotherapy* (2002) 56:365–379. doi: 10.1016/S0753-3322(02)00253-6
134. DiNicolantonio JJ, O'Keefe J. The Importance of Maintaining a Low Omega-6/Omega-3 Ratio for Reducing the Risk of Autoimmune Diseases, Asthma, and Allergies. *Mo Med* (2021) 118:453–459.
135. Simopoulos AP. Evolutionary aspects of diet, the omega-6/omega-3 ratio and genetic variation: nutritional implications for chronic diseases. *Biomedicine & Pharmacotherapy* (2006) 60:502–507. doi: 10.1016/j.biopha.2006.07.080
136. Swanson D, Block R, Mousa SA. Omega-3 fatty acids EPA and DHA: health benefits throughout life. *Adv Nutr* (2012) 3:1–7. doi: 10.3945/an.111.000893
137. Brenna JT, Salem N, Sinclair AJ, Cunnane SC. α-Linolenic acid supplementation and conversion to n-3 long-chain polyunsaturated fatty acids in humans. *Prostaglandins Leukot Essent Fatty Acids* (2009) 80:85–91. doi: 10.1016/j.plefa.2009.01.004

138. Blondeau N, Lipsky RH, Bourourou M, Duncan MW, Gorelick PB, Marini AM. Alpha-linolenic acid: an omega-3 fatty acid with neuroprotective properties-ready for use in the stroke clinic? *Biomed Res Int* (2015) 2015:519830. doi: 10.1155/2015/519830
139. Chevalier L, Plourde M. Comparison of pharmacokinetics of omega-3 fatty acid supplements in monoacylglycerol or ethyl ester in humans: a randomized controlled trial. *Eur J Clin Nutr* (2021) 75:680–688. doi: 10.1038/s41430-020-00767-4
140. Punia S, Sandhu KS, Siroha AK, Dhull SB. Omega 3-metabolism, absorption, bioavailability and health benefits–A review. *PharmaNutrition* (2019) 10:100162. doi: 10.1016/j.phanu.2019.100162
141. Fritsche KL. Too much linoleic acid promotes inflammation—doesn't it? *Prostaglandins Leukot Essent Fatty Acids* (2008) 79:173–175. doi: 10.1016/j.plefa.2008.09.019
142. Calder PC. Mechanisms of Action of (n-3) Fatty Acids,. *J Nutr* (2012) 142:592S-599S. doi: 10.3945/jn.111.155259
143. Riediger ND, Othman RA, Suh M, Moghadasian MH. A Systemic Review of the Roles of n-3 Fatty Acids in Health and Disease. *J Am Diet Assoc* (2009) 109:668–679. doi: 10.1016/j.jada.2008.12.022
144. Serhan CN, Savill J. Resolution of inflammation: the beginning programs the end. *Nat Immunol* (2005) 6:1191–1197. doi: 10.1038/ni1276
145. Lee JM, Lee H, Kang S, Park WJ. Fatty Acid Desaturases, Polyunsaturated Fatty Acid Regulation, and Biotechnological Advances. *Nutrients* (2016) 8: doi: 10.3390/nu8010023
146. Simopoulos AP. The Importance of the Omega-6/Omega-3 Fatty Acid Ratio in Cardiovascular Disease and Other Chronic Diseases. *Exp Biol Med* (2008) 233:674–688. doi: 10.3181/0711-MR-311
147. Burdge G. ??-Linolenic acid metabolism in men and women: nutritional and biological implications. *Curr Opin Clin Nutr Metab Care* (2004) 7:137–144. doi: 10.1097/00075197-200403000-00006
148. Giltay EJ, Gooren LJ, Toorians AW, Katan MB, Zock PL. Docosahexaenoic acid concentrations are higher in women than in men because of estrogenic effects. *Am J Clin Nutr* (2004) 80:1167–1174. doi: 10.1093/ajcn/80.5.1167
149. Jump DB. The Biochemistry of n-3 Polyunsaturated Fatty Acids. *Journal of Biological Chemistry* (2002) 277:8755–8758. doi: 10.1074/jbc.R100062200
150. Liput KP, Lepczyński A, Ogłuszka M, Nawrocka A, Poławska E, Grzesiak A, Ślaska B, Pareek CS, Czarnik U, Pierzchała M. Effects of Dietary n-3 and n-6 Polyunsaturated Fatty Acids in Inflammation and Cancerogenesis. *Int J Mol Sci* (2021) 22: doi: 10.3390/ijms22136965
151. Harris WS, Tintle NL, Imamura F, Qian F, Korat AVA, Marklund M, Djoussé L, Bassett JK, Carmichael P-H, Chen Y-Y, et al. Blood n-3 fatty acid levels and total and cause-specific mortality from 17 prospective studies. *Nat Commun* (2021) 12:2329. doi: 10.1038/s41467-021-22370-2
152. Anderson GJ, Neuringer M, Lin DS, Connor WE. Can Prenatal N-3 Fatty Acid Deficiency Be Completely Reversed after Birth? Effects on Retinal and Brain Biochemistry and Visual Function in Rhesus Monkeys. *Pediatr Res* (2005) 58:865–872. doi: 10.1203/01.pdr.0000182188.31596.5a
153. Messamore E, McNamara RK. Detection and treatment of omega-3 fatty acid deficiency in psychiatric practice: Rationale and implementation. *Lipids Health Dis* (2016) 15:25. doi: 10.1186/s12944-016-0196-5

154. von Schacky C. Use of Red Blood Cell Fatty-Acid Profiles as Biomarkers in Cardiac Disease. *Biomark Med* (2009) 3:25–32. doi: 10.2217/17520363.3.1.25
155. Harris WS, von Schacky C. The Omega-3 Index: a new risk factor for death from coronary heart disease? *Prev Med (Baltim)* (2004) 39:212–220. doi: 10.1016/j.ypmed.2004.02.030
156. Harris WS. Are n-3 fatty acids still cardioprotective? *Curr Opin Clin Nutr Metab Care* (2013) 16:141–149. doi: 10.1097/MCO.0b013e32835bf380
157. Harris WS, Sands SA, Windsor SL, Ali HA, Stevens TL, Magalski A, Porter CB, Borkon AM. Omega-3 Fatty Acids in Cardiac Biopsies From Heart Transplantation Patients. *Circulation* (2004) 110:1645–1649. doi: 10.1161/01.CIR.0000142292.10048.B2
158. Brasky TM, Darke AK, Song X, Tangen CM, Goodman PJ, Thompson IM, Meyskens FL, Goodman GE, Minasian LM, Parnes HL, et al. Plasma Phospholipid Fatty Acids and Prostate Cancer Risk in the SELECT Trial. *JNCI: Journal of the National Cancer Institute* (2013) 105:1132–1141. doi: 10.1093/jnci/djt174
159. Brasky TM, Till C, White E, Neuhouser ML, Song X, Goodman P, Thompson IM, King IB, Albanes D, Kristal AR. Serum Phospholipid Fatty Acids and Prostate Cancer Risk: Results From the Prostate Cancer Prevention Trial. *Am J Epidemiol* (2011) 173:1429–1439. doi: 10.1093/aje/kwr027
160. James M, Proudman S, Cleland L. Fish oil and rheumatoid arthritis: past, present and future. *Proceedings of the Nutrition Society* (2010) 69:316–323. doi: 10.1017/S0029665110001564
161. Stanley JC, Elsom RL, Calder PC, Griffin BA, Harris WS, Jebb SA, Lovegrove JA, Moore CS, Riemersma RA, Sanders TAB. UK Food Standards Agency Workshop Report: the effects of the dietary *n* -6: *n* -3 fatty acid ratio on cardiovascular health. *British Journal of Nutrition* (2007) 98:1305–1310. doi: 10.1017/S000711450784284X
162. Harris WS, Davidson MH. RE: Plasma Phospholipid Fatty Acids and Prostate Cancer Risk in the SELECT Trial. *JNCI Journal of the National Cancer Institute* (2014) 106:dju019–dju019. doi: 10.1093/jnci/dju019
163. Yaeger MJ, Leuenberger L, Shaikh SR, Gowdy KM. Omega-3 Fatty Acids and Chronic Lung Diseases: A Narrative Review of Impacts from Womb to Tomb. *J Nutr* (2025) 155:453–464. doi: 10.1016/j.tjnut.2024.10.028
164. Patchen BK, Balte P, Bartz TM, Barr RG, Fornage M, Graff M, Jacobs DR, Kalhan R, Lemaitre RN, O'Connor G, et al. Investigating Associations of Omega-3 Fatty Acids, Lung Function Decline, and Airway Obstruction. *Am J Respir Crit Care Med* (2023) 208:846–857. doi: 10.1164/rccm.202301-0074OC
165. Marcus AJ, Broekman MJ, Safier LB, Ullman HL, Islam N, Serhan CN, Weissmann G. Production of arachidonic acid lipoxygenase products during platelet-neutrophil interactions. *Clin Physiol Biochem* (1984) 2:78–83.
166. Serhan CN, Hong S, Gronert K, Colgan SP, Devchand PR, Mirick G, Moussignac R-L. Resolvins. *J Exp Med* (2002) 196:1025–1037. doi: 10.1084/jem.20020760
167. Panigrahy D, Gilligan MM, Serhan CN, Kashfi K. Resolution of inflammation: An organizing principle in biology and medicine. *Pharmacol Ther* (2021) 227:107879. doi: 10.1016/j.pharmthera.2021.107879
168. Chiang N, Serhan CN. Specialized pro-resolving mediator network: an update on production and actions. *Essays Biochem* (2020) 64:443–462. doi: 10.1042/EBC20200018
169. Arnold C, Konkel A, Fischer R, Schunck W-H. Cytochrome P450–dependent metabolism of ω-6 and ω-3 long-chain polyunsaturated fatty acids. *Pharmacological Reports* (2010) 62:536–547. doi: 10.1016/S1734-1140(10)70311-X

170. Serhan CN, Hamberg M, Samuelsson B. Lipoxins: novel series of biologically active compounds formed from arachidonic acid in human leukocytes. *Proc Natl Acad Sci U S A* (1984) 81:5335–9. doi: 10.1073/pnas.81.17.5335
171. Serhan CN. Pro-resolving lipid mediators are leads for resolution physiology. *Nature* (2014) 510:92–101. doi: 10.1038/nature13479
172. Serhan CN, Hong S, Lu Y. Lipid mediator informatics-lipidomics: novel pathways in mapping resolution. *AAPS J* (2006) 8:E284-97. doi: 10.1007/BF02854899
173. Cherpokova D, Jouvene CC, Libreros S, DeRoo EP, Chu L, de la Rosa X, Norris PC, Wagner DD, Serhan CN. Resolvin D4 attenuates the severity of pathological thrombosis in mice. *Blood* (2019) 134:1458–1468. doi: 10.1182/blood.2018886317
174. Li W, Shepherd HM, Terada Y, Shay AE, Bery AI, Gelman AE, Lavine KJ, Serhan CN, Kreisel D. Resolvin D1 prevents injurious neutrophil swarming in transplanted lungs. *Proc Natl Acad Sci U S A* (2023) 120:e2302938120. doi: 10.1073/pnas.2302938120
175. Karra L, Haworth O, Priluck R, Levy BD, Levi-Schaffer F. Lipoxin B4 promotes the resolution of allergic inflammation in the upper and lower airways of mice. *Mucosal Immunol* (2015) 8:852–862. doi: 10.1038/mi.2014.116
176. Libreros S, Shay AE, Nshimiyimana R, Fichtner D, Martin MJ, Wourms N, Serhan CN. A New E-Series Resolvin: RvE4 Stereochemistry and Function in Efferocytosis of Inflammation-Resolution. *Front Immunol* (2021) 11: doi: 10.3389/fimmu.2020.631319
177. Sato M, Aoki-Saito H, Fukuda H, Ikeda H, Koga Y, Yatomi M, Tsurumaki H, Maeno T, Saito T, Nakakura T, et al. Resolvin E3 attenuates allergic airway inflammation via the interleukin-23-interleukin-17A pathway. *FASEB J* (2019) 33:12750–12759. doi: 10.1096/fj.201900283R
178. Julliard WA, Myo YPA, Perelas A, Jackson PD, Thatcher TH, Sime PJ. Specialized pro-resolving mediators as modulators of immune responses. *Semin Immunol* (2022) 59:101605. doi: 10.1016/j.smim.2022.101605
179. Norling L V., Spite M, Yang R, Flower RJ, Perretti M, Serhan CN. Cutting Edge: Humanized Nano-Proresolving Medicines Mimic Inflammation-Resolution and Enhance Wound Healing. *The Journal of Immunology* (2011) 186:5543–5547. doi: 10.4049/jimmunol.1003865
180. Leoni G, Alam A, Neumann P-A, Lambeth JD, Cheng G, McCoy J, Hilgarth RS, Kundu K, Murthy N, Kusters D, et al. Annexin A1, formyl peptide receptor, and NOX1 orchestrate epithelial repair. *Journal of Clinical Investigation* (2013) 123:443–454. doi: 10.1172/JCI65831
181. Goh J, Baird AW, O'Keane C, Watson RWG, Cottell D, Bernasconi G, Petasis NA, Godson C, Brady HR, MacMathuna P. Lipoxin A4 and Aspirin-Triggered 15-Epi-Lipoxin A4 Antagonize TNF-α-Stimulated Neutrophil-Enterocyte Interactions In Vitro and Attenuate TNF-α-Induced Chemokine Release and Colonocyte Apoptosis in Human Intestinal Mucosa Ex Vivo. *The Journal of Immunology* (2001) 167:2772–2780. doi: 10.4049/jimmunol.167.5.2772
182. Chiang N, Sakuma M, Rodriguez AR, Spur BW, Irimia D, Serhan CN. Resolvin T-series reduce neutrophil extracellular traps. *Blood* (2022) 139:1222–1233. doi: 10.1182/blood.2021013422
183. Monge P, Astudillo AM, Pereira L, Balboa MA, Balsinde J. Dynamics of Docosahexaenoic Acid Utilization by Mouse Peritoneal Macrophages. *Biomolecules* (2023) 13: doi: 10.3390/biom13111635
184. Brezinski ME, Gimbrone MA, Nicolaou KC, Serhan CN. Lipoxins stimulate prostacyclin generation by human endothelial cells. *FEBS Lett* (1989) 245:167–172. doi: 10.1016/0014-5793(89)80214-5

185. Nascimento-Silva V, Arruda MA, Barja-Fidalgo C, Fierro IM. Aspirin-triggered lipoxin A4 blocks reactive oxygen species generation in endothelial cells: a novel antioxidative mechanism. *Thromb Haemost* (2007) 97:88–98.
186. Bonnans C, Fukunaga K, Levy MA, Levy BD. Lipoxin A4 Regulates Bronchial Epithelial Cell Responses to Acid Injury. *Am J Pathol* (2006) 168:1064–1072. doi: 10.2353/ajpath.2006.051056
187. Spite M, Norling L V., Summers L, Yang R, Cooper D, Petasis NA, Flower RJ, Perretti M, Serhan CN. Resolvin D2 is a potent regulator of leukocytes and controls microbial sepsis. *Nature* (2009) 461:1287–1291. doi: 10.1038/nature08541
188. Colby JK, Abdulnour R-EE, Sham HP, Dalli J, Colas RA, Winkler JW, Hellmann J, Wong B, Cui Y, El-Chemaly S, et al. Resolvin D3 and Aspirin-Triggered Resolvin D3 Are Protective for Injured Epithelia. *Am J Pathol* (2016) 186:1801–1813. doi: 10.1016/j.ajpath.2016.03.011
189. Lee TH, Horton CE, Kyan-Aung U, Haskard D, Crea AEG, Spur BW. Lipoxin A4 and Lipoxin B4 Inhibit Chemotactic Responses of Human Neutrophils Stimulated by Leukotriene B4 and *N* -Formyl- <scp>l</scp> -Methionyl- <scp>l</scp> -Leucyl- <scp>l</scp> -Phenylalanine. *Clin Sci* (1989) 77:195–203. doi: 10.1042/cs0770195
190. Serhan CN, Maddox JF, Petasis NA, Akritopoulou-Zanze I, Papayianni A, Brady HR, Colgan SP, Madara JL. Design of Lipoxin A4 Stable Analogs That Block Transmigration and Adhesion of Human Neutrophils. *Biochemistry* (1995) 34:14609–14615. doi: 10.1021/bi00044a041
191. Colgan SP, Serhan CN, Parkos CA, Delp-Archer C, Madara JL. Lipoxin A4 modulates transmigration of human neutrophils across intestinal epithelial monolayers. *Journal of Clinical Investigation* (1993) 92:75–82. doi: 10.1172/JCI116601
192. Bonnans C, Fukunaga K, Levy MA, Levy BD. Lipoxin A4 Regulates Bronchial Epithelial Cell Responses to Acid Injury. *Am J Pathol* (2006) 168:1064–1072. doi: 10.2353/ajpath.2006.051056
193. Papayianni A, Serhan CN, Brady HR. Lipoxin A4 and B4 inhibit leukotriene-stimulated interactions of human neutrophils and endothelial cells. *J Immunol* (1996) 156:2264–72.
194. Levy BD, Fokin V V., Clark JM, Wakelam MJO, Petasis NA, Serhan CN. Polyisoprenyl phosphate (PIPP) signaling regulates phospholipase D activity: a ‘stop’ signaling switch for aspirin-triggered lipoxin A $_4$. *The FASEB Journal* (1999) 13:903–911. doi: 10.1096/fasebj.13.8.903
195. Ariel A, Fredman G, Sun Y-P, Kantarci A, Van Dyke TE, Luster AD, Serhan CN. Apoptotic neutrophils and T cells sequester chemokines during immune response resolution through modulation of CCR5 expression. *Nat Immunol* (2006) 7:1209–1216. doi: 10.1038/ni1392
196. Ariel A, Li P-L, Wang W, Tang W-X, Fredman G, Hong S, Gotlinger KH, Serhan CN. The Docosatriene Protectin D1 Is Produced by TH2 Skewing and Promotes Human T Cell Apoptosis via Lipid Raft Clustering. *Journal of Biological Chemistry* (2005) 280:43079–43086. doi: 10.1074/jbc.M509796200
197. Maddox JF, Serhan CN. Lipoxin A4 and B4 are potent stimuli for human monocyte migration and adhesion: selective inactivation by dehydrogenation and reduction. *J Exp Med* (1996) 183:137–146. doi: 10.1084/jem.183.1.137
198. Rogerio AP, Haworth O, Croze R, Oh SF, Uddin M, Carlo T, Pfeffer MA, Priluck R, Serhan CN, Levy BD. Resolvin D1 and Aspirin-Triggered Resolvin D1 Promote Resolution of

Allergic Airways Responses. *The Journal of Immunology* (2012) 189:1983–1991. doi: 10.4049/jimmunol.1101665
199. Schwab JM, Chiang N, Arita M, Serhan CN. Resolvin E1 and protectin D1 activate inflammation-resolution programmes. *Nature* (2007) 447:869–874. doi: 10.1038/nature05877
200. Godson C, Mitchell S, Harvey K, Petasis NA, Hogg N, Brady HR. Cutting Edge: Lipoxins Rapidly Stimulate Nonphlogistic Phagocytosis of Apoptotic Neutrophils by Monocyte-Derived Macrophages. *The Journal of Immunology* (2000) 164:1663–1667. doi: 10.4049/jimmunol.164.4.1663
201. Schwab JM, Chiang N, Arita M, Serhan CN. Resolvin E1 and protectin D1 activate inflammation-resolution programmes. *Nature* (2007) 447:869–874. doi: 10.1038/nature05877
202. Serhan CN, Yang R, Martinod K, Kasuga K, Pillai PS, Porter TF, Oh SF, Spite M. Maresins: novel macrophage mediators with potent antiinflammatory and proresolving actions. *Journal of Experimental Medicine* (2009) 206:15–23. doi: 10.1084/jem.20081880
203. Herová M, Schmid M, Gemperle C, Hersberger M. ChemR23, the Receptor for Chemerin and Resolvin E1, Is Expressed and Functional on M1 but Not on M2 Macrophages. *The Journal of Immunology* (2015) 194:2330–2337. doi: 10.4049/jimmunol.1402166
204. Barnig C, Cernadas M, Dutile S, Liu X, Perrella MA, Kazani S, Wechsler ME, Israel E, Levy BD. Lipoxin A $_4$ Regulates Natural Killer Cell and Type 2 Innate Lymphoid Cell Activation in Asthma. *Sci Transl Med* (2013) 5: doi: 10.1126/scitranslmed.3004812
205. Thorén FB, Riise RE, Ousbäck J, Della Chiesa M, Alsterholm M, Marcenaro E, Pesce S, Prato C, Cantoni C, Bylund J, et al. Human NK Cells Induce Neutrophil Apoptosis via an NKp46- and Fas-Dependent Mechanism. *The Journal of Immunology* (2012) 188:1668–1674. doi: 10.4049/jimmunol.1102002
206. Barnig C, Cernadas M, Dutile S, Liu X, Perrella MA, Kazani S, Wechsler ME, Israel E, Levy BD. Lipoxin A $_4$ Regulates Natural Killer Cell and Type 2 Innate Lymphoid Cell Activation in Asthma. *Sci Transl Med* (2013) 5: doi: 10.1126/scitranslmed.3004812
207. Krishnamoorthy N, Burkett PR, Dalli J, Abdulnour R-EE, Colas R, Ramon S, Phipps RP, Petasis NA, Kuchroo VK, Serhan CN, et al. Cutting Edge: Maresin-1 Engages Regulatory T Cells To Limit Type 2 Innate Lymphoid Cell Activation and Promote Resolution of Lung Inflammation. *The Journal of Immunology* (2015) 194:863–867. doi: 10.4049/jimmunol.1402534
208. Miki Y, Yamamoto K, Taketomi Y, Sato H, Shimo K, Kobayashi T, Ishikawa Y, Ishii T, Nakanishi H, Ikeda K, et al. Lymphoid tissue phospholipase A2 group IID resolves contact hypersensitivity by driving antiinflammatory lipid mediators. *Journal of Experimental Medicine* (2013) 210:1217–1234. doi: 10.1084/jem.20121887
209. Karra L, Haworth O, Priluck R, Levy BD, Levi-Schaffer F. Lipoxin B4 promotes the resolution of allergic inflammation in the upper and lower airways of mice. *Mucosal Immunol* (2015) 8:852–862. doi: 10.1038/mi.2014.116
210. Bandeira-Melo C, Bozza PT, Diaz BL, Cordeiro RSB, Jose PJ, Martins MA, Serhan CN. Cutting Edge: Lipoxin (LX) A4 and Aspirin-Triggered 15-Epi-LXA4 Block Allergen-Induced Eosinophil Trafficking. *The Journal of Immunology* (2000) 164:2267–2271. doi: 10.4049/jimmunol.164.5.2267
211. Levy BD, De Sanctis GT, Devchand PR, Kim E, Ackerman K, Schmidt BA, Szczeklik W, Drazen JM, Serhan CN. Multi-pronged inhibition of airway hyper-responsiveness and inflammation by lipoxin A4. *Nat Med* (2002) 8:1018–1023. doi: 10.1038/nm748

212. Soyombo O, Spur BW, Lee TH. Effects of lipoxin A $_4$ on chemotaxis and degranulation of human eosinophils stimulated by platelet-activating factor and *N* -formyl-L-methionyl-L-leucyl-L-phenylalanine. *Allergy* (1994) 49:230–234. doi: 10.1111/j.1398-9995.1994.tb02654.x
213. Teague H, Fhaner CJ, Harris M, Duriancik DM, Reid GE, Shaikh SR. n-3 PUFAs enhance the frequency of murine B-cell subsets and restore the impairment of antibody production to a T-independent antigen in obesity. *J Lipid Res* (2013) 54:3130–8. doi: 10.1194/jlr.M042457
214. Cheng Q, Wang Z, Ma R, Chen Y, Yan Y, Miao S, Jiao J, Cheng X, Kong L, Ye D. Lipoxin A4 protects against lipopolysaccharide-induced sepsis by promoting innate response activator B cells generation. *Int Immunopharmacol* (2016) 39:229–235. doi: 10.1016/j.intimp.2016.07.026
215. Kim N, Lannan KL, Thatcher TH, Pollock SJ, Woeller CF, Phipps RP. Lipoxin B4 Enhances Human Memory B Cell Antibody Production via Upregulating Cyclooxygenase-2 Expression. *J Immunol* (2018) 201:3343–3351. doi: 10.4049/jimmunol.1700503
216. Ramon S, Bancos S, Serhan CN, Phipps RP. Lipoxin A$_4$ modulates adaptive immunity by decreasing memory B-cell responses via an ALX/FPR2-dependent mechanism. *Eur J Immunol* (2014) 44:357–69. doi: 10.1002/eji.201343316
217. Kim N, Ramon S, Thatcher TH, Woeller CF, Sime PJ, Phipps RP. Specialized proresolving mediators (SPMs) inhibit human B-cell IgE production. *Eur J Immunol* (2016) 46:81–91. doi: 10.1002/eji.201545673
218. Marques RM, Gonzalez-Nunez M, Walker ME, Gomez EA, Colas RA, Montero-Melendez T, Perretti M, Dalli J. Loss of 15-lipoxygenase disrupts Treg differentiation altering their pro-resolving functions. *Cell Death Differ* (2021) 28:3140–3160. doi: 10.1038/s41418-021-00807-x
219. Arrington JL, Chapkin RS, Switzer KC, Morris JS, McMurray DN. Dietary n-3 polyunsaturated fatty acids modulate purified murine T-cell subset activation. *Clin Exp Immunol* (2001) 125:499–507. doi: 10.1046/j.1365-2249.2001.01627.x
220. Ariel A, Fredman G, Sun Y-P, Kantarci A, Van Dyke TE, Luster AD, Serhan CN. Apoptotic neutrophils and T cells sequester chemokines during immune response resolution through modulation of CCR5 expression. *Nat Immunol* (2006) 7:1209–16. doi: 10.1038/ni1392
221. Xia H, Wang F, Wang M, Wang J, Sun S, Chen M, Huang S, Chen X, Yao S. Maresin1 ameliorates acute lung injury induced by sepsis through regulating Th17/Treg balance. *Life Sci* (2020) 254:117773. doi: 10.1016/j.lfs.2020.117773
222. Isaak M, Ulu A, Osunde A, Nordgren TM, Hanson C. Nutritional Factors in Occupational Lung Disease. *Curr Allergy Asthma Rep* (2021) 21:24. doi: 10.1007/s11882-021-01003-0
223. Nordgren T, Friemel T, Heires A, Poole J, Wyatt T, Romberger D. The Omega-3 Fatty Acid Docosahexaenoic Acid Attenuates Organic Dust-Induced Airway Inflammation. *Nutrients* (2014) 6:5434–5452. doi: 10.3390/nu6125434
224. Nordgren TM, Bauer CD, Heires AJ, Poole JA, Wyatt TA, West WW, Romberger DJ. Maresin-1 reduces airway inflammation associated with acute and repetitive exposures to organic dust. *Transl Res* (2015) 166:57–69. doi: 10.1016/j.trsl.2015.01.001
225. Nordgren TM, Heires AJ, Bailey KL, Katafiasz DM, Toews ML, Wichman CS, Romberger DJ. Docosahexaenoic acid enhances amphiregulin-mediated bronchial epithelial cell repair processes following organic dust exposure. *American Journal of Physiology-Lung Cellular and Molecular Physiology* (2018) 314:L421–L431. doi: 10.1152/ajplung.00273.2017
226. Ulu A, Burr A, Heires AJ, Pavlik J, Larsen T, Perez PA, Bravo C, DiPatrizio N V., Baack M, Romberger DJ, et al. A high docosahexaenoic acid diet alters lung inflammation and recovery following repetitive exposure to aqueous organic dust extracts. *Journal of Nutritional Biochemistry* (2021) 97: doi: 10.1016/j.jnutbio.2021.108797

227. Kang JX. Fat-1 transgenic mice: a new model for omega-3 research. *Prostaglandins Leukot Essent Fatty Acids* (2007) 77:263–7. doi: 10.1016/j.plefa.2007.10.010
228. Kang JX, Wang J, Wu L, Kang ZB. Fat-1 mice convert n-6 to n-3 fatty acids. *Nature* (2004) 427:504–504. doi: 10.1038/427504a
229. Ulu A, Velazquez J V., Burr A, Sveiven SN, Yang J, Bravo C, Hammock BD, Nordgren TM. Sex-Specific Differences in Resolution of Airway Inflammation in Fat-1 Transgenic Mice Following Repetitive Agricultural Dust Exposure. *Front Pharmacol* (2022) 12: doi: 10.3389/fphar.2021.785193

Chapter 2

Spectral Flow Cytometry Method for Immunophenotyping Neutrophil Activation and NET-forming Capabilities in an Acute Dust Exposure Model[1]

[1] Manuscript submitted for review to Infection and Immunity 4/30/25

Summary

Although the contributions of neutrophils and neutrophil extracellular trap (NET) in chronic respiratory diseases associated with environmental dust inhalation has advanced, changes in neutrophil populations and their response following acute dust inhalation are relatively limited. Our understanding of neutrophil response during acute lung injury relies on blood and lung samples, which limit investigations on neutrophil dynamics such as neutrophil production, release, trafficking, and NET formation in response to acute exposures. To address this limitation, we designed a spectral flow cytometry panel to identify neutrophil progenitors, banded, and mature neutrophils across different sites; bone marrow, blood, lung, and bronchoalveolar lavage fluid (BALF) following acute organic dust exposure (ODE). We demonstrate that acute ODE increases band and mature neutrophils in the lung and BALF while decreasing band neutrophils in the bone marrow and blood. Interestingly, the proportion of pro-neutrophils (ProNeu1 and ProNeu2) was altered following ODE in the blood, but not bone marrow. We also analyzed the expression of surface markers associated with neutrophil recruitment and activation, as well as their size and granularity after ODE. Regardless of their maturation status, neutrophils in BALF and lung exhibited significant changes in CD11b, CXCR2, and CXCR4 levels post-ODE, while CD62L levels were specifically elevated in the blood. Finally, we identified lytic and vital NET forming neutrophils via Hoechst 33342 intensity in the lung and BALF, demonstrating increases in NET-forming neutrophil counts following ODE. Our spectral flow cytometry method provides valuable insight into neutrophil response, activation, and NET-forming capacity in response to acute ODE.

Introduction

Neutrophils, the most abundant leukocytes in human blood, play an essential role in the initial response to acute infection and tissue damage against external insults (1). They rapidly deploy effector functions, such as degranulation, phagocytosis, and release of neutrophil extracellular traps (NET) to defend the host against invading pathogens and environmental insults (2,3). Neutrophil activation is a critical step for resolving inflammatory responses and maintaining homeostasis (4). However, excessive neutrophil infiltration and activation during initial inflammatory response can lead to granule release and persistent NET formation, perpetuating inflammatory responses, and causing additional tissue injury and/or impairing tissue repair (5,6).

Elevated NETs in circulation and within tissue have been observed in various chronic lung diseases, including asthma and chronic obstructive pulmonary disease (COPD) and infectious diseases, such as COVID-19 and streptococcal pneumonia (7–9). Studies have demonstrated that host inflammatory factors are involved in triggering NETosis and/ or that certain neutrophil subsets are more prone to forming NETs (10,11). Most often, NET formation triggers lytic cell death, but it can also proceed without lytic death, termed “vital NET formation”, that is non-lytic and maintains neutrophils’ ability to move and phagocytose following NET release (12). Accumulating evidence has demonstrated that both vital and lytic NETs have the potential to exacerbate inflammatory pathology and coagulopathy.

It is well demonstrated that neutrophilia is a major histopathologic response in the airway and lung tissue to acute exposure of dust extracts (13,14) and chronic dust exposures are linked to

development of chronic lung diseases (14–19). Still, neutrophil response, such as changes in neutrophil populations, phenotypes, and functionalities in response to acute insults are less understood, particularly, at mucosal barrier sites, such as the lung (20,21). Therefore, it is essential to understand temporal dynamics of neutrophil regulation and response during the acute phase of inflammatory response (22–24). In addition, understanding how acute stimuli regulate NET formation, and whether NETosis is lytic, vital, or both in response to such stimuli remains an area of active investigation.

Using an established mouse model of acute ODE, we have previously established that a single intranasal challenge with ODE leads to evidence of NETosis in the airways at 5 hours following exposure (13). These findings were limited by using a method that relies on cytocentrifugation of collected airway immune cell populations from bronchoalveolar lavage fluid and semi-quantitative scoring of "shooting star" morphologies on the slides (13). This method was limited in its ability to accurately quantify neutrophils that are undergoing NETosis, a lack of ability to differentiate lytic vs vital NETosis and finally presents a major challenge in identifying these cells from alternative samples, such as blood, tissue single cell suspensions, or bone marrow. A comprehensive overview of current methods for NET detection has been extensively reviewed elsewhere (25), but *in vitro* measurement of NET forming cells is reliant on flow cytometry as the gold standard (26–31). A comprehensive flow cytometry-based panel that incorporates neutrophil progenitors, NET-forming capacity, and differentiation of lytic vs vital NETosis across relevant tissues in response to an acute inflammatory stimulus, such as ODE, is lacking. To address this limitation, we developed a spectral flow cytometry panel that identifies neutrophil progenitors and banded and mature neutrophils in the bone marrow, blood, lung, and airway in response to acute

ODE. Our method allows for characterization of neutrophil phenotypes at the sites ODE, with the ability to examine NET-forming capacity and identify lytic/non-lytic NET-forming signatures via inclusion of the DNA dye Hoechst 33342 (32). Collectively this panel combines several aspects of a much-needed flow cytometry assay for neutrophil and NET formation processes *in vivo* using a model of acute inflammatory insult in the form of ODE.

Methods

Preparation of Dust Extracts

Dusts were collected as previously described from swine confinement facilities in the Midwest, United States, and stored at -20 ºC until preparation. Aqueous dust extracts were prepared as previously described (33); in brief, 5 g of dust was mixed into 50 mL of Hanks Balanced Salt Solution (HBSS) (HyClone, Logan, UT) at room temperature for 1 hour. The resulting extract was centrifuged at 2500 x g for 20 minutes at 4 ºC. Supernate was transferred to a new 50 mL conical, recentrifuged at 2500 x g for 20 minutes at 4 ºC, and subsequent supernate sterile-filtered with a 0.22 μm filter to produce 100% dust extract (DE). Aliquots of DE were stored at -20 ºC until use. Formulations of 12.5% DE were prepared for animal installations by diluting 100% DE with phosphate buffered saline (PBS) (Fisher Scientific, Waltham, MA). A dose of 12.5% DE has been previously demonstrated as appropriate for generating substantial lung inflammation characterized by airway neutrophilia with a single instillation and promoting histopathological markers of lung disease with repetitive exposure, while not leading to significant weight loss, lethargy, or other moribund phenotypes (34–38).

Animal Husbandry and Installations

Animal protocols were reviewed and approved by the Institutional Animal Care and Use Committee at Colorado State University (Protocol #2887). 7-month-old C57BL/6 male and female mice (Jackson Labs, Bar Harbor, ME) were used. Mice were allowed ad libitum food and water. For intranasal installations, mice were lightly anesthetized under 1.6-1.8% isoflurane and received a single 50 μL dose of 12.5% DE or PBS for the control group. Euthanasia of animals

was performed with 100% isoflurane overdose followed by cervical dislocation. All animals were used for the experiment, with none excluded. Mice were randomized by cage to determine saline or DE exposure. Exposures were given spaced so that euthanasia occurred at 5 hours post exposure for each mouse. Exposures received for each mouse were marked on the mouse by the doser and individual responsible for euthanasia.

Sample Extraction and Processing

Following euthanasia, an incision was made through the abdominal wall up to the diaphragm. The diaphragm was punctured and cleared away to allow the lungs to retract fully into the thoracic cavity. Another incision was made to remove the sternum and a cardiac puncture with a 23-gauge needle was used to collect approximately 500 μL of blood that was placed in K2EDTA Microtainer tubes (BD Biosciences, Franklin Lakes, NJ). Bronchoalveolar lavage fluid (BALF) was collected via three 1 mL lavages using ice cold Hanks Balanced Salt Solution (HBSS) (Cytiva, Marlborough, MA) with 0.25% of NaN_3. Left and right lungs were removed and placed in metal lysing matrix tubes (MP Biomedical, Santa Anna, CA) in 1 mL of HBSS+0.25% NaN_3 on ice. Lungs were gently mechanically dissociated utilizing a Bead Mill 24 (Fisherbrand, Waltham, MA) at 2.10 speed for 10 cycles of 15 seconds with 3 seconds rest between cycles. Resulting tissues were passed through a 70 μm filter with an additional rinse of 1 mL HBSS+0.25% NaN_3 to form a single cell suspension (SCS). To isolate bone marrow cells, femurs and tibias were placed in a 0.65 mL tube nested in a 1.5 mL Eppendorf tube and extracted via centrifugation at 12,000 x g for 30 seconds for cell collection. Bone marrow cell pellets were resuspended in HBSS+0.25% NaN_3 to form a bone marrow SCS. Lung and bone marrow SCS,

as well as BALF were centrifuged at 400 x g at 4 ºC for 8 minutes, the supernate aspirated off, and resulting cell pellets utilized for flow cytometry staining.

Flow Cytometry-mediated Analysis of Neutrophils in BALF, Lung SCS, Bone Marrow SCS, and Blood.

The flow cytometry panel was constructed using several recently published manuscripts on NET formation, neutrophil progenitor markers, and analysis of these populations across a range of tissues(29,32,39,40). All staining was performed protected from light. BALF, lung SCS, bone marrow SCS, and whole blood cell pellets were incubated for 30 minutes in Ghost Dye Red 780 (Tonbo Biosciences, San Diego CACA, 1:5000) at 4 ºC in a 96-well round bottom plate (Fisher Scientific, Waltham, MA). Two-hundred μL of flow buffer (HBSS+ 1% BSA, 0.25% NaN_3) was added and the cells were centrifuged at 400 x g for 8 minutes. Resulting supernate was decanted and cells were resuspended in 50 μL of TruStain FcX (BioLegend, San Diego, CA, 1:200) for 15 minutes at room temperature. Fifty μL of the extracellular antibody cocktail (**Supplementary Table 2.1**) including Hoechst 33342 was then added and incubated for 30 minutes at room temperature. Cells were washed and resuspended in BD Cytofix/Cytoperm (BD Biosciences, Franklin Lakes, NJ) for 30 minutes at 4 ºC. Cells were washed in BD Perm/Wash (BD Biosciences, Franklin Lakes, NJ) and then resuspended in an intracellular primary antibody cocktail (**Supplementary Table 2.1**) for 30 minutes. Cells were washed with BD Perm/Wash and then resuspended in the intracellular secondary antibody cocktail for 30 minutes. A final wash was performed and then cells were resuspended in flow buffer for analysis. Cells were acquired on a 4-laser (Violet 405 nm, Blue 488 nm, Yellow-Green 561 nm, and Red 640 nm) Cytek Auorora Flow Cytometer (Cytek Biosciences, Freemont, CA). Single color compensation

beads were utilized for spectral unmixing of fluorescent parameters and fluorescence minus ones (FMOs) were prepared for definitive gating placement (**Supplementary Figure 2.1**). The resulting data were exported and analyzed using FlowJo Version 10 (Treestar, Ashland, OR) software. Given the large number of events collected for bone marrow (averaged greater than 7 million events), bone marrow FCS files were pre-gated on "cells" then down sampled into 2 million events for each FCS file before final analysis.

Statistics

GraphPad Prism software (Version 10, La Jolla, CA) was utilized to perform ROUT outlier analysis (Q = 1%), with resulting data analyzed via a Mann-Whitney U test for between-groups comparisons if non-normally distributed. Differences between groups were considered significant if the p value ≤ 0.05. Data are represented with median ± 95% confidence interval on all figures unless otherwise noted. Power analysis was conducted to determine appropriate number of animals per sex per exposure condition.

Results

Total Band and Mature Neutrophils Increase in the Airway and Lung Following Acute Dust Extract Exposure.

To better understand the acute inflammatory response of neutrophils to inhaled dust, we utilized spectral flow cytometry to characterize and compare neutrophil populations (neutrophil progenitor, band, and mature neutrophils) in the bone marrow, circulation and airways under steady state and acute dust extract-exposed conditions. To assess changes in neutrophil populations after acute exposure of dust, we chose organic dust extracts (ODE) based on our previous observation, which showed neutrophilia in the airway as a notable pathologic feature in mice 5 hours after a single intranasal ODE instillation (36,41,42). We gave a single intranasal instillation to mice of 12.5% ODE or saline as a control group and collected bone marrow (BM), blood (BLD), lung (LNG), and bronchoalveolar lavage fluid (BALF) samples 5 hours post-instillation. Firstly, samples from saline-instilled (control) mice were used to establish and optimize flow gating to identify neutrophils in four different locations, such as BM, BLD, LNG, and BALF. We used makers for non-neutrophil lineage (CD3, CD19, B220, Ter119 hereafter referred to as Lin) and hematopoietic stem cells (CD117) to eliminate them prior to gating myeloid cells. Representative gating plots demonstrated band ($Lin^{-}/CD117^{-}/CD11b^{+}/Ly6G^{Lo}$) and mature neutrophils ($Lin^{-}/CD117^{-}/CD11b^{+}/Ly6G^{Hi}$) in the different locations based on the gating strategy in **Figure 2.1A**. The ODE group showed increased neutrophil populations in BLD and BALF, but not in BM and LNG compared to saline control group (**Figure 2.1B**). Further quantification of neutrophil proportions and counts demonstrated that the ODE group

had significantly decreased proportions of total neutrophils ($CD11b^{+}/Ly6G^{+}$) in the BM and BLD while the proportion significantly increased in LNG and BALF, compared to saline controls (**Figure 2.1C**). We also observed a similar trend with increased total neutrophil counts in LNG and BALF in ODE groups, but decreased neutrophil counts in BM. However, BLD neutrophil counts were comparable between groups (**Figure 2.1C**). When split into band ($Ly6G^{Lo}$) and mature ($Ly6G^{Hi}$) neutrophils based on Ly6G expression (43), total band neutrophils decreased in BM and BLD but drastically increased in LNG and BALF of ODE mice compared to control mice (**Figure 2.1D**). ODE exposure significantly increased mature neutrophil populations, but there were no changes in these populations in the BM or BLD (**Figure 2.1D**), suggesting that circulating neutrophils are rapidly recruited to the bronchoalveolar space and lung tissue in response to acute ODE.

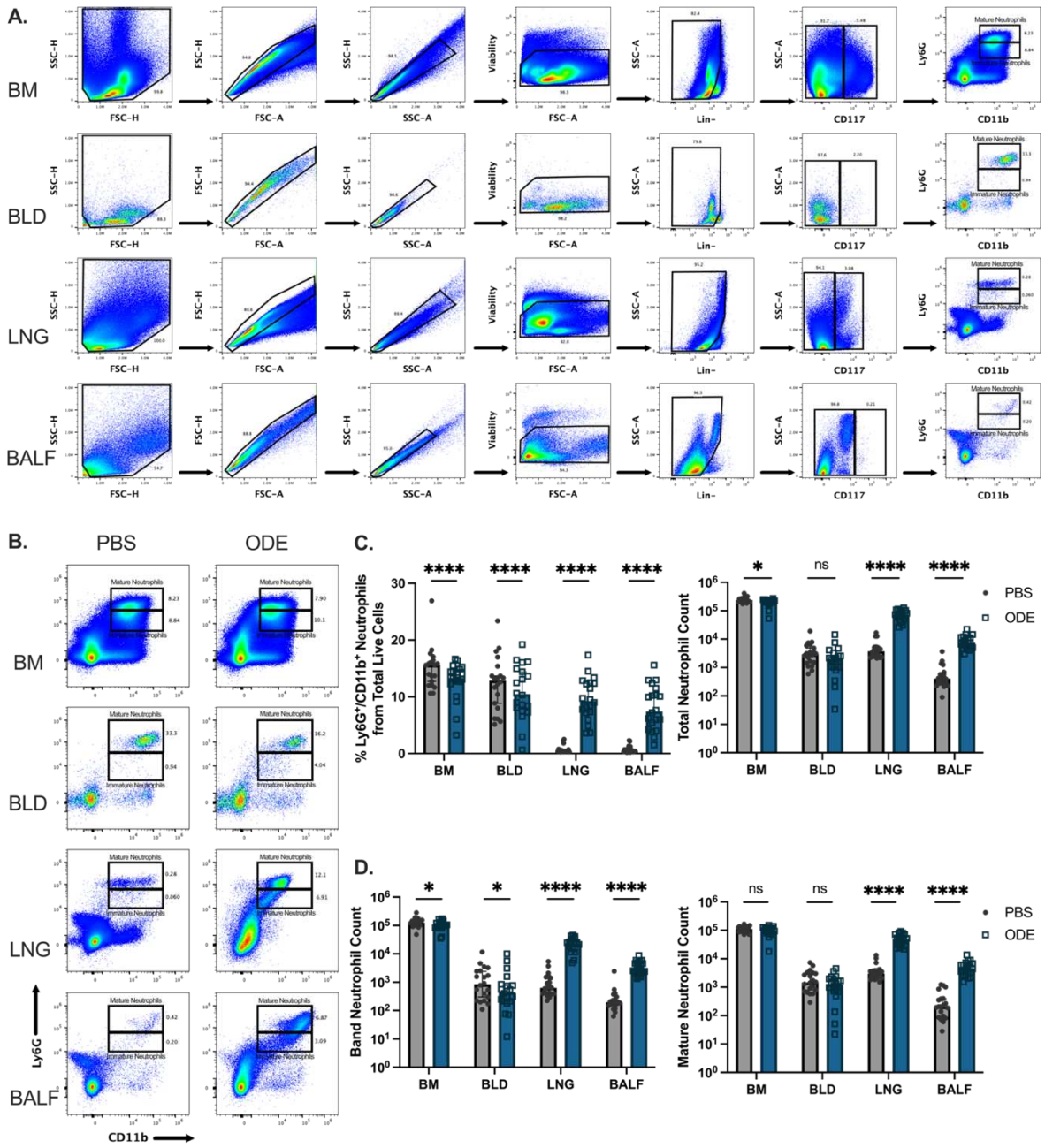

Figure 2.1. A.) Representative flowcytometry gating strategy of saline-exposed mice bone marrow (BM), blood (BLD), lung (LNG), and bronchoalveolar lavage (BALF) for total neutrophils (Live/Lin-/CD117-/Ly6G+/CD11b+). **B.)** Comparison of saline- and dust-exposed samples representative gating strategies for identification of total neutrophils and identification of band (Live/Lin-/CD117-/Ly6G^{Lo}/CD11b^{Lo}) and mature (Live/Lin-/CD117-/Ly6G^{Hi}/CD11b^{Hi}) neutrophils in BM, BLD, LNG, and BALF. **C.)** Percentage of total neutrophils from live cells in BM, BLD, LNG, and BALF in saline and dust exposed mice. Quantification of total neutrophils in BM, BLD, LNG, and BALF in saline- and dust-exposed mice. **D.)** Quantification of band and mature neutrophils in BM, BLD, LNG, and BALF in saline- and dust-exposed mice. Each dot represents a single animal. Saline (n=20) and dust (n=20) exposed mice were 50:50 male:female.

Bars are median with 95% confidence interval. Mann Whitney-U Test. *p<0.05, ****p<0.0001, ns= non-significant.

The Proportion of Neutrophil Precursors Are Altered in Bone Marrow and Blood of Dust-exposed Mice

To assess the effect of acute dust exposure on neutrophil development, we conducted a detailed analysis of neutrophil progenitors and precursors in the BM and BLD. To identify neutrophil progenitors in the BM, we analyzed the expression of CD117, CD11b, CXCR4, and Ly6G in Lin-negative cells by flow cytometry. We identified common myeloid progenitor (CMP, $Lin^-/CD117^{Hi}/CXCR4^+/CD11b^-$), granulocyte-monocyte progenitors (GMP, $Lin^-/CD117^{Hi}/CXCR4^-/CD11b^+$), Pro-Neu1 ($Lin^-/CD117^{Hi}$, $CXCR4^-/CD11b^{Lo}$), ProNeu2 ($Lin^-/CD117^{Hi}/CXCR4^-/CD11b^{Hi}$), and Pre-Neu ($Lin^-/CD117^{Mid}/CXCR4^+/CXCR2^-$) cells as neutrophil precursors in the BM of saline and ODE-exposed mice (**Figure 2.2A**). There were no changes in the proportion of neutrophil progenitors and precursors in BM between groups (**Figure 2.2B**). Interestingly, in circulation, CMP, GMP, and Pre-Neu proportions remained unchanged, but reductions in ProNeu1 and ProNeu2 proportions were observed in ODE mice (**Figure 2.2C**). These observations in ODE mice may explain the decreased band neutrophil counts in BLD.

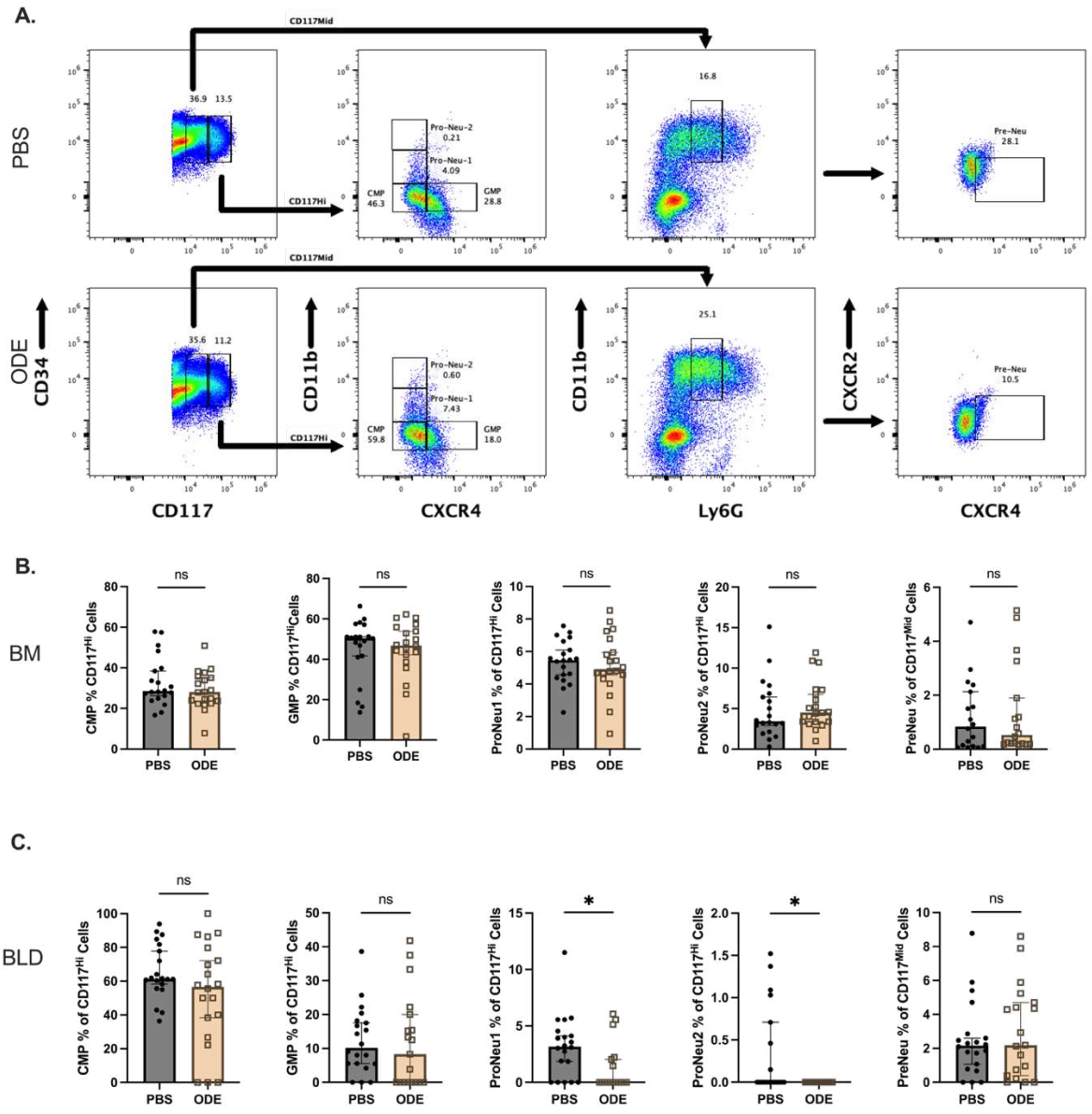

Figure 2.2: A.) Representative gating strategy of neutrophil precursor identification in bone marrow of saline- and dust-exposed mice. **B.)** Proportions of common myeloid progenitors (CMP), granulocyte myeloid progenitor (GMP), ProNeu1, ProNeu2, and PreNeu in saline- and dust-exposed mice bone marrow. **C.)** Proportions of common myeloid progenitors (CMP), granulocyte myeloid progenitor (GMP), ProNeu1, ProNeu2, and PreNeu in saline- and dust-exposed mice blood. Saline (n=20) and dust (n=20) exposed mice were 50:50 male:female. median with 95% confidence interval. Mann Whitney-U Test. *p<0.05, ns= non-significant.

Band and Mature Neutrophil Phenotypes Are Altered in Response to ODE

Next, to understand the activation state and phenotype of neutrophils at sites of neutrophil migration from blood to lung following acute ODE, we determined the expression of neutrophil-related markers (CD11b, CXCR4, CXCR2, Ly6G, CD62L, myeloperoxidase [MPO]) on band and mature neutrophils in BALF, LNG, and BLD. Neutrophil size and granularity can be indicative of functionality and activity, thus we also analyzed mean fluorescence intensity (MFI) of forward scatter (FSC) and side scatter (SSC), (40,44). When we analyzed MFI of indicated markers, band neutrophils in BALF and LNG showed increases in CD11b, Ly6G, and CXCR4 MFI in response to ODE (**Figure 2.3A, B**). ODE mice showed a markedly increased MFI of CD62L in mature and band neutrophils in LNG but exhibited no change in BALF. BALF band neutrophils decreased FSC and SSC MFI as well as CXCR2 in response to ODE (**Figure 2.3A**). Similarly, mature neutrophils in BALF and LNG increased CD11b, CD62L, and CXCR4, but decreased CXCR2 and MPO MFIs. (**Figure 2.3A, B**). LNG band neutrophils showed a significant increase in Ly6G MFI, while Ly6G and FSC MFI were decreased in mature neutrophils (**Figure 2.3B**). To determine if these phenotypic changes also occurred systemically, not just at the site of local inflammation, we further examined MFI of markers in BLD band and mature neutrophils. Only MPO MFI was statistically increased in both BLD band and mature neutrophils, but other marker MFIs were comparable between groups (**Figure 2.3C**). These data suggest that acute ODE exposure alters the expression of markers associated with neutrophil integrin-mediated movement (CD11b, Ly6G, and CD62L), chemotactic gradient response (CXCR4 and CXCR2), and morphologic changes (FSC and SSC) in band and mature neutrophils within the lower respiratory system.

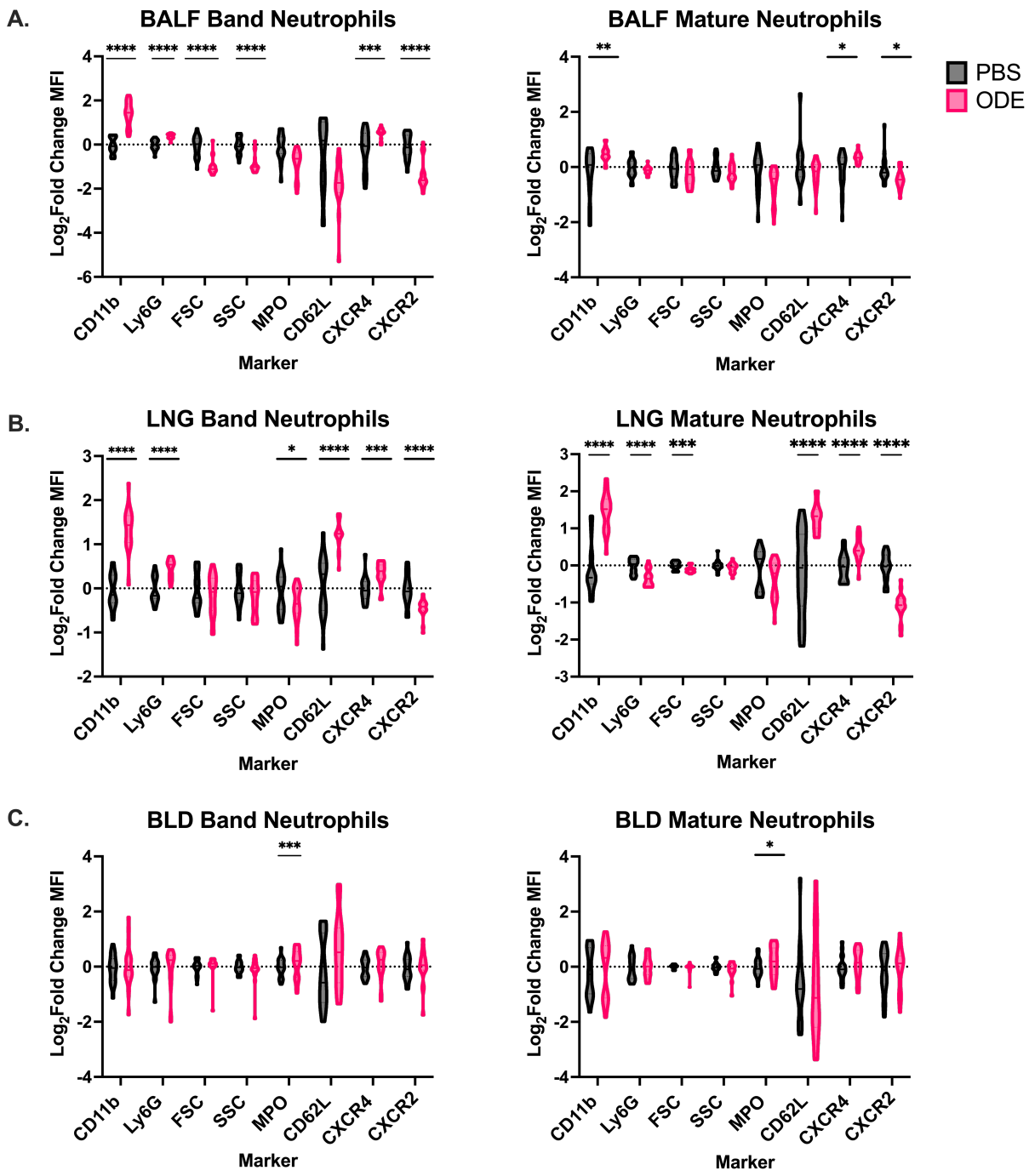

Figure 2.3: Log2 fold change of median fluorescent intensity (MFIs) of band and mature neutrophils in BALF (**A.**), lung (**B.**), and blood (**C.**) of saline- and dust-exposed animals. Saline (n=20) and dust (n=20) exposed mice were 50:50 male:female. Line is at mean. T-Test *p<0.05, **p<0.01, ***p<0.001, ****p<0.0001, no comparison shown equals non-significant.

NET-forming Band and Mature Neutrophils Increase in BALF and Lung Following Acute Dust Exposure

To better examine how acute ODE impacts neutrophils' capacity to form NETs, we included two NET markers (MPO and CitH3) in our flow panel to identify NET-forming neutrophils. We analyzed NET-forming neutrophils (MPO^{+} $CitH3^{+}$) in band and mature neutrophils from LNG (**Figure 2.4A**) and BALF samples (**Figure 2.4B**). ODE mice significantly increased the number of NET-forming neutrophils in LNG and BALF samples, regardless of neutrophil maturation status (**Figure 2.4C, D**). Interestingly, by examining the percentage of NET-forming neutrophils in LNG and BALF as a percentage of total identified band or neutrophils in LNG and BALF, it was revealed that the proportion of NET-forming neutrophils was increased in saline controls compared to acute ODE in all but NET-forming mature neutrophils in the LNG (**Figure 2.4C, D**). As the NETosis process can be lytic (full rupture of the neutrophil membrane) and/or non-lytic (maintaining membrane integrity), we utilized Hoechst 33342 signal intensity as a method to examine changes indicative of DNA presence or release of DNA from cells as previously described (**Figure 2.4E**) (32). $Hoechst^{Hi}$ indicates a more vital-like NET, $Hoechst^{Lo}$ indicates a more lytic NET, and $Hoechst^{Mid}$ is in between lytic and vital NET-release patterns. As the pre-processing gate uses a viability dye, where higher signal intensity equals non-live cells, these patterns of Hoechst intensity indicate NET-forming cells, not NET-released (cytoplast-like) cells. In the LNG, both band and mature neutrophil populations, regardless of ODE exposure, exhibited primarily $Hoechst^{Lo}$ and $Hoechst^{Mid}$ NET-forming populations (**Figure 2.4F**). In BALF samples, the $Hoechst^{Hi}$ populations dominated in NET-forming band and mature neutrophils, with a significant increase in $Hoechst^{Hi}$ cells in band neutrophils, but not mature neutrophils in the ODE group (**Figure 2.4G**). Collectively, these data demonstrate that acute dust exposure

increases both NET-forming band and mature neutrophils likely due to increased neutrophil counts due to inflammation, and that the lytic state of these neutrophils differs between BALF and LNG samples.

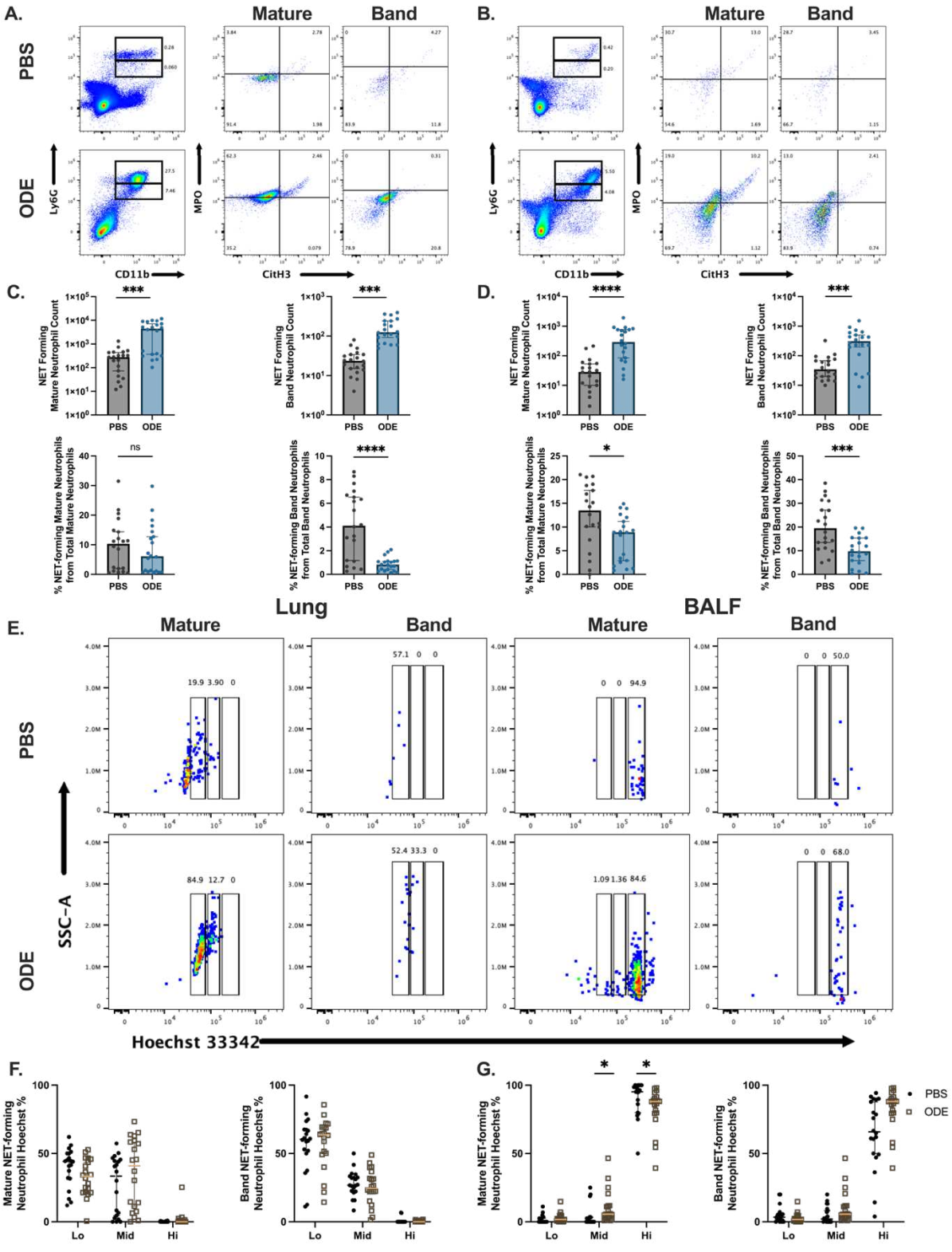

Figure 2.4: Representative gating strategy for identifying NET-forming neutrophils from parent band and mature neutrophil populations in the lung (**A.**) and BALF (**B.**) in saline- and dust-

exposed mice. Quantification of NET forming neutrophils in mature and band neutrophils in lung (**C.**) and BALF (**D.**) in saline- and dust-exposed mice. **E.**) Representative gating strategy for NET forming mature and band neutrophils from lung and BALF in saline- and dust-exposed mice. Proportions of mature and band NET forming neutrophils in lung (**F.**) and BALF (**G.**). Saline (n=20) and dust (n=20) exposed mice were 50:50 male:female. Samples on the left-most half of graphs/images are from lung and samples on the right-most half of graphs/images are from BALF. Line and bars are at the median with 95% confidence interval. Mann Whitney-U Test *$p<0.05$, ***$p<0.001$, ****$p<0.0001$, no comparison shown equals non-significant.

Discussion

Although the understanding of neutrophil diversity in chronic lung diseases is increasing and evolving, characteristics of neutrophils and their phenotypic and functional alterations during the early phase of inflammatory responses remain under active investigation. In this study, we aimed to gain more insight into changes in neutrophil populations and phenotype from neutrophil development to migration (bone marrow and blood) and at the site of acute inflammation (airway and lung tissue). Using a model of acute inhalational ODE-induced airway neutrophilia, we applied a spectral flow cytometry methodological framework to identify neutrophil progenitors, band and mature neutrophils, and identify changes in cellular phenotype within circulation and the lung following acute lung injury. Besides conventional flow cytometry for use in immunophenotyping, spectral flow cytometry presents increased panel resolution and marker selection due to the high sensitivity of detection, allowing more detailed characterization of cell types of interest. We demonstrate that neutrophil populations exhibit phenotypic alterations in both band and mature neutrophils in a location-dependent manner after acute ODE. More importantly, we validated a reliable method of identifying and quantifying lytic and non-lytic NET-forming neutrophils by flow cytometry analysis at the site of local inflammatory processes following exposure to acute ODE. Our data demonstrates that both mature and band neutrophils form NETs, and that NET-forming cell counts were significantly increased in BALF and LNG 5 hrs post instillation of ODE compared to saline vehicle-instilled mice.

Interestingly, the acute ODE instillation did not affect the capacity of neutrophils to form NETs, but this increase was due to the total increase of neutrophils following ODE for all but mature neutrophils within the LNG. Of note, we observed that the propensity for neutrophils to undergo

lytic versus non-lytic NET differed between BALF and LNG, regardless of exposure. Collectively, with a spectral flow cytometry-based analysis of neutrophils, this study provides additional insights into neutrophil dynamics and phenotypic changes during acute inflammation in the context of dust exposure.

Corroborated with the observed neutrophilia in mice 5 hours post-ODE instillation, we found increased numbers of band and mature neutrophils in LNG and BALF (13,36). This observation suggests that neutrophils extravasate sufficiently to the lung tissue and bronchoalveolar space by 5 hrs after ODE challenge. Interestingly, the decreased numbers of neutrophils in BM and BLD in response to ODE were observed only in band neutrophils, but not mature neutrophils. This suggests that acute ODE promotes recruitment of circulating mature neutrophils and likely promotes maturation of recruited band neutrophils in the lung and bronchoalveolar space rather than stimulating robust neutrophil production in the bone marrow. In an acute lung injury model utilizing LPS, neutrophil populations in the blood and lung, as well as bone marrow, followed similar kinetics at 6 hours post LPS administration as our 5-hour post instillation timepoint(45). Intriguingly, they demonstrated that GM-CSF levels peaked at 3 hours in the BALF samples, and its cognate receptor GM-CSFRα remained elevated up to 6 hrs post LPS on recruited neutrophils, with GM-CSFRβ increasing expression at 6 and 24 hours post LPS. These timepoints for neutrophil dynamics have been further corroborated in human challenge models with similar results and findings at the same 3- and 6-hour timepoints, regardless of dose(46). Another likely candidate for this potential maturation response in the lung is G-CSF. In the context of acute viral and bacterial infections within the respiratory tract, targeting G-CSF to

reduce neutrophilia has been proven successful, providing a potential means for therapeutic intervention in ODE-related disease (47).

Different capabilities of band and mature neutrophils to produce NETs have been reported, with band neutrophils traditionally exhibiting decreased ability and frequency of NET formation compared to their mature forms (48–50). Our data support the idea of niche-specific forms of NET formation, challenging the paradigm that band and mature neutrophils form NETs with different capacities. We observed lytic NET formation (characterized by decreased Hoechst signal) within LNG neutrophils regardless of maturity and ODE. In BALF samples, we observed vital NETosis, regardless of maturity state of neutrophils, with a significant reduction of vital NETosis percentage in mature neutrophils exposed to ODE. As mature neutrophils have canonically been associated with NET formation (51–53), our findings provide evidence that acute inflammatory environments induced by ODE within the bronchoalveolar space and lung tissue of the respiratory system may alter NET formation capability. This is particularly important, as non-lytic NET formation produces cytoplasts that have been demonstrated to be potent inducers of other inflammatory-based respiratory diseases such as severe asthma (54). The ability to distinguish between these forms of NET formation provides critical insight into how neutrophil cytoplasts after non-lytic NET release contribute to exacerbating the inflammatory environment present during more repetitive forms of ODE.

Our investigation into changes in neutrophil phenotype in response to acute dust exposure in the LNG, BALF, and BLD with analysis of MFIs of several markers associated with neutrophil activation yielded some interesting findings. The finding of increased MPO MFI in BLD

neutrophils could be indicative of MPO release by neutrophils at the site of ODE, and a potential priming effect on neutrophils found within the BLD post ODE. In a previous study with single ODE challenge, MPO levels in BALF were found to be significantly elevated, supporting this hypothesis (13). There was also a significant increase in lung mature and band neutrophils expression of CD62L following dust exposure. This markers' reduced expression ($CD62L^{Lo)}$ has been traditionally utilized in conjunction with $CXCR4^{Hi}$ expression to denote an aged neutrophil phenotype, and $CD62L^{Hi}$ expression to denote a younger phenotype (55). In the context of lung fibrosis, these aged neutrophils (denoted by $CD62L^{Lo}$ $CXCR4^{Hi}$) exhibit increased lung retention and an increase in inflammatory phenotype, neutrophil elastase production, and NET formation (56). $CD62L^{Lo}$ neutrophils within circulation are predictive for COPD disease severity and are associated with obstructive airway disease presence (57). In healthy BALF and blood, CD62L expression has been proposed as a marker of activation of neutrophils recruited to/extravasated into the lung, independent of inflammation (58). When CD62L expression decreases (some studies demonstrate that it is shed extracellularly and measurable in BALF) from lung neutrophils, this is indicative of an aging phenotype (57,59). Given that aging neutrophils exhibit an increased inflammatory profile and therefore propensity for exacerbating inflammatory lung disease, the ODE-induced increase in CD62L MFI within LNG, and reduction in BALF indicates that acute ODE may cause tissue-dependent modulation of this marker (60).

Previous methods to quantify NET-forming neutrophils in response to ODE have relied on the use of cytospins of BALF-derived cells followed by a differential staining and quantitative scoring of NET presence (13). Although useful, our flow cytometry method represents an advancement compared to the cytology-based NET-forming neutrophil identification in that it

allows for the characterization/phenotyping of cells and extends the ability to identify NETs to tissue samples. Within the lung, current published flow cytometry methods of analyzing NET-forming neutrophils utilize DAPI and SytoxOrange, which only measures release of DNA from neutrophils as a proxy for NET formation (28). Via the use of CitH3 and MPO as a dual positive marker, along with a viability dye and a DNA binding dye (Hoechst 33342), we ensure that NET formation identification has the molecular markers known to facilitate DNA decondensation and membrane disruption (CitH3 and MPO, respectively) (32). The multiparametric advantage of spectral flow cytometry allows for characterization of the phenotype of NET-forming neutrophils, allowing further identification of which neutrophil population is most involved in NET generation, increasing the specificity of further investigations interested in understanding NETs' contributions to inflammation and resolution processes (27).

Our study has several limitations, the first of which is that our identification of NET-forming neutrophils proceeds through a live cell gate via the use of a fixable viability dye. Given that the majority of what is known of NET formation is based on the lytic form of NETosis, our identification of NET-forming neutrophils relies on the identification of both MPO and CitH3, within a live cell (membrane intact) population. This identification strategy is meant to prevent non-specific binding of antibodies used for flow cytometry identification but does prevent the identification of NET-formed (those that have already released their NET) neutrophils. Secondly, the reagents available for CitH3 and MPO identification within murine samples are limited. Our strategy relies on a primary and fluorophore conjugated secondary for CitH3 and MPO identification, and secondary donkey-anti-goat and goat-anti-rabbit antibodies, possibly contributing to non-specific binding of these secondaries. To ensure appropriate gating, FMO's

can be used (**Supplementary Figure 2.1**), or staining can be done sequentially for the secondary antibodies. Thirdly, this study used a model of acute dust exposure, a known inducer of neutrophil airway recruitment, to examine how ODE alters maturation and activation of neutrophils following acute exposure. This acute timepoint only captures a snapshot of neutrophil response and recruitment, and future studies should examine the impact of repetitive dust exposure models and how they alter NET formation, as well as how recovery from repetitive ODE is mediated by neutrophils and their NET formation. How these neutrophil dynamics play out in repetitive exposure and recovery following ODE would offer translatable insights into the role of neutrophils in airway disease within workers repetitively exposed in agricultural and livestock occupations.

Acknowledgments and Funding

This work was supported by the NIH/NIMHD (U54MD007601) to J.P., NIH/NHLBI via R01HL158926 to T.M.N, and R01HL158926-04S1 to L.S.D.

Authorship Contribution

LSD- Conceptualization, Investigation, Data Analysis, Original Draft Writing, Review and Editing

MJLW- Investigation, Original Draft Writing, Review and Editing

TMN- Project Administration and Overview, Review and Editing

JP- Conceptualization, - Project Administration and Overview, Review and Editing

References

1. Nathan C. Neutrophils and immunity: challenges and opportunities. *Nat Rev Immunol* (2006) 6:173–82. doi: 10.1038/nri1785
2. Nauseef WM, Borregaard N. Neutrophils at work. *Nat Immunol* (2014) 15:602–11. doi: 10.1038/ni.2921
3. de Bont CM, Eerden N, Boelens WC, Pruijn GJM. Neutrophil proteases degrade autoepitopes of NET-associated proteins. *Clin Exp Immunol* (2019) 199:1–8. doi: 10.1111/cei.13392
4. Grommes J, Soehnlein O. Contribution of Neutrophils to Acute Lung Injury. *Molecular Medicine* (2011) 17:293–307. doi: 10.2119/molmed.2010.00138
5. Jasper AE, McIver WJ, Sapey E, Walton GM. Understanding the role of neutrophils in chronic inflammatory airway disease. *F1000Res* (2019) 8: doi: 10.12688/f1000research.18411.1
6. Tucker SL, Sarr D, Rada B. Neutrophil extracellular traps are present in the airways of ENaC-overexpressing mice with cystic fibrosis-like lung disease. *BMC Immunol* (2021) 22:7. doi: 10.1186/s12865-021-00397-w
7. Chen J, Wang T, Li X, Gao L, Wang K, Cheng M, Zeng Z, Chen L, Shen Y, Wen F. DNA of neutrophil extracellular traps promote NF-κB-dependent autoimmunity via cGAS/TLR9 in chronic obstructive pulmonary disease. *Signal Transduct Target Ther* (2024) 9:163. doi: 10.1038/s41392-024-01881-6
8. Porto BN, Stein RT. Neutrophil Extracellular Traps in Pulmonary Diseases: Too Much of a Good Thing? *Front Immunol* (2016) 7: doi: 10.3389/fimmu.2016.00311
9. Gray RD. NETs in pneumonia: is just enough the right amount? *European Respiratory Journal* (2018) 51:1800619. doi: 10.1183/13993003.00619-2018
10. Nappi F, Bellomo F, Avtaar Singh SS. Insights into the Role of Neutrophils and Neutrophil Extracellular Traps in Causing Cardiovascular Complications in Patients with COVID-19: A Systematic Review. *J Clin Med* (2022) 11: doi: 10.3390/jcm11092460
11. Dalan R. Metformin, neutrophils and COVID-19 infection. *Diabetes Res Clin Pract* (2020) 164:108230. doi: 10.1016/j.diabres.2020.108230
12. Pilsczek FH, Salina D, Poon KKH, Fahey C, Yipp BG, Sibley CD, Robbins SM, Green FHY, Surette MG, Sugai M, et al. A Novel Mechanism of Rapid Nuclear Neutrophil Extracellular Trap Formation in Response to *Staphylococcus aureus*. *The Journal of Immunology* (2010) 185:7413–7425. doi: 10.4049/jimmunol.1000675
13. Dominguez EC, Heires AJ, Pavlik J, Larsen TD, Guardado S, Sisson JH, Baack ML, Romberger DJ, Nordgren TM. A High Docosahexaenoic Acid Diet Alters the Lung Inflammatory Response to Acute Dust Exposure. *Nutrients* (2020) 12:2334. doi: 10.3390/nu12082334
14. Nordgren TM, Bailey KL. Pulmonary health effects of agriculture. *Curr Opin Pulm Med* (2016) 22:144–149. doi: 10.1097/MCP.0000000000000247
15. Nordgren TM, Charavaryamath C. Agriculture Occupational Exposures and Factors Affecting Health Effects. *Curr Allergy Asthma Rep* (2018) 18:65. doi: 10.1007/s11882-018-0820-8
16. Heires AJ, Samuelson D, Villageliu D, Nordgren TM, Romberger DJ. Agricultural dust derived bacterial extracellular vesicle mediated inflammation is attenuated by DHA. *Sci Rep* (2023) 13:2767. doi: 10.1038/s41598-023-29781-9
17. Poole JA, Wyatt TA, Von Essen SG, Hervert J, Parks C, Mathisen T, Romberger DJ. Repeat organic dust exposure–induced monocyte inflammation is associated with protein kinase C

activity. *Journal of Allergy and Clinical Immunology* (2007) 120:366–373. doi: 10.1016/j.jaci.2007.04.033
18. Poole JA, Nordgren TM, Heires AJ, Nelson AJ, Katafiasz D, Bailey KL, Romberger DJ. Amphiregulin modulates murine lung recovery and fibroblast function following exposure to agriculture organic dust. *American Journal of Physiology-Lung Cellular and Molecular Physiology* (2020) 318:L180–L191. doi: 10.1152/ajplung.00039.2019
19. Warren K, Wyatt T, Romberger D, Ailts I, West W, Nelson A, Nordgren T, Staab E, Heires A, Poole J. Post-Injury and Resolution Response to Repetitive Inhalation Exposure to Agricultural Organic Dust in Mice. *Safety* (2017) 3:10. doi: 10.3390/safety3010010
20. Jo A, Kim DW. Neutrophil Extracellular Traps in Airway Diseases: Pathological Roles and Therapeutic Implications. *Int J Mol Sci* (2023) 24: doi: 10.3390/ijms24055034
21. Pan T, Lee JW. A crucial role of neutrophil extracellular traps in pulmonary infectious diseases. *Chinese Medical Journal Pulmonary and Critical Care Medicine* (2024) 2:34–41. doi: 10.1016/j.pccm.2023.10.004
22. Mettelman RC, Allen EK, Thomas PG. Mucosal immune responses to infection and vaccination in the respiratory tract. *Immunity* (2022) 55:749–780. doi: 10.1016/j.immuni.2022.04.013
23. Hewitt RJ, Lloyd CM. Regulation of immune responses by the airway epithelial cell landscape. *Nat Rev Immunol* (2021) 21:347–362. doi: 10.1038/s41577-020-00477-9
24. Chamardani TM, Amiritavassoli S. Inhibition of NETosis for treatment purposes: friend or foe? *Mol Cell Biochem* (2022) 477:673–688. doi: 10.1007/s11010-021-04315-x
25. Stoimenou M, Tzoros G, Skendros P, Chrysanthopoulou A. Methods for the Assessment of NET Formation: From Neutrophil Biology to Translational Research. *Int J Mol Sci* (2022) 23: doi: 10.3390/ijms232415823
26. Masuda S, Shimizu S, Matsuo J, Nishibata Y, Kusunoki Y, Hattanda F, Shida H, Nakazawa D, Tomaru U, Atsumi T, et al. Measurement of NET formation in vitro and in vivo by flow cytometry. *Cytometry A* (2017) 91:822–829. doi: 10.1002/cyto.a.23169
27. Schneck E, Mallek F, Schiederich J, Kramer E, Markmann M, Hecker M, Sommer N, Weissmann N, Pak O, Michel G, et al. Flow Cytometry-Based Quantification of Neutrophil Extracellular Traps Shows an Association with Hypercoagulation in Septic Shock and Hypocoagulation in Postsurgical Systemic Inflammation-A Proof-of-Concept Study. *J Clin Med* (2020) 9: doi: 10.3390/jcm9010174
28. Zharkova O, Tay SH, Lee HY, Shubhita T, Ong WY, Lateef A, MacAry PA, Lim LHK, Connolly JE, Fairhurst A. A Flow Cytometry-Based Assay for High-Throughput Detection and Quantification of Neutrophil Extracellular Traps in Mixed Cell Populations. *Cytometry Part A* (2019) 95:268–278. doi: 10.1002/cyto.a.23672
29. McGill CJ, Lu RJ, Benayoun BA. Protocol for analysis of mouse neutrophil NETosis by flow cytometry. *STAR Protoc* (2021) 2:100948. doi: 10.1016/j.xpro.2021.100948
30. Cossarizza A, Chang H, Radbruch A, Abrignani S, Addo R, Akdis M, Andrä I, Andreata F, Annunziato F, Arranz E, et al. Guidelines for the use of flow cytometry and cell sorting in immunological studies (third edition). *Eur J Immunol* (2021) 51:2708–3145. doi: 10.1002/eji.202170126
31. Barbu EA, Dominical VM, Mendelsohn L, Thein SL. Detection and Quantification of Histone H4 Citrullination in Early NETosis With Image Flow Cytometry Version 4. *Front Immunol* (2020) 11: doi: 10.3389/fimmu.2020.01335

32. Zhu YP, Speir M, Tan Z, Lee JC, Nowell CJ, Chen AA, Amatullah H, Salinger AJ, Huang CJ, Wu G, et al. NET formation is a default epigenetic program controlled by PAD4 in apoptotic neutrophils. *Sci Adv* (2023) 9: doi: 10.1126/sciadv.adj1397
33. Romberger DJ, Bodlak V, Von Essen SG, Mathisen T, Wyatt TA. Hog barn dust extract stimulates IL-8 and IL-6 release in human bronchial epithelial cells via PKC activation. *J Appl Physiol* (2002) 93:289–296. doi: 10.1152/japplphysiol.00815.2001
34. Ulu A, Velazquez J V., Burr A, Sveiven SN, Yang J, Bravo C, Hammock BD, Nordgren TM. Sex-Specific Differences in Resolution of Airway Inflammation in Fat-1 Transgenic Mice Following Repetitive Agricultural Dust Exposure. *Front Pharmacol* (2022) 12: doi: 10.3389/fphar.2021.785193
35. Nordgren TM, Heires AJ, Bailey KL, Katafiasz DM, Toews ML, Wichman CS, Romberger DJ. Docosahexaenoic acid enhances amphiregulin-mediated bronchial epithelial cell repair processes following organic dust exposure. *American Journal of Physiology-Lung Cellular and Molecular Physiology* (2018) 314:L421–L431. doi: 10.1152/ajplung.00273.2017
36. Nordgren TM, Bauer CD, Heires AJ, Poole JA, Wyatt TA, West WW, Romberger DJ. Maresin-1 reduces airway inflammation associated with acute and repetitive exposures to organic dust. *Translational Research* (2015) 166:57–69. doi: 10.1016/j.trsl.2015.01.001
37. Ulu A, Sveiven S, Bilg A, Velazquez J V., Diaz M, Mukherjee M, Yuil-Valdes AG, Kota S, Burr A, Najera A, et al. IL-22 regulates inflammatory responses to agricultural dust-induced airway inflammation. *Toxicol Appl Pharmacol* (2022) 446:116044. doi: 10.1016/j.taap.2022.116044
38. Ulu A, Burr A, Heires AJ, Pavlik J, Larsen T, Perez PA, Bravo C, DiPatrizio N V., Baack M, Romberger DJ, et al. A high docosahexaenoic acid diet alters lung inflammation and recovery following repetitive exposure to aqueous organic dust extracts. *Journal of Nutritional Biochemistry* (2021) 97: doi: 10.1016/j.jnutbio.2021.108797
39. Carnevale S, Di Ceglie I, Grieco G, Rigatelli A, Bonavita E, Jaillon S. Neutrophil diversity in inflammation and cancer. *Front Immunol* (2023) 14: doi: 10.3389/fimmu.2023.1180810
40. Evrard M, Kwok IWH, Chong SZ, Teng KWW, Becht E, Chen J, Sieow JL, Penny HL, Ching GC, Devi S, et al. Developmental Analysis of Bone Marrow Neutrophils Reveals Populations Specialized in Expansion, Trafficking, and Effector Functions. *Immunity* (2018) 48:364-379.e8. doi: 10.1016/j.immuni.2018.02.002
41. Poole JA, Dooley GP, Saito R, Burrell AM, Bailey KL, Romberger DJ, Mehaffy J, Reynolds SJ. Muramic Acid, Endotoxin, 3-Hydroxy Fatty Acids, and Ergosterol Content Explain Monocyte and Epithelial Cell Inflammatory Responses to Agricultural Dusts. *J Toxicol Environ Health A* (2010) 73:684–700. doi: 10.1080/15287390903578539
42. Poole JA, Wyatt TA, Oldenburg PJ, Elliott MK, West WW, Sisson JH, Von Essen SG, Romberger DJ. Intranasal organic dust exposure-induced airway adaptation response marked by persistent lung inflammation and pathology in mice. *American Journal of Physiology-Lung Cellular and Molecular Physiology* (2009) 296:L1085–L1095. doi: 10.1152/ajplung.90622.2008
43. Grieshaber-Bouyer R, Nigrovic PA. Neutrophil Heterogeneity as Therapeutic Opportunity in Immune-Mediated Disease. *Front Immunol* (2019) 10:346. doi: 10.3389/fimmu.2019.00346
44. Adrover JM, Nicolás-Ávila JA, Hidalgo A. Aging: A Temporal Dimension for Neutrophils. *Trends Immunol* (2016) 37:334–345. doi: 10.1016/j.it.2016.03.005
45. De Alessandris S, Ferguson GJ, Dodd AJ, Juss JK, Devaprasad A, Piper S, Wyatt O, Killick H, Corkill DJ, Cohen ES, et al. Neutrophil GM-CSF receptor dynamics in acute lung injury. *J Leukoc Biol* (2019) 105:1183–1194. doi: 10.1002/JLB.3MA0918-347R

46. Mulvanny A, Jackson N, Pattwell C, Wolosianka S, Southworth T, Singh D. The dose response of inhaled LPS challenge in healthy subjects. *Eur J Inflamm* (2018) 16: doi: 10.1177/2058739218784820
47. Wang H, Aloe C, Wilson N, Bozinovski S. G-CSFR antagonism reduces neutrophilic inflammation during pneumococcal and influenza respiratory infections without compromising clearance. *Sci Rep* (2019) 9:17732. doi: 10.1038/s41598-019-54053-w
48. Martinelli S, Urosevic M, Daryadel A, Oberholzer PA, Baumann C, Fey MF, Dummer R, Simon H-U, Yousefi S. Induction of Genes Mediating Interferon-dependent Extracellular Trap Formation during Neutrophil Differentiation. *Journal of Biological Chemistry* (2004) 279:44123–44132. doi: 10.1074/jbc.M405883200
49. Amulic B, Knackstedt SL, Abu Abed U, Deigendesch N, Harbort CJ, Caffrey BE, Brinkmann V, Heppner FL, Hinds PW, Zychlinsky A. Cell-Cycle Proteins Control Production of Neutrophil Extracellular Traps. *Dev Cell* (2017) 43:449-462.e5. doi: 10.1016/j.devcel.2017.10.013
50. Qu J, Jin J, Zhang M, Ng LG. Neutrophil diversity and plasticity: Implications for organ transplantation. *Cell Mol Immunol* (2023) 20:993–1001. doi: 10.1038/s41423-023-01058-1
51. Ganesh K, Joshi MB. Neutrophil sub-types in maintaining immune homeostasis during steady state, infections and sterile inflammation. *Inflammation Research* (2023) 72:1175–1192. doi: 10.1007/s00011-023-01737-9
52. Adrover JM, del Fresno C, Crainiciuc G, Cuartero MI, Casanova-Acebes M, Weiss LA, Huerga-Encabo H, Silvestre-Roig C, Rossaint J, Cossío I, et al. A Neutrophil Timer Coordinates Immune Defense and Vascular Protection. *Immunity* (2019) 50:390-402.e10. doi: 10.1016/j.immuni.2019.01.002
53. Drifte G, Dunn-Siegrist I, Tissières P, Pugin J. Innate Immune Functions of Immature Neutrophils in Patients With Sepsis and Severe Systemic Inflammatory Response Syndrome*. *Crit Care Med* (2013) 41:820–832. doi: 10.1097/CCM.0b013e318274647d
54. Krishnamoorthy N, Douda DN, Brüggemann TR, Ricklefs I, Duvall MG, Abdulnour R-EE, Martinod K, Tavares L, Wang X, Cernadas M, et al. Neutrophil cytoplasts induce TH17 differentiation and skew inflammation toward neutrophilia in severe asthma. *Sci Immunol* (2018) 3: doi: 10.1126/sciimmunol.aao4747
55. Zhang D, Chen G, Manwani D, Mortha A, Xu C, Faith JJ, Burk RD, Kunisaki Y, Jang J-E, Scheiermann C, et al. Neutrophil ageing is regulated by the microbiome. *Nature* (2015) 525:528–32. doi: 10.1038/nature15367
56. Warheit-Niemi HI, Huizinga GP, Edwards SJ, Wang Y, Murray SK, O'Dwyer DN, Moore BB. Fibrotic Lung Disease Alters Neutrophil Trafficking and Promotes Neutrophil Elastase and Extracellular Trap Release. *Immunohorizons* (2022) 6:817–834. doi: 10.4049/immunohorizons.2200083
57. Lokwani R, Wark P, Baines K, Barker D, Fricker M, Simpson J. Circulatory neutrophils in COPD feature downregulated CD62L expression in comparison with asthma and healthy participants. *Allergy and immunology*. European Respiratory Society (2019). p. PA4384 doi: 10.1183/13993003.congress-2019.PA4384
58. Fortunati E, Kazemier KM, Grutters JC, Koenderman L, Van den Bosch van JMM. Human neutrophils switch to an activated phenotype after homing to the lung irrespective of inflammatory disease. *Clin Exp Immunol* (2009) 155:559–66. doi: 10.1111/j.1365-2249.2008.03791.x

59. Lokwani R, Wark PA, Baines KJ, Fricker M, Barker D, Simpson JL. Blood Neutrophils In COPD But Not Asthma Exhibit A Primed Phenotype With Downregulated CD62L Expression. *Int J Chron Obstruct Pulmon Dis* (2019) 14:2517–2525. doi: 10.2147/COPD.S222486
60. Williams AE, Chambers RC. The mercurial nature of neutrophils: still an enigma in ARDS? *Am J Physiol Lung Cell Mol Physiol* (2014) 306:L217-30. doi: 10.1152/ajplung.00311.2013

Chapter 3

Spectral Immune Cell Profiling Reveals Modulations in Immune Cell Response to Repetitive Inhaled Organic Dust Exposure in a High Omega-3 Fatty Acid Mouse Model[2]

[2] Manuscript accepted for publication in Lipids in Health and Disease 06/24/25

Summary

Exposure of the lungs to particulate matter (ie. dust, wildfire smoke, air pollution) places individuals at an increased risk for developing chronic respiratory disease. Recent work has demonstrated the efficacy of omega-3 fatty acids and their metabolites in promoting the resolution of prolonged inflammation, however a comprehensive understanding of how omega-3 fatty acid balance impacts immune cell populations and crosstalk remains undescribed. We developed a 17-marker, 14-color spectral flow cytometry method to characterize the immunophenotypic changes in the bronchoalveolar space and lung tissue following 14 days of repetitive organic dust exposure or PBS vehicle. The populations of immune cells were compared in C57BL/6 (WT) and a transgenic model of increased omega-3 fatty acid (Fat-1) mice. Histopathologic examination revealed no difference between WT and Fat-1 mice at baseline or following organic dust exposure. Immune cell makeup within the bronchoalveolar space and lung tissue differed between WT and Fat-1 mice, with and without organic dust exposure. Fat-1 mice demonstrated a monocyte-dominant response compared to WT in both the airway and the lung tissue. Intriguingly, this monocyte-dominance was more prominent in female Fat-1 mice in the lung tissue and male Fat-1 mice in the airway. This suggests that monocyte populations are a dominant cell type that contributes to omega-3 fatty acid metabolite-linked resolution to organic dust exposure within the lung, and that sex-dependent factors in this immune response are pivotal to consider in therapeutic strategies aimed at mitigating disease.

Introduction

Inhalation of organic dusts is a type of particulate matter (PM) exposure common to workers in agricultural production or livestock facility operations (1). Repetitive organic dust exposure (ODE) is linked to an increased incidence of chronic respiratory diseases, such as asthma and chronic obstructive pulmonary disease (COPD) (2,3). Current therapeutic strategies for chronic respiratory disease mitigation rely on preventing inflammation-promoting molecules or symptom management of bronchoconstriction, but such treatments are ineffective at promoting tissue recovery and damage reversal. Novel treatments that limit persistent inflammatory processes and promote resolution towards tissue recovery are critically needed.

Landmark discoveries three decades ago provided the first description of molecules intimately involved in the inflammatory process (4,5), including metabolites of omega-6 (n-6) and omega-3 (n-3) poly-unsaturated fatty acids (PUFAs) (6). Conversion of the n-6 arachidonic acid (AA) in early inflammation produces pro-inflammatory prostaglandins and leukotrienes, while metabolism via LOX enzymes of n-3 docosahexaenoic acid (DHA) and eicosopentanoic acid (EPA) creates potent pro-resolution-skewing metabolites (7). These metabolites are collectively referred to as specialized pro-resolving lipid mediators (SPMs) and include resolvins, protectins, and maresins which have demonstrated roles in promoting a pro-resolution state within individual immune cell populations and in disease contexts (8). A balance of these n-3 and n-6 precursor PUFAs in diet is recommended at a 1:1 ratio, however the typical westernized diet contains ratios of 24:1 to 60:1 n-6:n-3 PUFAs, promoting an imbalance of SPM generation (9). Such an imbalance has a detrimental impact on health, predisposing individuals to gut microbe dysbiosis, cancer development, and an increased risk of metabolic-based disease (10). Increasing

the ratio of n-6:n-3 PUFAs towards the optimal 1:1 ratio has previously shown efficacy in decreasing ODE-induced lung pathology and promoting recovery (11–15).

The last two decades have seen an increasing interest in understanding the immunologic drivers of ODE lung injury, including our research group's investigations exploring the use of SPMs to ameliorate ODE-induced inflammation (16–18). Previous studies have demonstrated that mice exposed to a single dose (1 intranasal installation) or a 3-week repetitive regimen (15 intranasal instillations) of ODE and treated with the SPM Maresin-1 (MaR1) demonstrated decreased inflammatory cytokines (TNF, IL-6, and CXCL1) and neutrophils within bronchoalveolar lavage fluid (BALF) (18). Interestingly, this same study observed increases in macrophage populations in the ODE + MaR1 groups. Subsequent studies have revealed that this SPM-induced macrophage population increase is reproducible in mouse models with increased n-3 FA via dietary and genetic manipulation methodologies (12,15).

Our understanding of the lungs' cell-mediated immune response to ODE has historically focused on differential population counts and identification of macrophages, neutrophils, and lymphocytes isolated from BALF via cytocentrifugation (14,19–22).This strategy has not allowed insight into identifying specific immune cells such as innate lymphoid cells (ILCs), differential lymphoid cells, and populations key to macrophage renewal such as monocytes. Since their discovery, ILCs (particularly ILC3s) are increasingly recognized as modulators of immunity at mucosal barrier surfaces through cytokine secretion (23–26). Monocytes are classically known as circulating macrophage and dendritic cell precursors, migrating to areas of ongoing tissue inflammation and differentiating via soluble mediator stimuli (27,28). Alveolar

macrophages (AM) and resident tissue macrophages (RTM) within the lung are primarily maintained via continuous self-renewal but require replenishment from circulating monocytes during acute and chronic insults (29). This recruitment is primarily mediated by monocyte chemoattractant protein-1 (MCP-1) and its' cognate receptor CCR2 (30). As such, identifying and understanding how these key immune cell populations are altered during ODE is crucial to developing an enhanced understanding of ODE-induced pathogenesis.

Our investigation aimed to understand the impact of increased omega-3 fatty acids on the comprehensive immune cell populations following repetitive organic dust exposure to better understand what cellular players are altered in the "loading" phase before resolution to inflammation occurs. We utilized C57BL/6 (WT) and a transgenic model of balanced n-6:n-3 fatty acid ratios (Fat-1) and demonstrated that the previous observations of a neutrophilic response to ODE hold true, but that monocyte populations, particularly within Fat-1 mice, are significantly increased in BALF and lung tissue compared to WT mice, both at baseline and following ODE. ILC populations were identified for the first time in this model of ODE and were particularly altered at baseline and following exposure in Fat-1 mice. Intriguingly, the monocyte populations were distinguished in a sex- and tissue location-dependent manner. Collectively, this study provides insight into the cellular diversity that omega-3 fatty acids induce to promote a resolution-like response following chronic organic dust inhalation.

Methods

Preparation of Dust Extracts

Dusts were collected as previously described from swine confinement facilities in the Midwest, United States, and stored at -20 ºC until preparation. Aqueous dust extracts were prepared as previously described (31); in brief, 5 g of dust was mixed into 50 mL of Hanks Balanced Salt Solution (HBSS) (HyClone, Logan, UT) at room temperature for 1 hour. The resulting extract was centrifuged at 2500 x g for 20 minutes at 4 ºC. Supernates were transferred to new tubes, recentrifuged at 2500 x g for 20 minutes at 4 ºC, and subsequent supernates were sterile filtered with a 0.22 um filter to produce 100% dust extract (DE). Aliquots were stored at -20 ºC until use. Formulations of 12.5% DE were prepared for animal installations by diluting 100% DE with phosphate buffered saline (PBS) (Fisher Scientific, Waltham, MA). A dose of 12.5% DE has been previously demonstrated as an appropriate dose for generating substantial lung inflammation with a single instillation and promoting histopathological markers of lung disease with repetitive exposure, while not leading to significant weight loss, lethargy, or other moribund phenotypes (15,18–20,31–33).

Animal Husbandry and Instillations

Animal protocols were reviewed and approved by the Institutional Animal Care and Use Committee at Colorado State University (Protocol #2887). 12 to 16-week-old C57BL/6 (WT) and Fat-1 transgenic mice [C57BL/6-Tg (CAG-*Fat-1*)1Jxk/J] (Jackson Labs, Bar Harbor, ME) were used, and a breeding colony of Fat-1 mice was established from an existing colony at the University of California Riverside. Breeding pairs were Fat-1 x Fat-1 while age- and sex-matched WT mice were ordered from Jackson Laboratories. Pups produced by the breeding

colony were genotyped by TransnetYX for Fat-1 transgene confirmation. Mice were allowed *ad libitum* food and water. For intranasal instillations, mice were lightly anesthetized under 1.6-2.2% isoflurane and received 50 uL of the 12.5% DE or PBS vehicle control for 3 weeks (total of 14 installations, provided 5 days/week).

Lung Extraction and Histopathology

Mice were euthanized via isoflurane overdose followed by a cervical dislocation 5 hours following the final installation. A cannula was inserted into the trachea and bronchoalveolar lavage fluid (BALF) was collected with three washes of 1 mL of ice cold HBSS (HyClone, Logan, UT) with 0.25% sodium azide (Millipore Sigma, Burlington, MA). The first wash was aliquoted into a separate tube while the 2nd and 3rd washes were combined. All washes were centrifuged and wash 1 supernate was aliquoted for downstream cytokine analysis via ELISA, while wash 2+3 supernate was discarded. Cells from all three fractions were combined for subsequent flow cytometry applications (detailed below). The left lung was tied off, separated, and utilized for flow cytometry assays, while the remaining right lobe was extracted, inflated with 10% neutral buffered formalin (NBF) (Cancer Diagnostics Inc, Durham, NC), and hung under 20 cm of pressure overnight while bathed in 10% NBF. The fixed right lung was inserted into tissue cassettes and sent to the Colorado State University Veterinary Diagnostic Laboratory Experimental Pathology Facility (EPF) for paraffin embedding and slicing. Resulting slides were stained following deparaffinization and a graded ethanol rehydration with hematoxylin and eosin (H&E).

Flow Cytometry Analysis of BALF and Lung Single Cell Suspensions

The two tubes of BALF (Wash 1 and Wash 2+3) were centrifuged at 4 ºC at 350 x g for 8 minutes. Wash 1 supernate was removed and stored at –20 °C for downstream cytokine analysis. Wash 2+3 supernate was aspirated off and the resulting cell pellets of wash 1 and 2+3 combined into a single tube.

Left lung lobes were gently homogenized utilizing a Bead Mill 24 (Fisherbrand, Waltham, MA) with metal bead lysing matrix tubes (2.25 speed, 4 cycles, 15 second cycle, 3 second rest) (MP Biomedical, Santa Anna, CA) and then strained through a 70 µm filter with 10, 1 mL rinses of HBSS + 0.25% sodium azide to create a single cell suspension (SCS). The SCS was centrifuged at 350 x g for 8 minutes at 4 ºC. The resulting supernate fraction was discarded, and the cell pellet processed along with the BALF cell pellet.

Cell pellets from BALF and SCS were incubated for 30 minutes in Ghost Dye Red 780 (Cytek, 1:4000) at 4 ºC protected from light. One mL of flow buffer (PBS+ 1% BSA, 0.25% sodium azide) was added, and the cells were centrifuged at 350 x g for 8 minutes. Resulting supernate was aspirated off and cells were resuspended in TruStain FcX (BioLegend, San Diego, CA, 1:200) for 15 minutes at room temperature, protected from light. Appropriate volumes of fluorophore antibody cocktail (**Supplementary Table 3.1**) were then added and incubated for 30 minutes at room temperature protected from light. Cells were washed and resuspended in BD Cytofix/Cytoperm (BD Technologies, East Rutherford, NJ) for 30 minutes at 4 ºC protected from light. Cells were washed in BD Perm/Wash (BD Biosciences, Franklin Lakes, NJ) and then resuspended for analysis in flow buffer.

Stained cells were acquired on a 4 Laser Cytek Aurora Spectral Flow Cytometer (Cytek Biosciences, Fremont, CA). Single color compensation beads were utilized for spectral unmixing parameters and fluorescent minus ones (FMOs) were utilized for appropriate gate placement. Resulting data were analyzed using FlowJo Version 10 (Treestar, Ashland, OR) software.

Measurement of BALF Cytokines via ELISA

BALF cytokines were measured using DuoSet ELISA (R&D Systems, Minneapolis, MN) kits according to manufacturer protocol for MCP-1 and CX_3CL1. Assays were conducted in 96-well half-area plates (Greiner Biotech, Kremunster, Austria) and read on a FLUOStar Omega (BMG Labtech, Ortenberg, Germany) plate reader at 450 nm. Resulting optical density (OD) data were analyzed in the Omega software (Version 5.70 R2) and values calculated via a four-point standard curve.

Right Lung Lobe Pathology Scoring

Slides were blinded and imaged at 20X magnification using an Olympus IX71 microscope (Evident, Waltham, MA, USA) with Retiga 2000R (Qimaging, Surrey, BC, Canada) and Qcolor3 (Evident, Waltham, MA, USA) cameras. Images were imported and visualized in QuPath for pathological scoring (34). H&E-stained right lung lobe sections were scored using a modified version of an established scoring criteria published previously (**Supplementary Table 3.2**) (35). All slides remained blinded and then 4 parameters were scored: the amount of immune cell aggregates, the presence of perivascular and peribronchiolar inflammation, alveolar space cellularity, and metaplasia of goblet cells. A mean pathology score consisted of the averaged scores in all 4 parameters.

Targeted RNA Expression of Left Lung Lobe via NanoString

Freshly isolated mouse lungs were homogenized in 1 mL of Trizol (Invitrogen, Carlsbad, CA) via a Bead Mill 24 (Fisherbrand, Waltham, MA) with metal bead lysing matrix tubes (5 speed, 4 cycles, 15 second cycle, 3 second rest). Extraction of RNA was performed as per manufacturer guidelines and resulting RNA placed on ice and sent to the Experimental Pathology Facility at Colorado State University for further processing. RNA purity was determined using 260/280 ratio (Agilent Bio Tek TAKE 3). Quality and DV200 concentration of the RNA was evaluated using the Agilent 4200 TapeStation System. The custom code set (XT_PGX_MmV2_Myeloid) was hybridized with 100 ng RNA during an overnight incubation at 65 ºC and processed on the NanoString nCounter® FLEX Analysis System. Each nCounter® XT panel included 15 housekeeping genes, 6 positive control probes, and 8 negative control probes. All samples that passed QC flags were combined and normalized using nSolver 4.0 (NanoString Technologies, Seattle, WA, United States) with recommended software parameters. Housekeeping genes for normalization were picked based on a lack of differential expression between experimental groups of genotype, sex, and exposure. The mouse myeloid innate immunity panel included 741 gene targets and utilized seven as housekeeping genes for count normalization (*Alas1, Edc3, Pol1rb1, Rpl19, Sap130, Sdha*). Raw and normalized NanoString data are deposited to GEO as GSE255787.

Analysis of Nanostring Gene Expression Data via Rosalind

Data were analyzed by ROSALIND® (https://rosalind.bio/), with a HyperScale architecture developed by ROSALIND, Inc. (San Diego, CA). Read distribution percentages, violin plots, identity heatmaps, and sample MDS plots were generated as part of the QC step. The limma R

library was used to calculate fold changes and p-values and perform optional covariate correction. Clustering of genes for the final heatmap of differentially expressed genes was done using the PAM (Partitioning Around Medoids) method using the fpc R library that takes into consideration the direction and type of all signals on a pathway, the position, role and type of every gene, etc. Hypergeometric distribution was used to analyze the enrichment of pathways, gene ontology, domain structure, and other ontologies. The topGO R library was used to determine local similarities and dependencies between GO terms to perform Elim pruning correction. Several database sources were referenced for enrichment analysis, including Interpro, NCBI, MSigDB, REACTOME, WikiPathways. Enrichment was calculated relative to a set of background genes relevant for the experiment.

Statistics

GraphPad Prism software (Version 10, La Jolla, CA) was utilized to perform ROUT outlier analysis (Q = 1%), with resulting data analyzed via two-way and three-way ANOVA tests to determine the main effects of exposure, sex, and genotype. Two-way ANOVA utilized Tukey's post-hoc multiple comparisons and three-way ANOVA utilized Fisher's LSD post-hoc multiple comparisons to identify significant differences among all groups. Differences between groups were considered significant if the p value ≤ 0.05. Data are represented with mean ± standard error of the mean on all figures unless otherwise noted.

Results

Lung Histopathology Suggests Similar Pathologic Severity in ODE in WT and Fat-1 Mice Regardless of Sex

We utilized a well-established murine model of repetitive organic dust exposure (ODE) in male and female WT and Fat-1 mice to delineate the impact of increased omega 3 fatty acids on the immune response to ODE. Given previous demonstrated findings of sex differences in the response to ODE in Fat-1 mice specifically, a 1:1 ratio of males to females was utilized in both genotypes. To examine the histopathologic characteristics of our ODE in WT and Fat-1 mice, right lung slices were stained with H&E for blinded histopathological scoring **(Supplementary Table 3.2)**. Visual inspection revealed similar lung architecture in WT and Fat-1 mice who received saline, irrespective of sex **(Figure 3.1B)**. ODE mice exhibited profound alveolar inflammation, immune cell aggregation formation, and immune cell presence around bronchioles and vessels, irrespective of genotype or sex **(Figure 3.1C)**. Quantification of pathologic features demonstrated that repetitive ODE resulted in significant increases in immune cell infiltration into the alveolar space around vasculature and bronchioles, formation of immune cell aggregations, and metaplasia of goblet cells within bronchi **(Figure 3.1D-H)**. For all scored pathologic features, a main effect of exposure was observed **(Figure 3.1D-H)**. Averaged pathology scores revealed a main effect of exposure x genotype, seemingly driven by Fat-1 females **(Figure 3.1H)**.

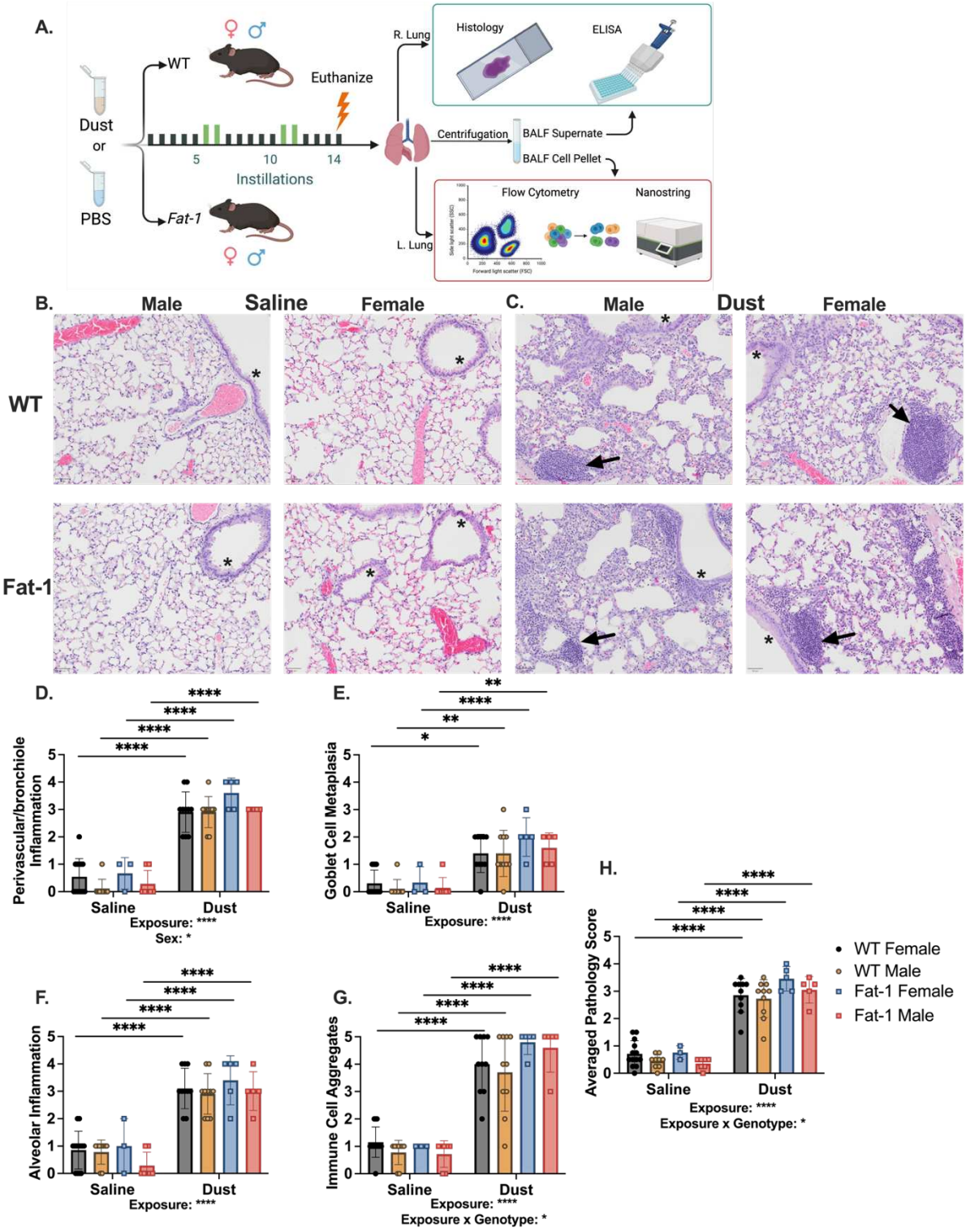

Figure 3.1. Experimental schematic detailing the timeline of repetitive ODE in WT and Fat-1 mice. Samples collected downstream assays performed with each sample type are detailed **(A.)**

Representative H&E pathology of right lung lobes in WT and Fat-1 mice treated with saline or 12.5% organic dust extract over a 3-week period for a total of 14 installations. Images are taken at 20x with a scale bar of 50 μm for reference in the bottom left-hand corner **(B-C).** Pathology scores for perivascular and bronchiole inflammation **(D)**, goblet cell metaplasia **(E)**, alveolar inflammation **(F)**, immune cell aggregates **(G)**, and the averaged pathology score **(H)**. Graphs are plotted by exposure (saline or dust), then delineated by sex (male or female) and genotype (WT or Fat-1). Mouse group numbers are as follows; WT saline n=22, WT dust n=20, Fat-1 saline n=10, Fat-1 dust n=10. Each genotype by exposure group is split 50:50, female to male. Scale bar is 50 μm. Arrows denote immune cell aggregates; asterisks denote goblet cell metaplasia of the airway. Main effects are shown below each graph. 3-Way ANOVA with Dunn's Multiple Comparisons Test. *p<0.05, **p<0.01, ***p<0.001, ****p<0.0001.

No differences between WT and Fat-1 mice were noted in saline treated groups, and no sex differences were observed in either exposure group **(Figure 3.1D-H)**. Collectively, this suggests that WT and Fat-1 mice have similar tissue architecture at baseline and pathologic similarities following ODE, independent of the sex of the animal.

Lung Tissue Immune Cell Makeup is Altered in both Saline- and Dust-exposed Fat-1 Mice Compared to WT

We utilized an extracellular marker-based spectral flow cytometry panel to identify the cellular makeup of a single cell suspension of the lung tissue. We identified 7 separate myeloid lineage immune cell populations, which have been grouped according to parent ontology for examining overall makeup of immune cells identified **(Figure 3.2B)**. Saline-exposed WT and Fat-1 mice

were found to have differing immune cell proportions, suggesting a genotype-dependence on immune cell makeup within the lung in saline-exposed conditions **(Figure 3.2B)**. Saline-exposed Fat-1 mice exhibited decreased proportions of neutrophils, but increased proportions of monocytes, macrophages, and ILCs compared to saline-exposed WT **(Figure 3.2B)**. Irrespective of genotype, ODE significantly influenced the observed proportions of immune cells within the lung tissue, with a notable increase of neutrophils and subsequent decrease of macrophage proportions, consistent with previously described patterns of ODE-mediated inflammation **(Figure 3.2B)**. Population proportions appeared relatively similar between WT and Fat-1 mice after ODE; however, ODE Fat-1 demonstrated an increase in monocyte and ILC populations as well as decreased neutrophil proportions compared to ODE WT mice **(Figure 3.2B)**.

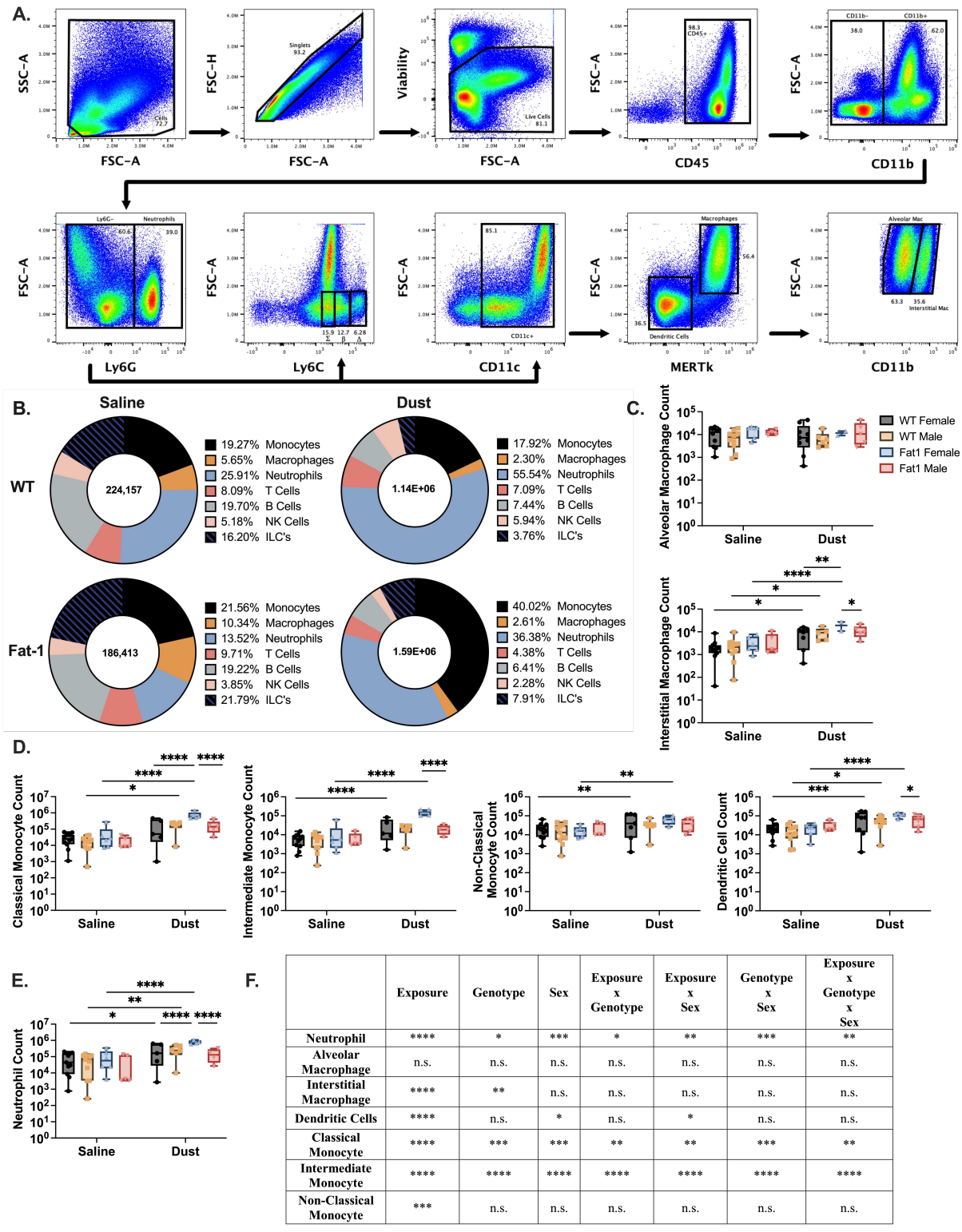

F.

	Exposure	Genotype	Sex	Exposure x Genotype	Exposure x Sex	Genotype x Sex	Exposure x Genotype x Sex
Neutrophil	****	*	***	*	**	***	**
Alveolar Macrophage	n.s.	n.s.	n.s.	n.s.	n.s.	n.s.	n.s.
Interstitial Macrophage	****	**	n.s.	n.s.	n.s.	n.s.	n.s.
Dendritic Cells	****	n.s.	*	n.s.	*	n.s.	n.s.
Classical Monocyte	****	***	***	**	**	***	**
Intermediate Monocyte	****	****	****	****	****	****	****
Non-Classical Monocyte	***	n.s.	n.s.	n.s.	n.s.	n.s.	n.s.

Figure 3.2. Representative gating strategy for identifying myeloid cells in the lung tissue via spectral flow cytometry. All cell populations are labeled with percentages of gates and final cell

population names. Σ= non-classical monocytes, β= intermediate monocytes , Δ=classical monocytes **(A.)** Median immune cell proportions in lung tissue of saline and ODE WT and Fat-1 mice **(B.)** Alveolar and interstitial macrophage counts in saline and ODE WT and Fat-1 mice **(C.)** Classical, intermediate, and non-classical monocyte counts in saline and ODE WT and Fat-1 mice **(D.)** Neutrophil counts in saline and ODE WT and Fat-1 mice **(E.)** Main effects of each immune cell type and variable interactions **(F.)** Mouse group numbers are as follows; WT saline n=22 (11 male, 11 female), WT dust n=21 (11 male, 10 female), Fat-1 saline n=11 (5 male, 6 female), Fat-1 dust n=11 (6 male, 5 female. 3-Way ANOVA with Dunn's Multiple Comparisons Test. *p<0.05, **p<0.01, ***p<0.001, ****p<0.0001

When the macrophage population was delineated into alveolar and interstitial, we observed no significant change in alveolar macrophage counts in the lung tissue in saline or ODE WT or Fat-1 mice, regardless of sex **(Figure 3.2C)**. Interstitial macrophage counts in lung tissue significantly increase in both WT and Fat-1 mice after dust exposure **(Figure 3.2C)**. Fat-1 female interstitial macrophage counts post ODE were significantly increased compared to Fat-1 male ODE mice **(Figure 3.2C)**.

We were particularly intrigued by the observable differences in monocyte populations identified in saline and ODE Fat-1 mice, given the genetic pre-disposition of this model towards a more resolution-specific phenotype. When separated into their respective populations (classical, intermediate, and non-classical), we observed significant ODE-induced increases in all monocyte population counts in Fat-1 mice, with classical monocytes also demonstrating an ODE-induced increase in WT mice **(Supplementary Figure 3.1A)**. In response to ODE, classical and

intermediate monocyte counts were significantly elevated in Fat-1 mice compared to WT, with significant main effects of exposure, genotype, and the interaction of both also observed **(Supplementary Figure 3.2A)**. When split by sex, classical and intermediate monocyte counts in ODE Fat-1 mice were increased in females compared to males, with a similar pattern noted in dendritic cells **(Figure 3.2D)**. Neutrophil counts increased in response to ODE in all but Fat-1 males, with ODE Fat-1 females demonstrating increased counts compared to their male counterparts **(Figure 3.2E)**. No sex differences were noted in WT ODE, or saline-exposed mice regardless of sex or genotype **(Figure 3.2C-E)**.

Previous investigations in our lab utilizing Fat-1 mice in models of ODE have noted sex-dependent differences in histopathology resolution, as well as immune cell counts (12,37). Within the lung tissue monocyte compartment, sex, and interactions of sex with exposure and genotype were found as significant main effects in classical monocytes and intermediate monocyte counts **(Figure 3.2F)**. Only a significant main effect of exposure was found in non-classical monocyte counts **(Figure 3.2F)**. Overall, main effects of exposure, genotype, and sex independently, or the interaction of these variables, were found significant in neutrophils, classical and intermediate monocyte counts **(Figure 3.2F**). These data suggest that neutrophil, interstitial macrophage, and classical/intermediate monocyte population increases within the lung tissue are enhanced in Fat-1 mice in a female-dominant manner.

Sex, Exposure, and Genotype-Dependent Lymphocyte Alterations at the Cellular and Transcriptomic Level Within the Lung Tissue

As lymphocytes, and more recently ILCs, have been found responsible for monocyte/macrophage recruitment to the lungs, we aimed to identify population level changes in response to ODE, and altered by the Fat-1 genotype (38–41). We identified 8 separate lymphoid cell types, delineating $CD4^+$ and $CD8^+$ T cells, B cells, and ILC1, ILC2, and ILC3 **(Figure 3.3A)**. B cell counts increased following ODE in only WT males and NK cell count increased following ODE in WT females **(Figure 3.3B)**. Both $CD4^+$ and $CD8^+$ T cells increased following ODE in Fat-1 females, with $CD4^+$ T cells exhibiting a sex difference between ODE Fat-1 males and females **(Figure 3.3B)**. No alteration of ILC1 count or NCR^+ ILC3 counts was observed following ODE **(Figure 3.3B).** ILC2 counts increased following ODE in Fat-1 males only, with a significant difference in Fat-1 males and females after ODE **(Figure 3.3B).** NCR^+ ILC3 counts in ODE mice demonstrated a significant increase in Fat-1 females compared to WT females, and WT females were significantly reduced compared to ODE WT males **(Figure 3.3B).** NCR^- ILC3 increased following ODE in only WT male mice **(Figure 3.3B)**.

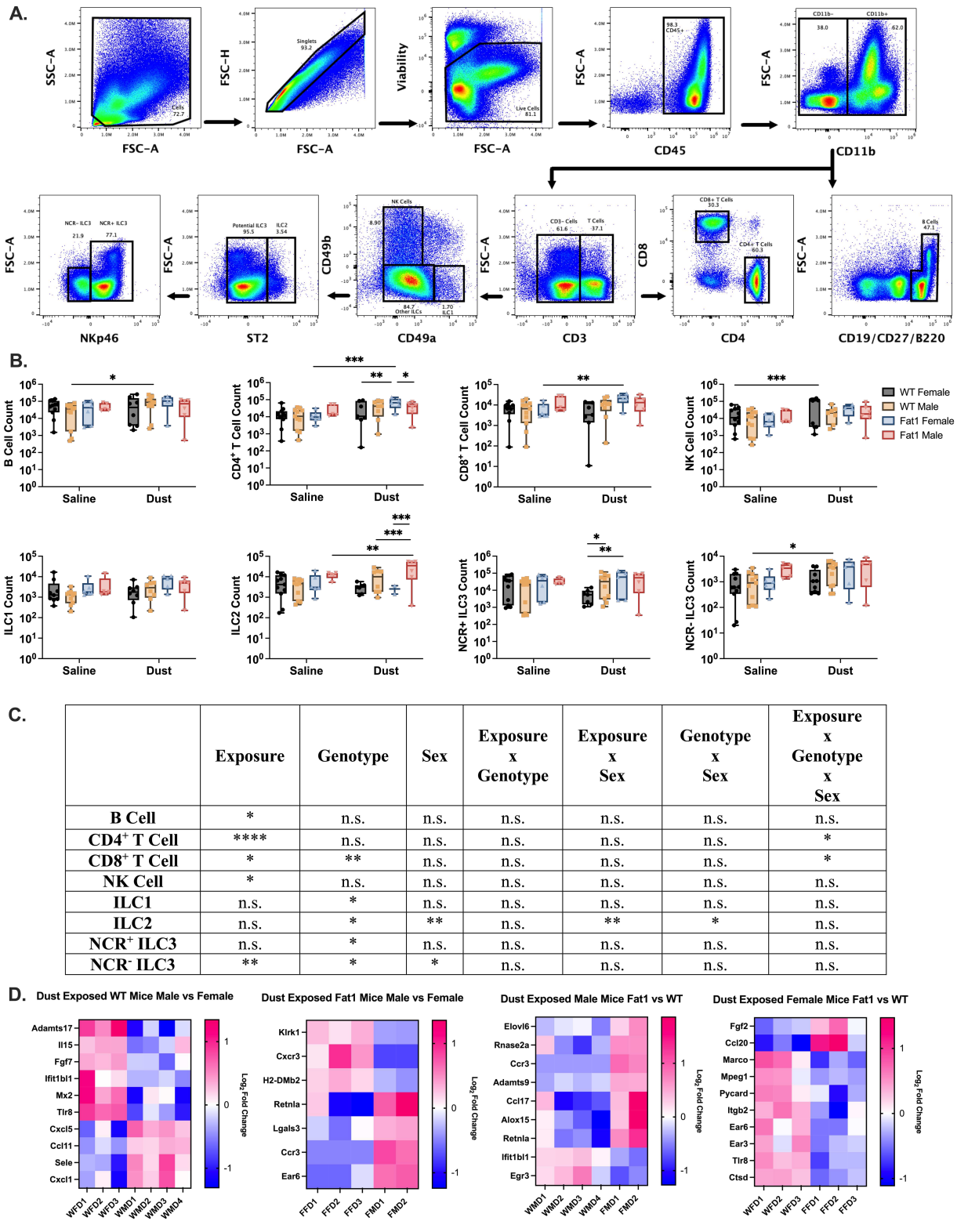

	Exposure	Genotype	Sex	Exposure x Genotype	Exposure x Sex	Genotype x Sex	Exposure x Genotype x Sex
B Cell	*	n.s.	n.s.	n.s.	n.s.	n.s.	n.s.
CD4$^+$ T Cell	****	n.s.	n.s.	n.s.	n.s.	n.s.	*
CD8$^+$ T Cell	*	**	n.s.	n.s.	n.s.	n.s.	*
NK Cell	*	n.s.	n.s.	n.s.	n.s.	n.s.	n.s.
ILC1	n.s.	*	n.s.	n.s.	n.s.	n.s.	n.s.
ILC2	n.s.	*	**	n.s.	**	*	n.s.
NCR$^+$ ILC3	n.s.	*	n.s.	n.s.	n.s.	n.s.	n.s.
NCR$^-$ ILC3	**	*	*	n.s.	n.s.	n.s.	n.s.

Figure 3.3. Representative gating strategy for lymphoid cells identified in the lung tissue via spectral flow cytometry **(A.)** Lymphoid cell counts in the lung tissue of saline and ODE WT and

Fat-1 mice **(B.)** Main effects of each immune cell type and variable interactions **(C.)** Differentially expressed genes from left lung RNA in saline- and dust-exposed WT and Fat-1 mice. Analysis was conducted via Nanostring Myeloid panel. Significant differentially expressed genes with an adjusted p value <0.05 with log_2fold change ± 1.5 graphed in the heat maps. Mouse group numbers for cell counts are as follows; WT saline n=22 (11 male, 11 female), WT dust n=21 (11 male, 10 female), Fat-1 saline n=11 (5 male, 6 female), Fat-1 dust n=11 (6 male, 5 female. Mouse group numbers for Nanostring are as follows; WT dust n=6 (3 male, 3 female) Fat-1 dust (3 male, 2 female). 3-Way ANOVA with Dunn's Multiple Comparisons Test. *p<0.05, **p<0.01, ***p<0.001, ****p<0.0001.

Main effects of exposure were found to be significant in B Cells, CD4 and CD8 T cells, NK cells, and NCR- ILC3s **(Figure 3.3C)**. Main effects of genotype were found significant in CD8 T cells, ILC1, ILC2, NCR+ ILC3, and ILC- ILC3 **(Figure 3.3C)**. ILC2 exhibited significant main effects of sex and sex interactions with exposure or genotype **(Figure 3.3C).**

With the demonstrated sex-driving factor in our myeloid, but not lymphoid, cell populations in response to ODE in Fat-1 mice, we were interested in determining if the transcriptome could provide insight into the transcriptional drivers of this observation. We conducted targeted RNA sequencing from homogenized left lung from saline and ODE, male and female WT and Fat-1 mice. Dust exposure in both genotypes significantly increased fold change expression of genes assessed **(Supplementary Table 3.3)**. ODE Fat-1 mice appeared less responsive with regards to these transcriptomic effects, with a total of 156 differentially expressed genes (DEG) (148 up, 8 down) compared to the ODE WT mice with 266 DEG (230 up, 36 down) **(Supplementary**

Table 3.3). When stratified by sex, ODE animals in both genotypes demonstrated sex-dependent DEG signatures **(Figure 3.3D)**. ODE Fat-1 male mice demonstrated upregulation of long chain fatty acid processing genes such as *Elov6* and *Alox15,* as well as upregulation of *Ccr3* and *Ccl17* compared to their WT male counterparts **(Figure 3.3D)**. ODE Fat-1 female mice exhibited downregulation of scavenger receptor *Marco* and *Mpeg1* and upregulation of *Ccl20* and *Fgf2* **(Figure 3.3D)**. ODE WT mice exhibited alterations in primarily innate immunity linked genes such as *Cxcl5*, *Cxcl1*, *Mx2*, and *Adamts17* **(Figure 3.3D)**. ODE Fat-1 mice transcript alterations appeared more adaptive in nature, with alterations of *Cxcr3*, *Retnla*, and *Ccr3* **(Figure 3.3D)**.

ODE-induced Effects on Airway Myeloid Cell Counts in WT and Fat-1 Mice

We were intrigued by the drastic differences in immune cells observed in the lung tissue between WT and Fat-1 mice at baseline and following ODE. As most inhalable insults are encountered on the external epithelial surface within the bronchi and alveoli, we sought to characterize the cellular and soluble mediators of ODE within the airway. The same panel for myeloid cell identification was successfully applied to immune cells isolated from bronchioalveolar lavage fluid (BALF) to the BALF cells **(Figure 3.4A)**. The proportions of cells isolated in BALF demonstrated drastic differences in immune cell proportions between WT and Fat-1 mice exposed to saline or ODE **(Figure 3.4B)**. Proportions of neutrophils were drastically reduced in saline exposed Fat-1 mice, while all other immune cell proportions were increased compared to WT counterparts **(Figure 3.4B)**. Following ODE, Fat-1 mice exhibited increased monocyte and macrophage proportions compared to WT's and decreased neutrophil proportions **(Figure 3.4B).**

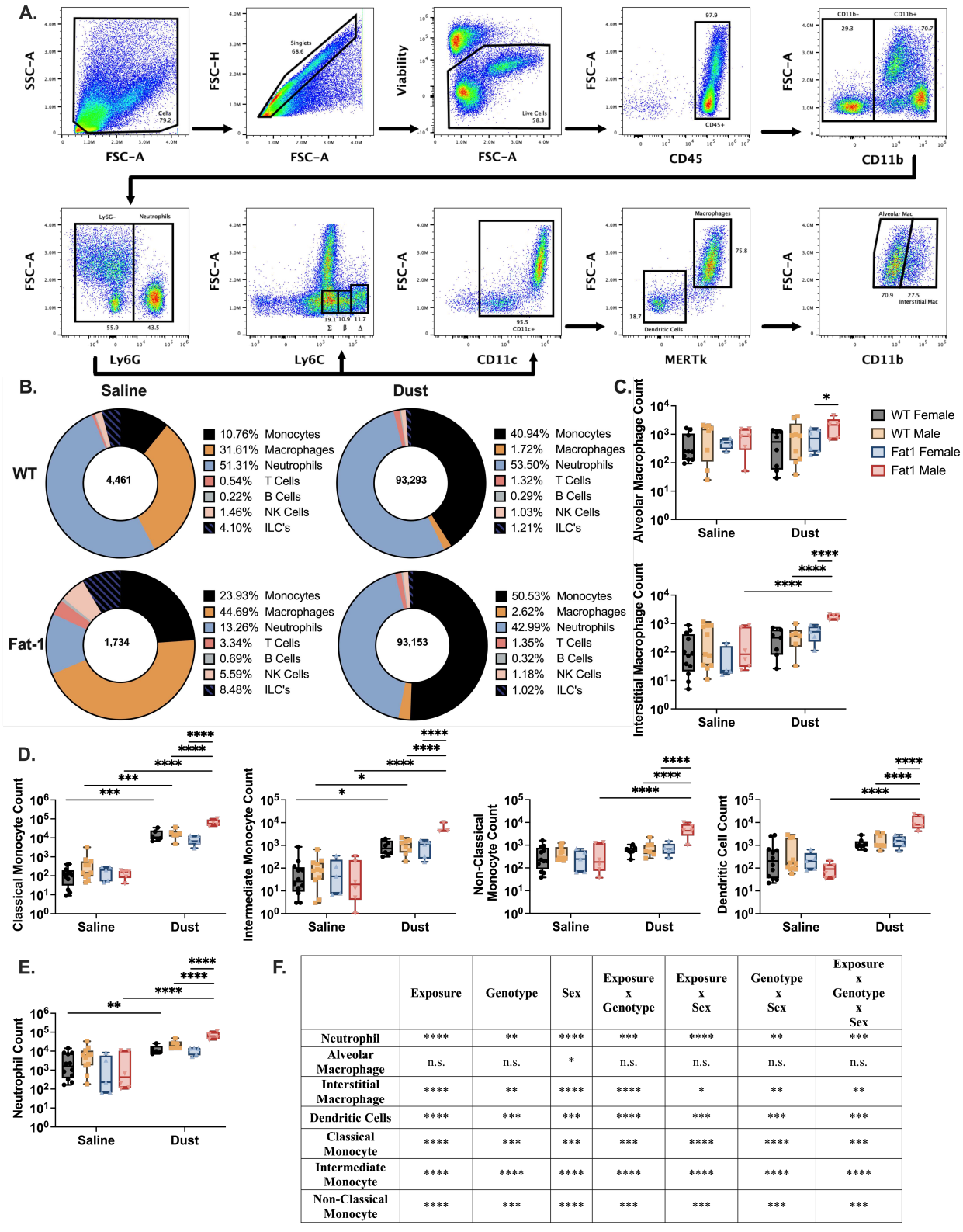

F.

	Exposure	Genotype	Sex	Exposure x Genotype	Exposure x Sex	Genotype x Sex	Exposure x Genotype x Sex
Neutrophil	****	**	****	***	****	**	***
Alveolar Macrophage	n.s.	n.s.	*	n.s.	n.s.	n.s.	n.s.
Interstitial Macrophage	****	**	****	****	*	**	**
Dendritic Cells	****	***	***	****	***	***	***
Classical Monocyte	****	***	***	***	****	****	***
Intermediate Monocyte	****	****	****	****	****	****	****
Non-Classical Monocyte	****	***	****	***	***	***	***

Figure 3.4. Representative gating strategy for myeloid cells identified in bronchoalveolar lavage fluid via spectral flow cytometry. All cell populations are labeled with percentages of gates and final cell population names. Σ= non-classical monocytes, β= intermediate monocytes , Δ=classical monocytes **(A.)** Median immune cell proportions in airways of WT and Fat-1 saline and ODE mice **(B.)** Alveolar and interstitial macrophage counts in saline and ODE WT and Fat-1 mice **(C.)** Classical, intermediate, and non-classical monocyte counts in saline and ODE WT and Fat-1 mice **(D.)** Neutrophil counts in saline and ODE WT and Fat-1 mice **(E.)**. Main effects of each immune cell type and variable interactions **(F.)** Mouse group numbers for cell counts are as follows; WT saline n=22 (11 male, 11 female), WT dust n=21 (11 male, 10 female), Fat-1 saline n=11 (5 male, 6 female), Fat-1 dust n=11 (6 male, 5 female. 3-Way ANOVA with Dunn's Multiple Comparisons Test *p<0.05 **p<0.01, ***p<0.001****p<0.0001.

Examination of each monocyte subtype individually revealed ODE-dependent increases in classical and intermediate monocyte counts, but not non-classical monocytes regardless of genotype **(Supplementary Figure 3.1B)**. In ODE-exposed mice, there was a significant decrease in classical monocyte counts and increase in intermediate monocyte counts in Fat-1 compared to WT mice **(Supplementary Figure 3.1B)**. Significant main effects of exposure were found for all three monocyte subsets, while main effects of genotype and genotype interacting with exposure were demonstrated in classical and intermediate monocytes only **(Supplementary Figure 3.1B)**.

Alveolar macrophage counts following ODE were significantly increased in Fat-1 males compared to Fat-1 males, while interstitial macrophages exhibited an ODE-associated increase in counts in Fat-1 males only, with a significant increase compared to ODE-challenged Fat-1

females **(Figure 3.4C).** ODE significantly increased classical and intermediate monocyte counts in all but Fat-1 females **(Figure 3.4D)**. Non-classical monocytes and dendritic cell counts were increased post ODE in Fat-1 males only **(Figure 3.4D)**. For all three monocyte populations, in response to ODE, Fat-1 males had increased counts compared to Fat-1 females, the inverse findings that Fat-1 female dominance in monocyte populations in the lung tissue **(Figure 3.4D)**. Neutrophil populations were found significantly elevated in ODE in WT females and Fat-1 males, and a significant increase in neutrophils post ODE in Fat-1 males compared to their female counterparts **(Figure 3.4E)**. Significant main effects of exposure, genotype, sex, or the interaction of both, or all, variables were found in all but alveolar macrophage populations for myeloid cell counts **(Figure 3.4F)**.

A.

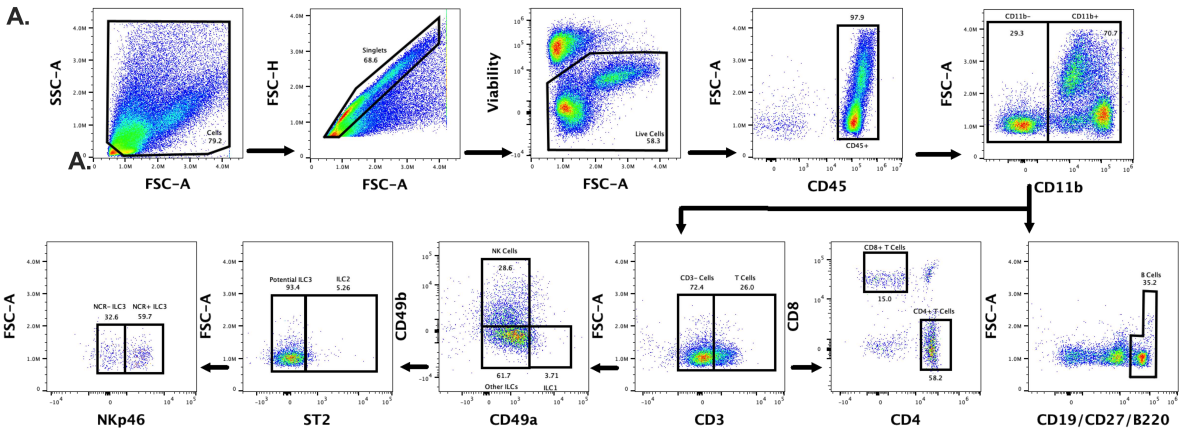

B.

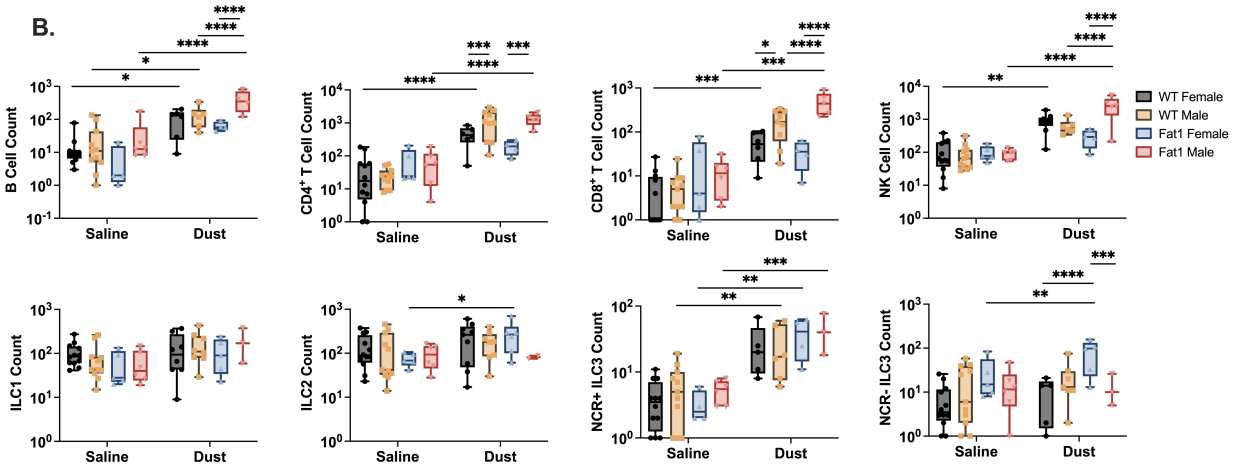

C.

	Exposure	Genotype	Sex	Exposure x Genotype	Exposure x Sex	Genotype x Sex	Exposure x Genotype x Sex
B Cell	****	n.s.	***	n.s.	**	**	*
CD4$^+$ T Cell	****	n.s.	***	n.s.	***	n.s.	n.s.
CD8$^+$ T Cell	****	**	****	*	****	**	**
NK Cell	****	*	**	*	**	***	***
ILC1	**	n.s.	n.s.	n.s.	n.s.	n.s.	n.s.
ILC2	n.s.	n.s.	n.s.	n.s.	n.s.	n.s.	n.s.
NCR$^+$ ILC3	*	n.s.	n.s.	n.s.	n.s.	n.s.	n.s.
NCR$^-$ ILC3	n.s.	**	n.s.	n.s.	n.s.	***	n.s.

D.

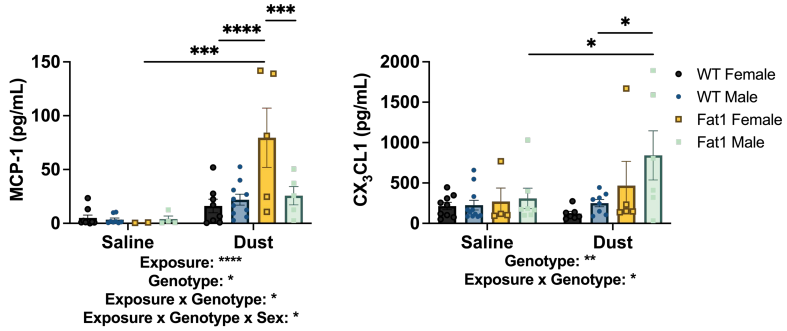

Figure 3.5. Representative gating strategy for lymphoid cell identification in bronchoalveolar lavage fluid via spectral flow cytometry **(A.)** Lymphoid cell counts in the lung tissue of saline and ODE WT and Fat-1 mice **(B.)** Main effects of each immune cell type and variable interactions **(C.)** Levels of MCP-1 and CX_3CL1 in bronchoalveolar lavage fluid of = saline and ODE exposed WT and Fat-1, with main effects shown below the graphs. Mouse group numbers for cell counts are as follows; WT saline n=22 (11 male, 11 female), WT dust n=21 (11 male, 10 female), Fat-1 saline n=11 (5 male, 6 female), Fat-1 dust n=11 (6 male, 5 female. 3-Way ANOVA with Dunn's Multiple Comparisons Test *p<0.05 **p<0.01, ***p<0.001****p<0.0001.

The lymphoid compartment of cells was examined **(Figure 3.5A)**, with similar findings to their myeloid counterparts. B cell, $CD4^+$ and $CD8^+$ T cell, and NK cell counts were found increased in WT females, with a significant increase in ODE Fat-1 males compared to Fat-1 females **(Figure 3.5B)**. ODE exposed WT males had significantly elevated CD4 and CD8 T cells compared to WT females **(Figure 3.5B)**. Changes in ILC1 populations were observed in the airway in response to ODE, but an increase in ILC2 counts specifically in Fat-1 females was demonstrated **(Figure 5B)**. NCR^+ ILC3 counts increased in all but WT females in response to ODE **(Figure 3.5B)**. Conversely, NCR^- ILC3 counts were significantly elevated post ODE in Fat-1 females only, significantly so compared to Fat-1 males **(Figure 3.5B)**. Main effects of exposure were found in all identified lymphoid cells except ILC2 and NCR^- ILC3 **(Figure 3.5C)**. NK cells exhibited main effects of exposure, genotype, sex, and the interaction between both or all of these features **(Figure 3.5C).**

MCP-1 levels increased in Fat-1 females following ODE exposure, significantly so compared to Fat-1 males and WT females **(Figure 3.5D)**. MCP-1 variation was driven by exposure, genotype, and the combination of both factors **(Figure 3.5D)**. CX_3CL1 levels were increased in Fat-1 males only post ODE, significantly so compared to WT males **(Figure 3.5D)**. Variation of CX_3CL1 levels was found to have a genotype-specific driver with alterations driven by the Fat-1 genotype or the interaction with exposure **(Figure 3.5D)**. A comprehensive summary of these findings by immune cell type, organized by sex and location demonstrates that ODE has a primary impact on increasing immune cell populations in females within the lung tissue, and males in the airway **(Figure 3.6**). Furthermore, this female dominance in the lung tissue appears primarily grouped in myeloid-lineage cells, with little to no perturbation in lymphoid lineage cells **(Figure 3.6**). Within the airway, the male dominance of response appears visually distributed across both myeloid and lymphoid cell subsets **(Figure 3.6**).

A.

Location, Genotype, and Sex Difference-induced Myeloid Population Changes from ODE		Lung Tissue ♂	Lung Tissue ♀	Airway ♂	Airway ♀
Classical Monocyte	WT	+	+	+	+
	Fat-1	+	+++	+++	++
Intermediate Monocyte	WT	+	+	+	+
	Fat-1	++	+++	+++	++
Non-Classical Monocyte	WT	-	-	-	-
	Fat-1	+	+	+++	-
Neutrophils	WT	+	+	+	+
	Fat-1	+	+++	+++	+
Alveolar Macrophages	WT	-	-	-	-
	Fat-1	-	-	+	-
Interstitial Macrophages	WT	+	+	-	-
	Fat-1	++	+++	+++	+
Dendritic Cells	WT	+	+	-	-
	Fat-1	-	+++	+++	-

B.

Location, Genotype, and Sex Difference-induced Lymphoid Population Changes from ODE		Lung Tissue ♂	Lung Tissue ♀	Airway ♂	Airway ♀
$CD4^+$ T Cells	WT	-	-	+	++
	Fat-1	-	+	++	+
$CD8^+$ T Cells	WT	-	-	+	+++
	Fat-1	-	+	++	+
B Cells	WT	+	-	+	+
	Fat-1	-	-	+++	-
NK Cells	WT	++	-	-	+++
	Fat-1	-	-	+++	+
ILC1	WT	-	-	-	-
	Fat-1	-	-	-	-
ILC2	WT	-	-	-	-
	Fat-1	++	-	-	+
NCR+ ILC3	WT	-	-	+	-
	Fat-1	-	-	++	+
NCR- ILC3	WT	+	-	-	-
	Fat-1	-	-	-	++

Figure 3.6. Comprehensive summary of myeloid **(A)** and lymphoid **(B)** immune cell population changes in response to ODE in WT and Fat-1 mice, delineated by sex and location (lung tissue vs airway).

Discussion

Inhalational insults continuously plague agricultural workers, with the prevalence of COPD among this group twice that of those who do not have an occupation with agricultural activity (42). The crux of the issue is the spatiotemporal nature of inhalation; the continuity of exposure creates a chronically inflamed environment within the lungs, where traditional immunologic dogma of acute vs chronic cell population mobility breaks down, increasing susceptibility of an individual to COPD (42), asthma (43), and other insults more infectious in nature (44). In the fight against chronic lung inflammation and COPD endpoints, therapeutics are significantly lacking and are targeted towards symptom reduction or inflammatory stimuli mitigation, rather than a promotion of inflammation resolution (45). Succinctly summarized in Shakeel et al., inhibition of proinflammatory signals, protease inhibitors, or cAMP/cGMP inhibitors have struggled to demonstrate efficacy in reducing COPD endpoints during clinical trials (46). As such, an approach that harnesses the benefits of resolution within the inflammatory process is needed.

We herein demonstrate a monocyte-dominant immune response to repetitive inhalational dust exposure, furthermore in a transgenic mouse model of increased n-3 FA in a sex-dependent manner. Early characterization of monocytes in the literature began with two “flavors”, the tissue resident, anti-inflammatory and patrolling “non-classical monocyte,” and the blood-recruited and pro-inflammatory “classical monocyte” (47,48). Within humans, these subsets are delineated via variable expression of CD14 and CD16 (49). With the advent and popularity of flow cytometry, a third “intermediate monocyte” subset was identified, and nomenclature accepted in 2010 (50–52). Intermediate monocytes are pro-inflammatory in nature and were initially hypothesized as a transient population between classical to non-classical monocyte populations but have since been

defined as their own unique subset with primarily pro-inflammatory functions (47,49,50,53–55). Intermediate monocytes express decreased CCR2 and increased CCR5 than their classical counterparts, a result of decreased migratory necessity (56). In addition, increased CX_3CR1, HLA-DR, and CD86 on intermediate monocytes compared to their classical counterparts suggests a primary role in phagocytosis and altered reliance on chemotactic migration (49,57,58).

Within mice, the classic CD14/CD16 marking paradigm is not used, and identification of monocytes and their subsets relies on the use of lymphocyte antigen 6 family member C1 (Ly6C) (49). Nonetheless, the 3 primary subsets of monocytes hold within mice, with classical ($Ly6c^{Hi}$), intermediate ($Ly6c^{mid}$), and non-classical ($Ly6c^{lo}$) subpopulations having been characterized (56,57,59). Similar roles as to those described among humans are ascribed to these murine monocyte populations as well. It is important to note that Ly6c is additionally found on T cells, and use of Ly6c requires lineage-based gating strategies that separate myeloid and lymphoid cell populations (via CD11b and/or CD3 co-staining) (60).

Classical monocyte recruitment via the MCP-1/CCR2 mechanism into chronically inflamed areas such as in the settings of cystic fibrosis or COPD are traditionally associated with poorer pathologic and functional outcomes (54,61). Conversely, CCR2 deficiency has been demonstrated to contribute to progression of polycystic lung disease (30), suggesting that a balance of CCR2/MCP-1 is imperative in maintaining lung homeostasis. Our own findings suggest that monocytes are more abundantly recruited to the lung and airways in a pro-resolution model during chronic inflammation. In addition, our repetitive exposure model demonstrated that

Fat-1 mice exposed to dust have significantly increased intermediate monocyte populations, with no significant difference in non-classical monocyte populations (**Supplementary Figure 3.2A, B**). This suggests a previously undescribed role for intermediate monocyte populations in responding to this inflammatory inhalational exposure, but further studies are needed to confirm the directionality of this monocyte population increase, and whether it is likely to enhance resolution features at recovery timepoints. Previous work attempted to reduce ODE-induced inflammation through reduction of monocyte populations via $CCR2^{-/-}$ mice and chlodronate treatment, demonstrating that depletion via clodronate independently led to reduced inflammation in response to ODE (36). Further studies that examine timepoints indicative of inflammatory resolution 3 days to several weeks post halting of dust exposure would demonstrate the resolution kinetics and necessity of this observed monocyte population response.

The use of n-3 FA has shown promise in reducing the inflammatory signatures associated with chronic inhalation of organic dusts (11,12,16,18,62). These studies have utilized single n-3 FA metabolites, such as aspirin-triggered resolvin D1 (AT-RvD1) or MaR1, diet-based interventions to artificially mimic a 1:1 n-6:n-3 fatty acid ratio, or the transgenic Fat-1 model used herein. The use of once weekly AT-RvD1 in ODE mice over a 24-week period was found to significantly increase IL-10, as well as decrease alveolar inflammation and overall fibrotic severity (16). Utilizing MaR1, another downstream metabolite of n-3 FA, led to a reduction of neutrophils, IL-6, TNF, and CXCL2 in the airways following a single- or 3-week exposure of organic dust (18). Both studies utilized differential cell counts via cytocentrifugation to determine cell populations, with neutrophils dominating acute and chronic dust exposure, similar to what we observed.

Models that utilize supplementation of n-3 FA docosahexaenoic acid (DHA), the precursor molecule to MaR1 and AT-RvD1, corroborate these findings. In a single exposure of organic dust following a week of oral DHA supplementation, pre-treated mice demonstrated decreased neutrophils, and total cell counts isolated from BALF (11). Similar to single metabolite studies, DHA pretreatment reduced IL-6, TNF, CXCL1, and CXCL2 amounts compared to acute dust exposure alone. In studies where the length of time of DHA pre-treatment, via dietary supplementation rather than oral gavage, was expanded from 1 week to a month, similar trends were observed. The total amount of BALF cells were found to be less significantly increased compared to ODE alone (14). In addition, long-term pre-treatment was found to significantly increase the macrophage proportion isolated from BALF in dust-exposed animals. Interestingly, this study found that DHA treatment alone was responsible for dust-induced MCP-1 increases, corroborating our findings of ODE-induced MCP-1 increases **(Figure 3.5D)**. Of note, this study demonstrated that the prolonged DHA diet also increased the presence of DHA metabolites, like AT-RvD1 specifically, in saline and dust exposed animals (14).

Similarly, repetitive dust exposure during dietary DHA supplementation has revealed that pretreatment reduces cell counts in the BALF, albeit non-significantly, compared to non-DHA pretreatment (15). At a one-week recovery period, these patterns held, with less cells recovered from the airway in DHA diet-fed mice exposed to dust. Collectively, this suggests that DHA presence decreases cellularity within the airways of chronically dust-exposed mice. In a chronic dust exposure model that utilizes the Fat-1 mouse, total cell counts, or individual cell counts did not differ between WT or Fat-1 mice (37). It does corroborate the pathologic scoring similarity we observed between saline and dust exposed WT and Fat-1 mice, regardless of sex (37).

This same study reported sex-based differences in BALF cell counts, demonstrating that Fat-1 females had increased total cell populations compared to their male counterparts when exposed to dust. As we observed increased cell counts in male Fat-1 mice compared to females post dust exposure, there is a discrepancy in our findings. A possible explanation could be methodology based, as our study utilized flow cytometry while the comparator study utilized cytocentrifugation with differential staining. Flow cytometry allows for enumeration of greater amounts of immune cell populations, increasing the accuracy of cell type identification, especially important in identifying monocytes. In our data, the sex differences in dust-exposed animals of the Fat-1 genotype presents an interesting case. In BALF, after exposure to dust and within the Fat-1 mice, male sex appears to drive monocyte populations, which switches to female sex when lung tissue is examined. When MCP-1 levels are measured within the airway, they are increased in dust-exposed Fat-1 females, despite the monocyte response being male dominant. Sex differences in immune response are well documented (63); however, no reports yet within the chronic dust exposure literature suggests a reason. In models of obesity, it has been shown that monocytes from males were more robust in their pro-inflammatory skewing and more likely to mature into macrophages than monocytes from females (64). So et al. in 2021 determined that sex differences exist in the monocyte transcriptome using a cohort of individuals while testing the efficacy of omega-3 fatty acids on chronic low-grade inflammation (65). They reported that upregulation of innate immune cell activation genes (CEACAM1, FCCR2B, and SLAMF7) and antigen recognition and presentation (AIM2, CD1E, and UBA1) were all increased in female monocytes. Male monocytes displayed an X-linked increase in SERPINB2 and EPBL. Our investigation into the transcript level differences of the whole lung in a targeted myeloid panel

did not yield similar differentially expressed genes but did demonstrate that dust exposure primarily enhanced pathways associated with innate immune cell activation and scavenger receptor processes, regardless of sex. We also demonstrated a Fat-1-dependent increase in genes involved in lipid metabolism (*Alox15*, *Elovl6*) specifically in ODE male mice **(Figure 3.3D)**.

These same alterations were not found in ODE females, suggesting that transcriptional-levels of fatty acid modifying enzymes appears mor significantly upregulated in ODE Fat-1 males compared to WT counterparts, and that females of both Fat-1 and WT ODE groups are resistant to such differences.

This study faces some limitations, the first of which relates to the timepoint of animal sacrifice post chronic installation. Based on previous literature, 5 hours post the final installation was used to investigate the immune cell population perturbations and cytokine production environment. As a result, it should be noted that our n-3 FA model, which demonstrates a "pro-resolution" skew, shows similar pathology to our WT mice. Future studies using extended recovery periods are needed to fully demonstrate how the populations observed at our 5-hour post installation timepoint contribute to tissue resolution processes.

Conclusions

Collectively this study reveals a previously undescribed role for monocyte-dominant immune responses as a hallmark of the initial response needed in the resolution of chronic inflammation caused by inhalation of organic dusts. This study demonstrates that use of the Fat-1 model corroborates cellular makeup and inflammatory mediator signatures within the field, while revealing a baseline difference in immune cell makeup, prior to and following, organic dust

exposure. Interestingly, we uncover a sex-dependent link, specifically in Fat-1 mice, suggesting that future investigations that utilize the model, or models of increased n-3 FA, must account for sex as a primary confounding variable.

Funding
Research reported in this publication was supported by the National Heart, Lung, and Blood Institute of the National Institute of Health under award number R01HL158926 to TMN and R01HL158926-04S1 to LSD.

Acknowledgements
The authors would like to acknowledge Dr. Brad Burke and Lizzie Creisen formerly of the Colorado State University Flow Cytometry Core as well as the Lab Animal Resources technicians and staff.

Data Availability Statement
Raw and normalized NanoString data are deposited to GEO as GSE255787.

References

1. Crawford MS, Nordgren TM, McCole DF. Every breath you take: Impacts of environmental dust exposure on intestinal barrier function–from the gut-lung axis to COVID-19. *American Journal of Physiology-Gastrointestinal and Liver Physiology* (2021) 320:G586–G600. doi: 10.1152/ajpgi.00423.2020
2. Nordgren TM, Bailey KL. Pulmonary health effects of agriculture. *Curr Opin Pulm Med* (2016) 22:144–149. doi: 10.1097/MCP.0000000000000247
3. Nordgren TM, Charavaryamath C. Agriculture Occupational Exposures and Factors Affecting Health Effects. *Curr Allergy Asthma Rep* (2018) 18:65. doi: 10.1007/s11882-018-0820-8
4. Marcus AJ, Broekman MJ, Safier LB, Ullman HL, Islam N, Serhan CN, Weissmann G. Production of arachidonic acid lipoxygenase products during platelet-neutrophil interactions. *Clin Physiol Biochem* (1984) 2:78–83.
5. Serhan CN, Hamberg M, Samuelsson B. Lipoxins: novel series of biologically active compounds formed from arachidonic acid in human leukocytes. *Proc Natl Acad Sci U S A* (1984) 81:5335–9. doi: 10.1073/pnas.81.17.5335
6. Serhan CN, Hong S, Gronert K, Colgan SP, Devchand PR, Mirick G, Moussignac R-L. Resolvins: a family of bioactive products of omega-3 fatty acid transformation circuits initiated by aspirin treatment that counter proinflammation signals. *J Exp Med* (2002) 196:1025–37. doi: 10.1084/jem.20020760
7. Basil MC, Levy BD. Specialized pro-resolving mediators: endogenous regulators of infection and inflammation. *Nat Rev Immunol* (2016) 16:51–67. doi: 10.1038/nri.2015.4
8. Schebb NH, Kühn H, Kahnt AS, Rund KM, O'Donnell VB, Flamand N, Peters-Golden M, Jakobsson PJ, Weylandt KH, Rohwer N, et al. Formation, Signaling and Occurrence of Specialized Pro-Resolving Lipid Mediators—What is the Evidence so far? *Front Pharmacol* (2022) 13: doi: 10.3389/fphar.2022.838782
9. Simopoulos AP. The importance of the ratio of omega-6/omega-3 essential fatty acids. *Biomedicine & Pharmacotherapy* (2002) 56:365–379. doi: 10.1016/S0753-3322(02)00253-6
10. Kaliannan K, Li X-Y, Wang B, Pan Q, Chen C-Y, Hao L, Xie S, Kang JX. Multi-omic analysis in transgenic mice implicates omega-6/omega-3 fatty acid imbalance as a risk factor for chronic disease. *Commun Biol* (2019) 2:276. doi: 10.1038/s42003-019-0521-4
11. Nordgren T, Friemel T, Heires A, Poole J, Wyatt T, Romberger D. The Omega-3 Fatty Acid Docosahexaenoic Acid Attenuates Organic Dust-Induced Airway Inflammation. *Nutrients* (2014) 6:5434–5452. doi: 10.3390/nu6125434
12. Ulu A, Velazquez J V., Burr A, Sveiven SN, Yang J, Bravo C, Hammock BD, Nordgren TM. Sex-Specific Differences in Resolution of Airway Inflammation in Fat-1 Transgenic Mice Following Repetitive Agricultural Dust Exposure. *Front Pharmacol* (2022) 12: doi: 10.3389/fphar.2021.785193
13. Hanson C, Ponce J, Isaak M, Heires A, Nordgren T, Wichman C, Furtado JD, LeVan T, Romberger D. Fatty Acids, Amphiregulin Production, and Lung Function in a Cohort of Midwestern Veterans. *Frontiers in Rehabilitation Sciences* (2022) 3: doi: 10.3389/fresc.2022.773835
14. Dominguez EC, Heires AJ, Pavlik J, Larsen TD, Guardado S, Sisson JH, Baack ML, Romberger DJ, Nordgren TM. A High Docosahexaenoic Acid Diet Alters the Lung Inflammatory Response to Acute Dust Exposure. *Nutrients* (2020) 12:2334. doi: 10.3390/nu12082334

15. Ulu A, Burr A, Heires AJ, Pavlik J, Larsen T, Perez PA, Bravo C, DiPatrizio N V., Baack M, Romberger DJ, et al. A high docosahexaenoic acid diet alters lung inflammation and recovery following repetitive exposure to aqueous organic dust extracts. *Journal of Nutritional Biochemistry* (2021) 97: doi: 10.1016/j.jnutbio.2021.108797
16. Dominguez EC, Phandthong R, Nguyen M, Ulu A, Guardado S, Sveiven S, Talbot P, Nordgren TM. Aspirin-Triggered Resolvin D1 Reduces Chronic Dust-Induced Lung Pathology without Altering Susceptibility to Dust-Enhanced Carcinogenesis. *Cancers (Basel)* (2022) 14:1900. doi: 10.3390/cancers14081900
17. Nordgren TM, Heires AJ, Wyatt TA, Poole JA, LeVan TD, Cerutis DR, Romberger DJ. Maresin-1 reduces the pro-inflammatory response of bronchial epithelial cells to organic dust. *Respir Res* (2013) 14:51. doi: 10.1186/1465-9921-14-51
18. Nordgren TM, Bauer CD, Heires AJ, Poole JA, Wyatt TA, West WW, Romberger DJ. Maresin-1 reduces airway inflammation associated with acute and repetitive exposures to organic dust. *Translational Research* (2015) 166:57–69. doi: 10.1016/j.trsl.2015.01.001
19. Poole JA, Nordgren TM, Heires AJ, Nelson AJ, Katafiasz D, Bailey KL, Romberger DJ. Amphiregulin modulates murine lung recovery and fibroblast function following exposure to agriculture organic dust. *American Journal of Physiology-Lung Cellular and Molecular Physiology* (2020) 318:L180–L191. doi: 10.1152/ajplung.00039.2019
20. Warren K, Wyatt T, Romberger D, Ailts I, West W, Nelson A, Nordgren T, Staab E, Heires A, Poole J. Post-Injury and Resolution Response to Repetitive Inhalation Exposure to Agricultural Organic Dust in Mice. *Safety* (2017) 3:10. doi: 10.3390/safety3010010
21. Nordgren TM, Heires AJ, Bailey KL, Katafiasz DM, Toews ML, Wichman CS, Romberger DJ. Docosahexaenoic acid enhances amphiregulin-mediated bronchial epithelial cell repair processes following organic dust exposure. *American Journal of Physiology-Lung Cellular and Molecular Physiology* (2018) 314:L421–L431. doi: 10.1152/ajplung.00273.2017
22. Nordgren TM, Heires AJ, Bailey KL, Katafiasz DM, Toews ML, Wichman CS, Romberger DJ. Docosahexaenoic acid enhances amphiregulin-mediated bronchial epithelial cell repair processes following organic dust exposure. *Am J Physiol Lung Cell Mol Physiol* (2018) 314: doi: 10.1152/ajplung.00273.2017
23. Seillet C, Jacquelot N. Sensing of physiological regulators by innate lymphoid cells. *Cell Mol Immunol* (2019) 16:442–451. doi: 10.1038/s41423-019-0217-1
24. Panda SK, Colonna M. Innate lymphoid cells in mucosal immunity. *Front Immunol* (2019) 10: doi: 10.3389/fimmu.2019.00861
25. Sonnenberg GF, Artis D. Innate lymphoid cells in the initiation, regulation and resolution of inflammation. *Nat Med* (2015) 21:698–708. doi: 10.1038/nm.3892
26. Klose CSN, Artis D. Innate lymphoid cells control signaling circuits to regulate tissue-specific immunity. *Cell Res* (2020) 30:475–491. doi: 10.1038/s41422-020-0323-8
27. van der Vorst EPC, Weber C. Novel Features of Monocytes and Macrophages in Cardiovascular Biology and Disease. *Arterioscler Thromb Vasc Biol* (2019) 39:e30–e37. doi: 10.1161/ATVBAHA.118.312002
28. Schyns J, Bai Q, Ruscitti C, Radermecker C, De Schepper S, Chakarov S, Farnir F, Pirottin D, Ginhoux F, Boeckxstaens G, et al. Non-classical tissue monocytes and two functionally distinct populations of interstitial macrophages populate the mouse lung. *Nat Commun* (2019) 10:3964. doi: 10.1038/s41467-019-11843-0
29. Evren E, Ringqvist E, Willinger T. Origin and ontogeny of lung macrophages: from mice to humans. *Immunology* (2020) 160:126–138. doi: 10.1111/imm.13154

30. Neehus A-L, Carey B, Landekic M, Panikulam P, Deutsch G, Ogishi M, Arango-Franco CA, Philippot Q, Modaresi M, Mohammadzadeh I, et al. Human inherited CCR2 deficiency underlies progressive polycystic lung disease. *Cell* (2023) doi: 10.1016/j.cell.2023.11.036
31. Romberger DJ, Bodlak V, Von Essen SG, Mathisen T, Wyatt TA. Hog barn dust extract stimulates IL-8 and IL-6 release in human bronchial epithelial cells via PKC activation. *J Appl Physiol* (2002) 93:289–296. doi: 10.1152/japplphysiol.00815.2001
32. Nordgren TM, Wyatt TA, Sweeter J, Bailey KL, Poole JA, Heires AJ, Sisson JH, Romberger DJ. Motile cilia harbor serum response factor as a mechanism of environment sensing and injury response in the airway. *American Journal of Physiology-Lung Cellular and Molecular Physiology* (2014) 306:L829–L839. doi: 10.1152/ajplung.00364.2013
33. Romberger DJ, Heires AJ, Nordgren TM, Souder CP, West W, Liu X, Poole JA, Toews ML, Wyatt TA. Proteases in agricultural dust induce lung inflammation through PAR-1 and PAR-2 activation. *American Journal of Physiology-Lung Cellular and Molecular Physiology* (2015) 309:L388–L399. doi: 10.1152/ajplung.00025.2015
34. Bankhead P, Loughrey MB, Fernández JA, Dombrowski Y, McArt DG, Dunne PD, McQuaid S, Gray RT, Murray LJ, Coleman HG, et al. QuPath: Open source software for digital pathology image analysis. *Sci Rep* (2017) 7:16878. doi: 10.1038/s41598-017-17204-5
35. Burr AC, Velazquez J V, Ulu A, Kamath R, Kim SY, Bilg AK, Najera A, Sultan I, Botthoff JK, Aronson E, et al. Lung Inflammatory Response to Environmental Dust Exposure in Mice Suggests a Link to Regional Respiratory Disease Risk. *J Inflamm Res* (2021) Volume 14:4035–4052. doi: 10.2147/JIR.S320096
36. Ulu A, Velazquez J V., Burr A, Sveiven SN, Yang J, Bravo C, Hammock BD, Nordgren TM. Sex-Specific Differences in Resolution of Airway Inflammation in Fat-1 Transgenic Mice Following Repetitive Agricultural Dust Exposure. *Front Pharmacol* (2022) 12: doi: 10.3389/fphar.2021.785193
37. Yin G, Zhao C, Pei W. Crosstalk between macrophages and innate lymphoid cells (ILCs) in diseases. *Int Immunopharmacol* (2022) 110:108937. doi: 10.1016/j.intimp.2022.108937
38. Lechner AJ, Driver IH, Lee J, Conroy CM, Nagle A, Locksley RM, Rock JR. Recruited Monocytes and Type 2 Immunity Promote Lung Regeneration following Pneumonectomy. *Cell Stem Cell* (2017) 21:120-134.e7. doi: 10.1016/j.stem.2017.03.024
39. Ardain A, Porterfield JZ, Kløverpris HN, Leslie A. Type 3 ILCs in Lung Disease. *Front Immunol* (2019) 10:92. doi: 10.3389/fimmu.2019.00092
40. Öz HH, Cheng E-C, Di Pietro C, Tebaldi T, Biancon G, Zeiss C, Zhang P-X, Huang PH, Esquibies SS, Britto CJ, et al. Recruited monocytes/macrophages drive pulmonary neutrophilic inflammation and irreversible lung tissue remodeling in cystic fibrosis. *Cell Rep* (2022) 41:111797. doi: 10.1016/j.celrep.2022.111797
41. Guillien A, Puyraveau M, Soumagne T, Guillot S, Rannou F, Marquette D, Berger P, Jouneau S, Monnet E, Mauny F, et al. Prevalence and risk factors for COPD in farmers: a cross-sectional controlled study. *Eur Respir J* (2016) 47:95–103. doi: 10.1183/13993003.00153-2015
42. Reeb-Whitaker CK, Bonauto DK. Respiratory disease associated with occupational inhalation to hop (Humulus lupulus) during harvest and processing. *Annals of Allergy, Asthma & Immunology* (2014) 113:534–538. doi: 10.1016/j.anai.2014.07.029
43. Croft DP, Zhang W, Lin S, Thurston SW, Hopke PK, van Wijngaarden E, Squizzato S, Masiol M, Utell MJ, Rich DQ. Associations between Source-Specific Particulate Matter and Respiratory Infections in New York State Adults. *Environ Sci Technol* (2020) 54:975–984. doi: 10.1021/acs.est.9b04295

44. Molfino NA, Jeffery PK. Chronic obstructive pulmonary disease: Histopathology, inflammation and potential therapies. *Pulm Pharmacol Ther* (2007) 20:462–472. doi: 10.1016/j.pupt.2006.04.003
45. Shakeel I, Ashraf A, Afzal M, Sohal SS, Islam A, Kazim SN, Hassan MI. The Molecular Blueprint for Chronic Obstructive Pulmonary Disease (COPD): A New Paradigm for Diagnosis and Therapeutics. *Oxid Med Cell Longev* (2023) 2023:2297559. doi: 10.1155/2023/2297559
46. Kapellos TS, Bonaguro L, Gemünd I, Reusch N, Saglam A, Hinkley ER, Schultze JL. Human Monocyte Subsets and Phenotypes in Major Chronic Inflammatory Diseases. *Front Immunol* (2019) 10: doi: 10.3389/fimmu.2019.02035
47. van Furth R, Cohn ZA. THE ORIGIN AND KINETICS OF MONONUCLEAR PHAGOCYTES. *J Exp Med* (1968) 128:415–435. doi: 10.1084/jem.128.3.415
48. Wolf AA, Yáñez A, Barman PK, Goodridge HS. The Ontogeny of Monocyte Subsets. *Front Immunol* (2019) 10: doi: 10.3389/fimmu.2019.01642
49. Zawada AM, Rogacev KS, Rotter B, Winter P, Marell R-R, Fliser D, Heine GH. SuperSAGE evidence for CD14++CD16+ monocytes as a third monocyte subset. *Blood* (2011) 118:e50–e61. doi: 10.1182/blood-2011-01-326827
50. Passlick B, Flieger D, Ziegler-Heitbrock H. Identification and characterization of a novel monocyte subpopulation in human peripheral blood. *Blood* (1989) 74:2527–2534. doi: 10.1182/blood.V74.7.2527.2527
51. Ziegler-Heitbrock L, Ancuta P, Crowe S, Dalod M, Grau V, Hart DN, Leenen PJM, Liu Y-J, MacPherson G, Randolph GJ, et al. Nomenclature of monocytes and dendritic cells in blood. *Blood* (2010) 116:e74–e80. doi: 10.1182/blood-2010-02-258558
52. Shahid F, Lip GYH, Shantsila E. Role of Monocytes in Heart Failure and Atrial Fibrillation. *J Am Heart Assoc* (2018) 7: doi: 10.1161/JAHA.117.007849
53. Öz HH, Cheng E-C, Di Pietro C, Tebaldi T, Biancon G, Zeiss C, Zhang P-X, Huang PH, Esquibies SS, Britto CJ, et al. Recruited monocytes/macrophages drive pulmonary neutrophilic inflammation and irreversible lung tissue remodeling in cystic fibrosis. *Cell Rep* (2022) 41:111797. doi: 10.1016/j.celrep.2022.111797
54. Kratofil RM, Kubes P, Deniset JF. Monocyte Conversion During Inflammation and Injury. *Arterioscler Thromb Vasc Biol* (2017) 37:35–42. doi: 10.1161/ATVBAHA.116.308198
55. Williams H, Mack C, Baraz R, Marimuthu R, Naralashetty S, Li S, Medbury H. Monocyte Differentiation and Heterogeneity: Inter-Subset and Interindividual Differences. *Int J Mol Sci* (2023) 24:8757. doi: 10.3390/ijms24108757
56. Rodero MP, Poupel L, Loyher P-L, Hamon P, Licata F, Pessel C, Hume DA, Combadière C, Boissonnas A. Immune surveillance of the lung by migrating tissue monocytes. *Elife* (2015) 4:e07847. doi: 10.7554/eLife.07847
57. Mildner A, Marinkovic G, Jung S. Murine Monocytes: Origins, Subsets, Fates, and Functions. *Microbiol Spectr* (2016) 4: doi: 10.1128/microbiolspec.MCHD-0033-2016
58. Schyns J, Bai Q, Ruscitti C, Radermecker C, De Schepper S, Chakarov S, Farnir F, Pirottin D, Ginhoux F, Boeckxstaens G, et al. Non-classical tissue monocytes and two functionally distinct populations of interstitial macrophages populate the mouse lung. *Nat Commun* (2019) 10:3964. doi: 10.1038/s41467-019-11843-0
59. Hänninen A, Maksimow M, Alam C, Morgan DJ, Jalkanen S. Ly6C supports preferential homing of central memory CD8 $^{+}$ T cells into lymph nodes. *Eur J Immunol* (2011) 41:634–644. doi: 10.1002/eji.201040760

60. Cui TX, Brady AE, Fulton CT, Zhang Y-J, Rosenbloom LM, Goldsmith AM, Moore BB, Popova AP. CCR2 Mediates Chronic LPS-Induced Pulmonary Inflammation and Hypoalveolarization in a Murine Model of Bronchopulmonary Dysplasia. *Front Immunol* (2020) 11: doi: 10.3389/fimmu.2020.579628
61. Schwab AD, Wyatt TA, Moravec G, Thiele GM, Nelson AJ, Gleason A, Schanze O, Duryee MJ, Romberger DJ, Mikuls TR, et al. Targeting transitioning lung monocytes/macrophages as treatment strategies in lung disease related to environmental exposures. *Respir Res* (2024) 25:157. doi: 10.1186/s12931-024-02804-3
62. Heires AJ, Samuelson D, Villageliu D, Nordgren TM, Romberger DJ. Agricultural dust derived bacterial extracellular vesicle mediated inflammation is attenuated by DHA. *Sci Rep* (2023) 13:2767. doi: 10.1038/s41598-023-29781-9
63. Klein SL, Flanagan KL. Sex differences in immune responses. *Nat Rev Immunol* (2016) 16:626–638. doi: 10.1038/nri.2016.90
64. Varghese M, Clemente J, Lerner A, Abrishami S, Islam M, Subbaiah P, Singer K. Monocyte Trafficking and Polarization Contribute to Sex Differences in Meta-Inflammation. *Front Endocrinol (Lausanne)* (2022) 13: doi: 10.3389/fendo.2022.826320
65. So J, Tai AK, Lichtenstein AH, Wu D, Lamon-Fava S. Sexual dimorphism of monocyte transcriptome in individuals with chronic low-grade inflammation. *Biol Sex Differ* (2021) 12:43. doi: 10.1186/s13293-021-00387-y

Chapter 4

Repetitive Inhaled Dust Exposure Protects from *S. pneumoniae* Infection and Mortality[3]

[3] Manuscript submitted for publication 07/31/25 in Infection and Immunity

Summary

The temporal nature of the immune response to inhaled organic dusts (ODE) leads to the development of respiratory diseases such as asthma and chronic obstructive pulmonary disease (COPD). Dysregulation of normal inflammatory to resolution processes are critical to disease development, and can pre-dispose individuals to opportunistic respiratory pathogens, such as *Streptococcus pneumoniae*. An obligate extracellular bacterium, *Streptococcus pneumoniae* is the leading cause of community acquired pneumonia within the United States and is linked to asthmatic and COPD exacerbations. Whether the chronic inflammatory environment created by repetitive ODE pre-disposes individuals to *S. pneumoniae* infection is unknown. Utilizing an established murine model of repetitive ODE, we sought to determine if and how the inflammatory nature of ODE alters susceptibility to secondary infection with *S. pneumoniae*. We found that ODE prior to challenge with *S. pneumonia* led to complete clearance of the bacterium from the airway, lung, and spleen tissue. Histopathologic analysis revealed profound induction of iBALT structures within the lung tissue in dust pre-exposed animals secondarily challenged with *S. pneumoniae*. Cellular analysis using flow cytometry suggest that ODE induces effector memory $CD4^+$ and terminally differentiated effector memory reactivated (TEMRA) $CD8^+$ T cell populations and ILC1s within the lung, without any profound additional innate immune cell population alterations. Within the airway, $CD4^+$ TEMRAs were primarily increased. When fatally challenged with an increased dose of *S. pneumoniae*, pre-ODE mice were protected from the 50% mortality rate and exhibited reduced recoverable CFU in lung and spleen, but not BALF, samples. Cellularly, the primary immune cell population increased in the fatal challenge was interstitial and alveolar macrophage populations, and effector memory $CD8^+$ T cells. Collectively these data implicate a role for ODE in training lymphocyte populations to enhance

efficacy in *S. pneumoniae* clearance and reveals a macrophage-specific role for cell populations in the airway during fatal *S. pneumoniae* challenge.

Introduction

Inhalational organic dust exposure (ODE) leads to development of asthma and chronic obstructive pulmonary disease (COPD), disproportionately impacting workers in the agricultural and livestock industries (1–8). The inflammatory response to ODE is meant to be a self-limiting process with three canonical steps leading to resolution; First, cessation of neutrophil influx, followed by induced apoptosis of neutrophils and neutrophil extracellular traps (NETs), and finally macrophage-mediated clearance and stimulation of tissue repair programs (9,10). Within a chronically inflamed environment, such as that created by repetitive ODE, this normally stepwise process fails to progress, creating a prolonged inflammatory environment within the lung, characterized by sustained neutrophil and lymphocyte infiltration, decreases in inflammation resolution kinetics, and potentially increased susceptibility to secondary infection (11–14).

Streptococcus pneumoniae (*S. pneumoniae*) is an obligate, extracellular, and opportunistic bacterial pathogen (15). As a leading cause of community acquired pneumonia, sepsis, and bacterial meningitis, the bacterium is of significant public health importance (15,16). The commensal nature of *S. pneumoniae* requires an altered immune state for non-resident organ colonization, such as concurrent viral infection, immunosuppressive treatment, or development and maintenance of a chronic inflammatory environment within the respiratory tract (15,17). Repetitive ODE creates a sustained inflammatory environment, and epidemiologic evidence demonstrates increased incidence of bacterial pneumonia in individuals who work or live in close proximities to a farm (18–22). How, and if, concurrent exposures increase disease susceptibility, and the manner in which ODE-induced inflammation predisposes an organism to secondary infection remains uninvestigated via experimental means.

Utilizing an established murine model of repetitive (3 week) ODE followed by infection of *Streptococcus pneumoniae*, we herein probe the immune response to ODE followed by infection with *S. pneumoniae*, revealing that ODE prior to infection increases central and effector memory lymphocytes. Additionally, fatal infection demonstrates a more myeloid-skewed response for dust-induced protection, suggesting that the duality of the immune response in ODE-exposed individuals is infection severity-dependent.

Methods

Preparation of Dust Extracts

Dusts were collected as previously described from swine confinement facilities in the Midwest, United States, and stored at -20 ºC until preparation. Aqueous dust extracts were prepared as previously described (23); in brief, 5 g of dust was mixed into 50 mL of Hanks Balanced Salt Solution (HBSS) (HyClone, Logan, UT) at room temperature for 1 hour. The resulting extract was centrifuged at 2500 x g for 20 minutes at 4 ºC. Supernates were transferred to new tubes, recentrifuged at 2500 x g for 20 minutes at 4 ºC, and subsequent supernates were sterile filtered with a 0.22 um filter to produce 100% dust extract (DE). Aliquots were stored at -20 ºC until use. Formulations of 12.5% DE were prepared for animal installations by diluting 100% DE with phosphate buffered saline (PBS) (Fisher Scientific, Waltham, MA). A dose of 12.5% DE has been previously demonstrated as an appropriate dose for generating substantial lung inflammation with a single instillation and promoting histopathological markers of lung disease with repetitive exposure, while not leading to significant weight loss, lethargy, or other moribund phenotypes (23–29).

Animal Husbandry and Instillations

Animal protocols were reviewed and approved by the Institutional Animal Care and Use Committee at Colorado State University (Protocol #2887). 12 to 16-week-old C57BL/6 (WT) male and female mice (Jackson Labs, Bar Harbor, ME) were utilized and allowed *ad libitum* food and water. For intranasal instillations, mice were lightly anesthetized under 1.6-2.2% isoflurane and received 50 uL of the 12.5% DE or PBS vehicle control for 3 weeks (total of 14 installations, provided 5 days/week).

Streptococcus pneumoniae Growth and Infection

Streptococcus pneumoniae (*S. pneumoniae*) strain serotype 2 strain D39 was grown to log phase in Todd Hewitt Broth (Fisher Scientific, Cat# DF0492176) with 0.5% yeast extract (Fisher Scientific, Cat#212750) and 50 ug/mL streptomycin at 37°C and 5% CO_2 without shaking. Resulting bacteria were resuspended in PBS at a final concentration of 10^7 or 1.2^8 CFU per infectious dose of 50 uL. Infections were completed under light isoflurane intranasally. For plate growth to determine colony forming unit determination, samples were serially diluted and streaked onto tryptic soy broth (TSB) (Fisher Scientific, Cat# ICN1010717) plates with 5 ug/mL neomycin, 50 ug/mL streptomycin, and freshly spread catalase (Worthington Chemical, Cat#LS001898). Plates were grown overnight at 37°C and 5% CO_2 and resulting colonies counted via ImageJ.

Organ Extraction and Lung Histopathology

Mice were euthanized via isoflurane overdose followed by a cervical dislocation. A cannula was inserted into the trachea and bronchoalveolar lavage fluid (BALF) was collected with three washes of 1 mL of ice cold HBSS (HyClone, Logan, UT). Spleens were extracted and processed for flow cytometry and CFU determinations (detailed below). The left lung was tied off, separated, and utilized for flow cytometry assays, while the remaining right lobe was extracted, inflated with 10% neutral buffered formalin (NBF) (Cancer Diagnostics Inc, Durham, NC), and hung under 20 cm of pressure overnight while bathed in 10% NBF. The fixed right lungs were inserted into tissue cassettes and sent to the Colorado State University Veterinary Diagnostic Laboratory Experimental Pathology Facility (EPF) for paraffin embedding and slicing. Resulting slides were stained following deparaffinization and a graded ethanol rehydration with

hematoxylin and eosin (H&E). Slides were blinded and imaged at 40X magnification using the Vectra Polaris Automated Quantitative Pathology Imaging System (Akoya Biosciences, Marlborough, MA). Images were imported and visualized in QuPath for pathological scoring (30). H&E-stained right lung lobe sections were scored using a modified version of an established scoring criteria published previously (**Supplementary Table 4.1**) (31). All slides remained blinded and then 4 parameters were scored: the amount of immune cell aggregates, the presence of perivascular and peribronchiolar inflammation, alveolar space cellularity, and metaplasia of goblet cells. A mean pathology score consisted of the averaged scores in all 4 parameters.

Sample Processing and Colony Forming Unit Determination

BALF was centrifuged at 350 x g for 8 minutes at 4°C. Resulting supernatant was removed and centrifuged at 12,000 x g for 10 minutes to pellet bacteria for CFU. The remaining BALF cell pellet was utilized for subsequent flow cytometry applications (detailed below). Extracted left lung and spleens were gently mechanically dissociated utilizing a Bead Mill 24 (Fisherbrand, Waltham, MA) with metal bead lysing matrix tubes (1.95 speed, 6 cycles, 15 second cycle, 3 second rest) (MP Biomedical, Santa Anna, CA) and then strained and rinsed with 1 mL of HBSS + 0.25% sodium azide through a 70 µm filter to create a single cell suspension (SCS). The resulting SCSs were centrifuged at 350 x g for 8 minutes at 4°C, with supernatant fractions removed and centrifuged at 12,0000 x g at 4°C for bacterial pellet formation. Remaining cell pellets were used for subsequent flow cytometry applications (detailed below). Bacterial pellets were resuspended in PBS, serially diluted and plated on TSB plates with 5 ug/mL neomycin, 50 ug/mL streptomycin, and 130 uL of freshly spread catalase (Worthington Chemical,

Cat#LS001898). Plates were grown overnight at 37°C and 5% CO_2 and resulting colonies counted via ImageJ to determine recoverable CFU.

Flow Cytometry Analysis of BALF and Organ Single Cell Suspensions

BALF, lung, and spleen SCS were split into 3 portions for staining with a T cell panel, myeloid panel, and innate lymphoid cell panel (**Supplementary Table 4.2**). Regardless of panel, samples were initially resuspended in viability dye at the appropriate concentration for 30 minutes at 4 ºC protected from light. One mL of flow buffer (HBSS+ 1% BSA, 0.25% sodium azide) was added, and the cells were centrifuged at 400 x g for 8 minutes at 4ºC. Resulting supernates were aspirated off and cells were resuspended in TruStain FcX (BioLegend, San Diego, CA, 1:200) for 15 minutes at room temperature, protected from light. Appropriate volumes of fluorophore antibody cocktail (**Supplementary Table 4.2**) were then added and incubated for 30 minutes at room temperature protected from light. Cells were washed and resuspended in BD Cytofix/Cytoperm (BD Technologies, East Rutherford, NJ) for 30 minutes at 4 ºC protected from light. Cells were washed in BD Perm/Wash (BD Biosciences, Franklin Lakes, NJ) and centrifuged at 500 x g for 8 minutes at 4ºC. Samples were then resuspended in intracellular staining cocktails and incubated for 30 minutes protected from light. Cells were then washed in BD Perm/Wash and resuspended in flow buffer for analysis. Stained cells were acquired on a custom 3 Laser Attune NxT Flow Cytometer (Thermofisher Scientific, Waltham, MA). Single color compensation beads (Cat#424602, Biolegend, San Diego, CA) were utilized for compensation control and fluorescent minus one samples (FMOs) were utilized for appropriate gate placement. Resulting data were analyzed using FlowJo Version 10 (Treestar, Ashland, OR) software.

Statistics

GraphPad Prism software (Version 10, La Jolla, CA) was utilized to perform ROUT outlier analysis (Q = 1%), with resulting data analyzed via two-way ANOVA tests to determine the main effects of exposure and infection. Fisher's LSD method was used to perform post-hoc multiple comparisons to identify significant differences between groups. Mann-Whitney U was utilized for stand-alone between group comparisons in SP^{Hi} and DP^{Hi} infection outcomes. Differences between groups were considered significant if the p value ≤ 0.05. For Spearman correlation analysis, all values of designated parameters were included and a two-tailed test with a 95% confidence interval was utilized. Non-significant values are not denoted in figures, unless otherwise noted. Data are represented with median ± confidence intervals on all figures unless otherwise noted.

Results

Infection of C57BL/6 Mice with S. pneumoniae Following Repetitive ODE Leads to Complete Clearance of Bacterial Infection.

Male and female mice pre-exposed to 3 weeks of dust extract (DE) or saline (PBS) control were given 3 days rest to allow DE-induced cell populations to reduce, as previously published (32). Mice were infected with *S. pneumoniae* and euthanized on the third day post infection (DPI) **(Figure 4.1A)**. BALF, right lung, and spleen were homogenized and plated for colony forming unit determination **(Figure 4.1B)**, while cell suspensions were utilized for flow cytometry and the left lung for histopathology **(Figure 4.1B**). CFU of *S. pneumoniae* was recovered in BALF, lung tissue, and spleen of saline pre-exposed animals, demonstrating systemic dissemination of *S. pneumoniae* **(Figure 4.1C)**. No CFU was recoverable from mice pre-exposed to DE, regardless of sample.

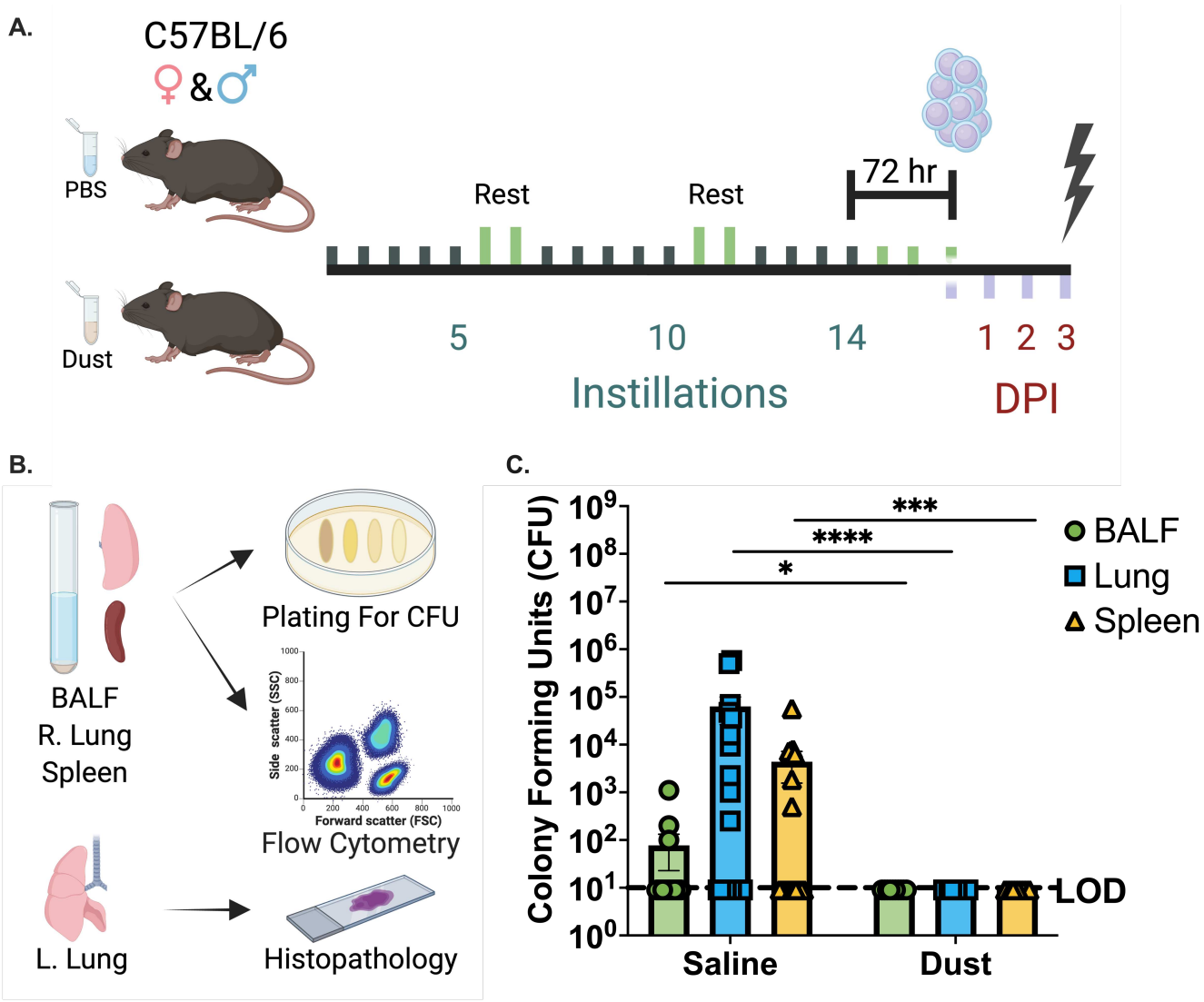

Figure 4.1. Experimental schematic that depicts instillation of C57BL/6 male and female mice with saline (PBS) or dust for 3 weeks intranasally before a 3-day recovery before infection with 10^7 CFU of *Streptococcus pneumoniae* strain D39. Mice were euthanized at 3 days post infection (DPI) **(A.)**. Bronchoalveolar lavage fluid, right lung, and spleen were utilized for CFU determination, while the cells from these samples underwent flow cytometry for immunophenotyping. The left lung was stained and utilized for histopathology **(B.)**. Colony forming units recovered from BALF, lung, and spleen in saline and dust exposed animals at 3 DPI **(C.)**. Mann-Whitney U test, *p<0.05, **p<0.01, ***p<0.001, ****p<0.0001.

Histopathologic Analysis Demonstrates a Dust-induced Increase in iBALT Formation but Similar Inflammatory Scores Otherwise

To further explore potential mechanisms by which DE pre-exposure demonstrates a seemingly protective effect on subsequent *S. pneumoniae* infection, we probed the pathologic consequences of DE-*S. pneumoniae* (DP) combinations via a blinded scoring methodology **(Supplementary Table 4.2)**. Gross examination revealed that DE-exposure induced iBALT formation, independent of *S. pneumoniae* infection status **(Figure 4.2A)**. Saline-*S. pneumoniae* (SP) lungs demonstrated significant alveolar inflammation **(Figure 4.2A)**. When quantified, dust-saline (DS), saline-*S. pneumoniae* (SP), and dust-*S. pneumoniae* (DP) mice exhibited significant increases in peribronchial and alveolar inflammation, goblet cell metaplasia, and averaged pathology scores compared to saline-saline (SS) mice **(Figure 4.2 B-D, F, G)**. Increased scores for all parameters except perivascular and alveolar inflammation were found in DP compared to SP lungs **(Figure 4.2 B-D, F)**. DS and DP groups had increase iBALT scores compared to saline-*S. pneumoniae* mice **(Figure 4.2F)**. Total numbers of immune cell aggregates were increased in DS and DP compared to SS and SP groups **(Figure 4.2E)**. DP mice demonstrated increased averaged pathology scores compared to all other groups **(Figure 4.2G)**. The DP group exhibited increased average pathology scores compared to both SP and DS groups, demonstrating a combinatory impact on pathologic score of dust and *S. pneumoniae* infection **(Figure 4.2G)**. Given these histopathologic insights, we hypothesized an alteration of lung resident and recruited immune cells contributes to the protective impact of ODE on secondary bacterial challenge.

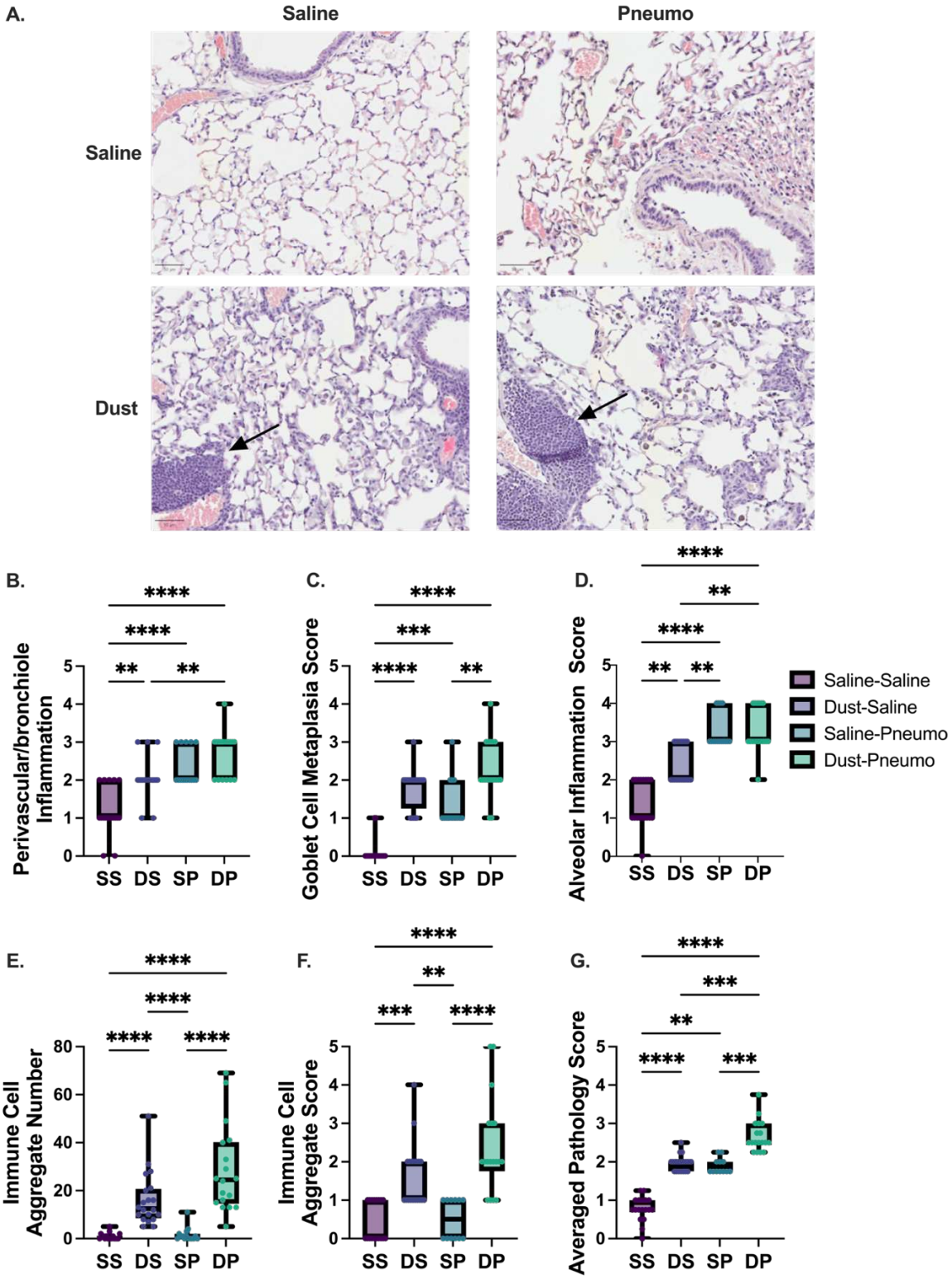
A.
Saline
Pneumo
Saline
Dust
B.
Perivascular/bronchiole Inflammation
C.
Goblet Cell Metaplasia Score
D.
Alveolar Inflammation Score
Saline-Saline
Dust-Saline
Saline-Pneumo
Dust-Pneumo
E.
Immune Cell Aggregate Number
F.
Immune Cell Aggregate Score
G.
Averaged Pathology Score
SS DS SP DP

Figure 4.2. Representative pathology images of right lung stained with H&E for saline-saline, dust-saline, saline-*S. pneumoniae* and dust-*S. pneumoniae* exposed mice **(A.)**. Perivascular/bronchiole inflammation **(B.)**, goblet cell metaplasia **(C.)**, alveolar inflammation **(D.)**, immune cell aggregate number **(E.)**, immune cell aggregate score **(F.)**, and averaged pathology **(G.)** scores. Line on graphs denote mean value, while range demonstrates minimum and maximum scores for each group. SS= saline-saline, DS=dust-saline, SP=saline-*S. pneumoniae*, DP=dust-*S. pneumoniae*. Arrows denote immune cell aggregate formation. Kruskal Wallis test with Dunn's Multiple comparisons for post-hoc analysis. *p<0.05, **p<0.01, ***p<0.001, ****p<0.0001.

Pre-Exposure to Dust Differentially Generates Effector and Central Memory Lymphocytes

Within the lung tissue, our findings of iBALT development prompted us to examine the T-lymphocyte repertoire as a potential driver of dust-induced *S. pneumoniae* infection protection. We developed a flow cytometry panel to examine these T cell populations (**Figure 4.3A**) via the repurposing of a spleen-based T cell immunophenotyping panel (33). Total $CD4^+$ counts were elevated in SP compared to SS, and SP $CD4^+$s were increased compared to DP **(Figure 4.3B)**. $CD3^+/CD4^+/FoxP3^+$ T-regulatory (Treg) populations followed similar trends, seemingly drive by the parent $CD4^+$ count numbers, but when plotted as a percentage to avoid parent population impact, Treg percentage was decreased in DS and increased in SP compared to SS groups, with no statistical significance in the DP group **(Supplementary Figure 4.1A)**. $CD8^+$ T cell counts were elevated in response to *S. pneumoniae* infection, regardless of PBS or ODE pre-exposure compared to SS **(Figure 4.3D)**. SP populations were increased compared to DP, and DP was increased compared to DS, suggesting that *S. pneumoniae* infection, regardless of pre-exposure

status was a driver of $CD8^+$ T cell number increases **(Figure 4.3D)**. These elevations carried forward in delineated T cell subsets **(Supplementary Figure 4.1B-I)**, so percentages of parent population were utilized to observe population level shifts. Naïve populations of both $CD4^+$ and $CD8^+$ T cells were reduced in DS, SP, and DP mice compared to SS mice **(Figure 4.3E, G)**. pre-exposure to dust followed by *S. pneumoniae* infection significantly reduced naïve $CD4^+$ and $CD8^+$ T cell populations compared to PBS pre-exposure and *S. pneumoniae* infection **(Figure 4.3E, G)**. Central memory $CD4^+$ T cells were significantly increased in SP compared to all other exposure-by-infection groups **(Figure 4.3F)**. Dust pre-exposure increased effector memory $CD4^+$ T cell proportions significantly compared to saline pre-exposure, regardless of infection status **(Figure 4.3I)**. $CD4^+$ EMRA proportions increased in DS, SP, and DP compared to SS groups **(Figure 4.3J)**. $CD8^+$ T cells yielded altered proportions compared to their $CD4^+$ counterparts. Central memory $CD8^+$ populations decreased in DS and DP compared to SS **(Figure 4.3H)**. DP was significantly increased compared to DS, suggesting a pneumo-based reliance on porportion alterations **(Figure 4.3H)**. Effector memory $CD8^+$ T cells were increased in all exposure-by-infection groups compared to SS **(Figure 4.3K)**. Intriguingly, DS was signifianctly reduced compared to DP, suggesting a *S. pneumoniae*-based role in population maintenance. $CD8^+$ EMRA populations were signifianctly elevated in DS and DP compared to SS, and DP compared to SP, suggesting a dust-based role in $CD8^+$ EMRA population generation **(Figure 4.3L)**. Collectivley these results demonstrate a dust-based signature in generating specific effector memory $CD4^+$ populations and terminally differentiated effector memory $CD8^+$ populations, which may play a role in the dust-induced *S. pneumoniae* clearance. Additionally, a role for dust-induced maintence of effector memory generation against *S. pneumoniae* infection is extremely likely.

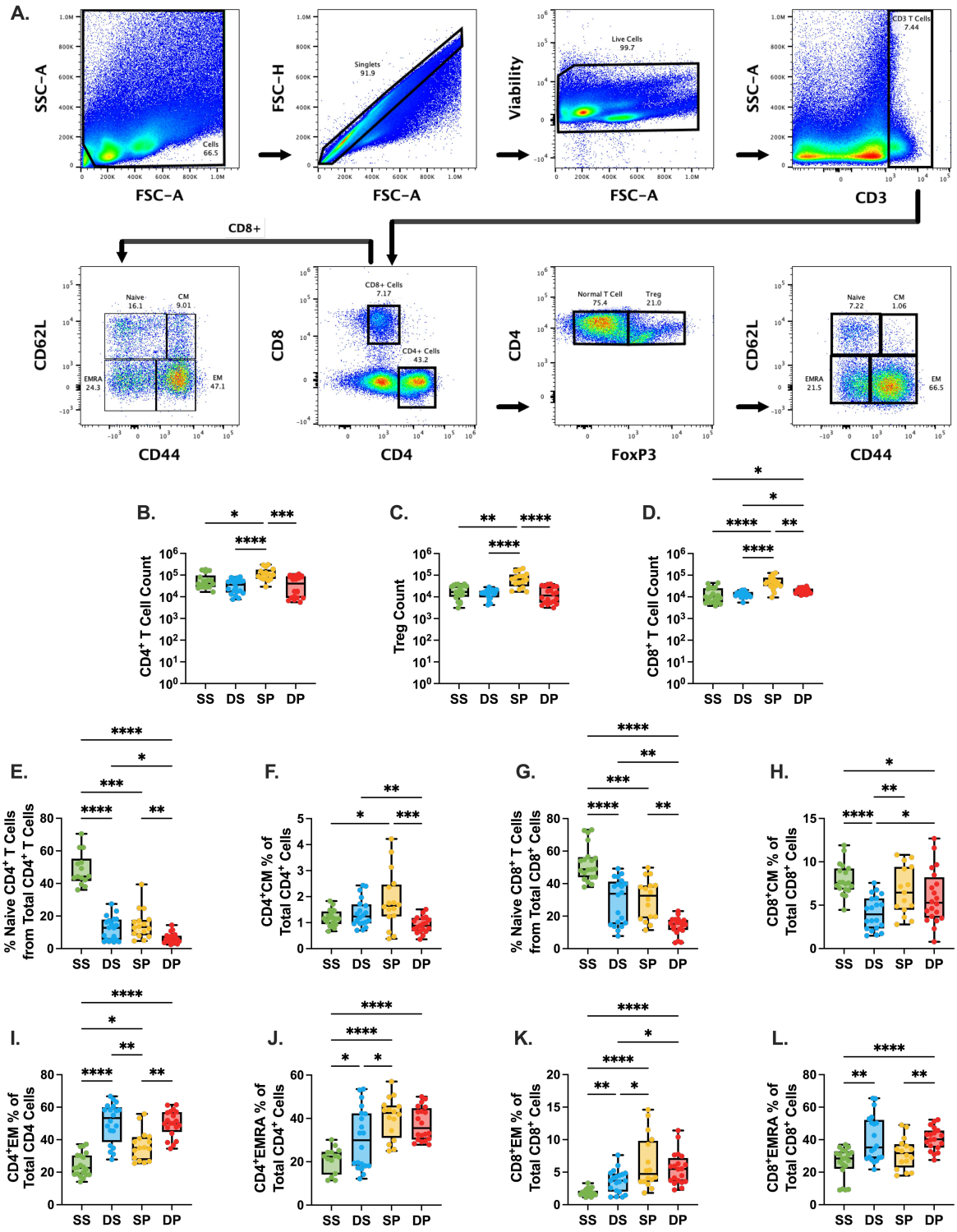
A.
SSC-A
FSC-A
Cells
66.5
FSC-H
Singlets
91.9
Viability
Live Cells
99.7
CD3 T Cells
7.44
CD3
CD8+
CD62L
CD44
Naive
16.1
CM
9.01
EMRA
24.3
EM
47.1
CD8
CD4
CD8+ Cells
7.17
CD4+ Cells
43.2
FoxP3
Normal T Cell
75.4
Treg
21.0
Naive
7.22
CM
1.06
EMRA
21.5
EM
66.5
B.
CD4+ T Cell Count
C.
Treg Count
D.
CD8+ T Cell Count
SS DS SP DP
E.
% Naive CD4+ T Cells from Total CD4+ T Cells
F.
CD4+CM % of Total CD4+ Cells
G.
% Naive CD8+ T Cells from Total CD8+ Cells
H.
CD8+CM % of Total CD8+ Cells
I.
CD4+EM % of Total CD4 Cells
J.
CD4+EMRA % of Total CD4+ Cells
K.
CD8+EM % of Total CD8+ Cells
L.
CD8+EMRA % of Total CD8+ Cells

Figure 4.3. Representative flow cytometry gating strategy for identification of T cells and their subsets from lung SCS **(A.)**. Total $CD4^+$ T cells **(B.)**, $FoxP3^+$ T-regulatory cells **(C.)**, and $CD8^+$ T cell **(D.)** numbers enumerated from lung single cell suspension. Percentage of naïve **(E.)**, central memory **(F.)**, effector memory **(I.)**, and terminal effector memory **(J.)** from total $CD4^+$ T cells. Percentage of naïve **(G.)**, central memory **(H.)**, effector memory **(K.)**, and terminal effector memory **(L.)** from total $CD8^+$ T cells. Box and whisker plots depict minimum to maximum values with all data points shown and the midline at the median value. SS= saline-saline, DS=dust-saline, SP=saline-*S. pneumoniae*, DP=dust-*S. pneumoniae*. Kruskal Wallis test with Dunn's Multiple comparisons for post-hoc analysis. *p<0.05, **p<0.01, ***p<0.001, ****p<0.0001.

Innate Lymphoid but not Myeloid Cell Population Frequencies were Differentially Altered in Mice Pre-exposed to Dust before S. pneumoniae Infection Compared to No Pre-exposure and Infection Alone

Given the requirement of innate immune cells in clearing and modulating adaptive-mediated responses to pathogens, we probed population shifts of these cells in response to dust exposure and *S. pneumoniae* infection in the lung tissue compartment. Innate lymphoid cell (ILC) populations were successfully identified **(Supplementary Figure 4.2A)**, but no change in population was noted for ILC2, NCR+ ILC3, and only an increase in the DP group of NCR- ILC3 was demonstrated compared to SS **(Supplementary Figure 4.2 C-E)**. ILC1 populations were significantly increased in the DP group compared to SS, DS, and SP groups **(Supplementary Figure 4.2B)**. Myeloid lineage innate immune cells were also investigated **(Supplementary Figure 4.2F)**. Here, no myeloid lineage cell populations exhibited increases in counts in the DP group compared to the SP group **(Supplementary Figure 4.2G-M)**. Neutrophil

and dendritic cell counts were driven by *S. pneumoniae* infection, irrespective of dust pre-exposure **(Supplementary Figure 4.2G, H)**. Alveolar macrophage counts increased only within the DS group, consistent with the initiation of inflammation resolution processes **(Supplementary Figure 4.2I)**. Interstitial macrophages were increased in all exposure-by-infection groups compared to SS **(Supplementary Figure 4.2J)**. Classical, intermediate, and non-classical monocyte populations all increased in SP and DP groups, but not DS groups compared to SS **(Supplementary Figure 4.2K-M)**.

Correlation Analysis Reveals Requirement of Innate and Adaptive Responses to Drive Exposure-induced CFU Reduction.

Given these findings of primarily lymphoid-specific alterations induced by dust in the lung, we were curious how differential cell populations identified correlated with CFU burden reductions, and pathologic scoring within the lung. As expected, all pathologic scoring parameters correlated with each other, but the correlative driver between pathology score was dust exposure, not *S. pneumoniae* infection **(Figure 4.4)**. BALF, lung, and spleen CFU were positively correlated with each other **(Figure 4.4)**. Pathologic scores within the lung inversely correlated with Naïve $CD4^+$ and $CD8^+$ T cell percentages, as well as CFU **(Figure 4.4)**. Exposure and *S. pneumoniae* infection synergistically correlated with $CD4^+$ and $CD8^+$ EM % **(Figure 4.4)**, findings not revealed in cell percentages. Conflicting correlations from exposure and infection were found in $CD4^+$ and $CD8^+$ count, as well as Treg and dendritic cell count **(Figure 4.4)**. Intriguingly, all ILC counts only exhibited weak correlations, despite elevated ILC1s being 1 of the 2 cell populations found increased in DP compared to SP groups **(Figure 4.4)**. The strongest correlates of increasing Lung CFU were dendritic cell, classical monocyte, intermediate monocyte, and

neutrophil counts, and these populations were specifically reliant on *S. pneumoniae* infection **(Figure 4.4)**. No identified population increases correlated with reduced CFU, lung or otherwise **(Figure 4.4)**. These correlative findings reveal an increasingly complex cellular interplay involved in CFU reduction within the lung.

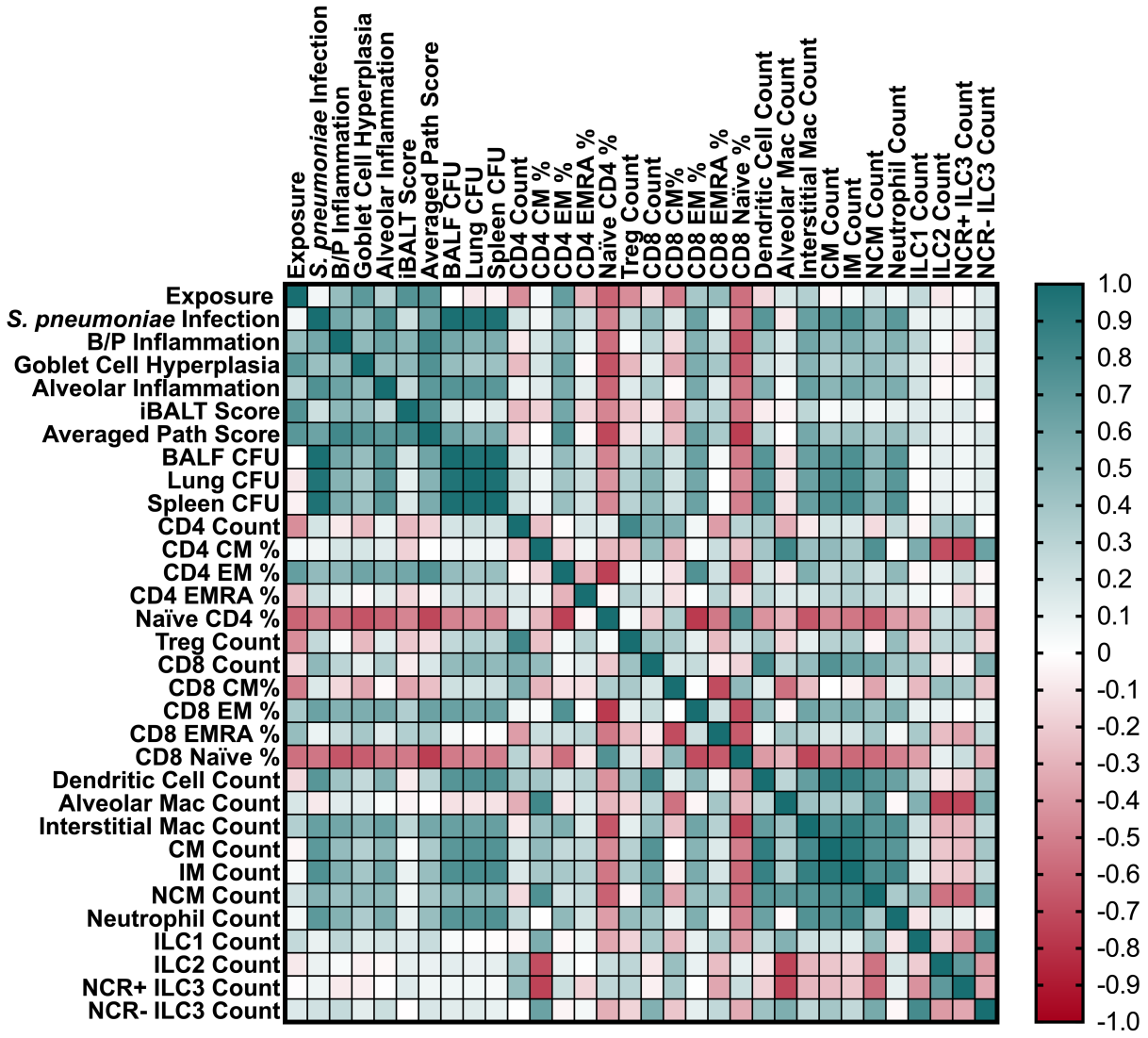

Figure 4.4. Heatmap of Spearman Correlations for pathology, infection, exposure, and major cell populations identified within lung tissue. Spearman R value is denoted on the scale bar. CM = classical monocyte, IM = intermediate monocyte, NCM = non-classical monocyte.

Given these findings of dust-induced increases in "trained" lymphocyte populations and the correlation of myeloid cells in response to increased pathology, and CFU, it is likely that there is a coordinated adaptive-to-innate clearance mechanism involved in the dust-associated increased clearance observed. We examined these populations at the site of successful clearance: the airway. As expected, neutrophil populations increased in response to dust, *S. pneumoniae* infection, or the combination thereof compared to SS animals **(Figure 4.5A)**. Dendritic cell counts were elevated in SP and DP groups, but not DS groups **(Figure 4.5B)**. Alveolar macrophages were significantly elevated in DS, SP, and DP groups **(Figure 4.5C).** Interstitial macrophages were elevated in DS, SP, and DP groups, but more so in SP and DP compared to DS, suggesting a pneumo-dependence **(Figure 4.5D)**. This same pattern of elevations was found in classical monocyte populations **(Figure 4.5E)**, while intermediate and non-classical monocyte populations exhibited increases in DS, SP, and DP groups compared to SS **(Figure 4.5F-G**). T-regulatory $CD4^+$ cells were elevated in DS and SP compared to SS, but these populations were reduced in DP compared to SP **(Figure 4.5H)**. ILC1 and NCR+/- ILC3s all exhibited significant increases in DS, SP, and DP groups compared to SS **(Figure 4.5I, K, L)**. ILC2 populations appeared dependent on *S. pneumoniae* infection for increases, with only SP and DP increasing compared to SS, but also increased compared to DS **(Figure 4.5J)**. Total $CD4^+$ and $CD8^+$ populations were elevated in DS, SP, and DP compared to SS, and reduced, albeit not-significantly so, cell counts in DP compared to SP groups (p=0.0543 and p=0.3891, respectively) **(Figure 4.5M, R)**. Dust pre-exposure was sufficient to increase DP Naïve $CD4^+$ but not DP $CD4^+$ central memory T cell populations compared to SS groups **(Figure 4.5N, O)**. DE and *S. pneumoniae* infection, alone or in combination, increased $CD4^+$ effector memory and EMRA

populations, however $CD4^+$EMRAs also exhibited a significant increase in the DP vs SP group **(Figure 4.5Q)**. All $CD8^+$ derivative populations followed similar trends as total $CD8^+$ populations, with some noted exceptions; Naïve $CD8^+$'s were reduced in DP compared to SP, and $CD8^+$ naïve and central memory populations were not elevated in DS compared to the SS group **(Figure 4.5 R-V)**.

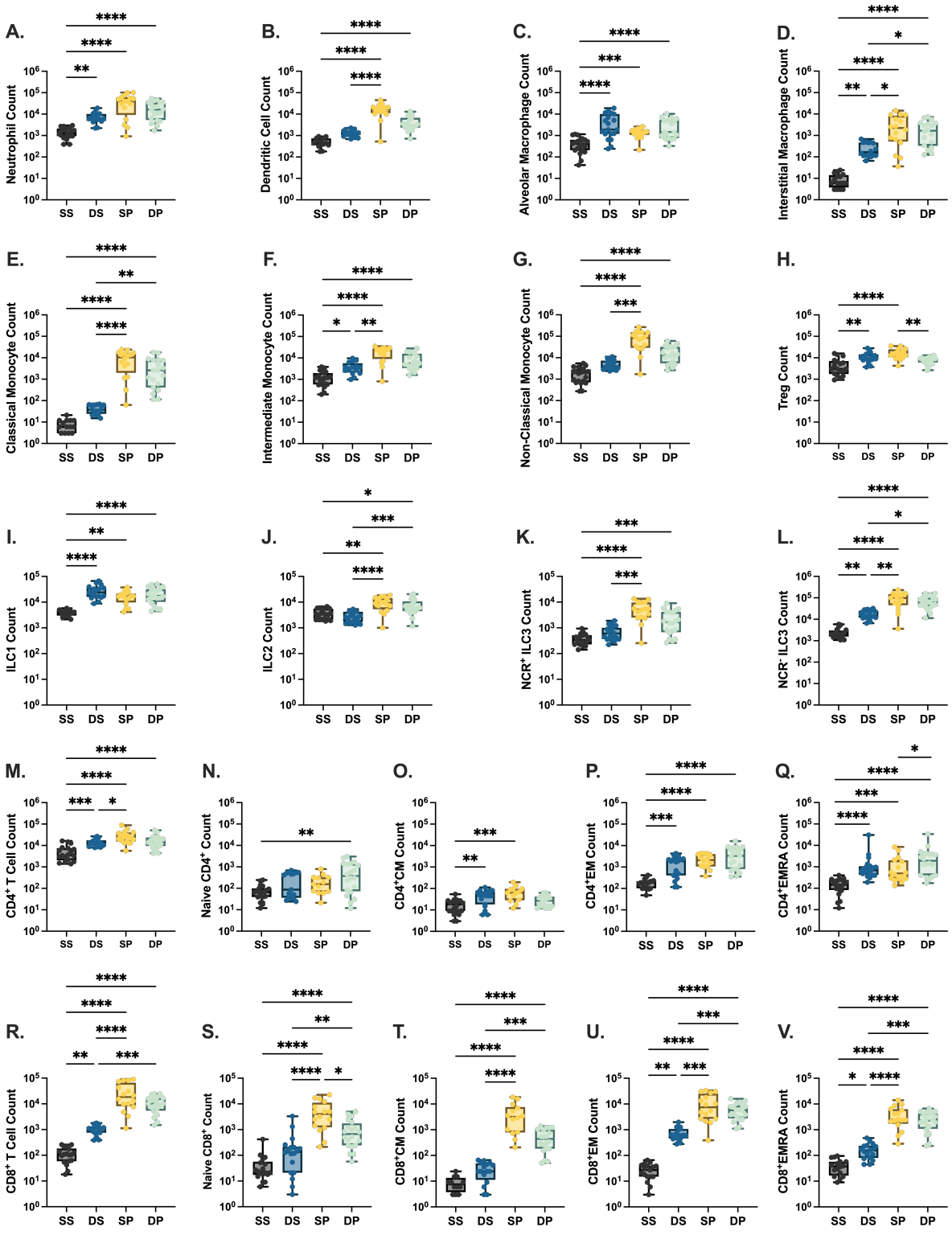

Figure 4.5. Immune cell counts in BALF. Neutrophil **(A.)**, dendritic cell **(B.)**, alveolar macrophage **(C.)**, interstitial macrophage **(D.)**, classical monocyte **(E.)**, intermediate monocyte

(F.), non-classical monocyte **(G.)**, T-regulatory **(H.)**, ILC1 **(I.)**, ILC2 **(J.)**, NCR+ ILC3 **(K.)**, NCR-ILC3 **(L.)**, $CD4^+$ T cell **(M.)**, Naïve $CD4^+$T cell **(N.)**, $CD4^+$ central memory **(O.)**, $CD4^+$ effector memory **(P.)**, $CD4^+$ EMRA **(Q.)**, $CD8^+$ T cell **(R.)**, Naïve $CD8^+$ T cell **(S.)**, $CD8^+$central memory **(T.)**, $CD8^+$effector memory **(U.)**, and $CD8^+$EMRA **(V.)** counts. Box and whisker plots depict minimum to maximum values with all data points shown and the midline at the median value. SS= saline-saline, DS=dust-saline, SP=saline-S. *pneumoniae*, DP=dust-*S. pneumoniae*. Kruskal Wallis test with Dunn's Multiple comparisons for post-hoc analysis. *p<0.05, **p<0.01, ***p<0.001, ****p<0.0001.

Dust Pre-exposure Protects from Fatal Challenge with S. pneumoniae and Reduces Systemic Dissemination

Our findings thus far have revealed dust-based lymphoid cell population alterations, in both the lung tissue and airway, that suggest generation of an adaptive-immune skew that leads to clearance of *S. pneumoniae* infection in a sub-lethal dose. We alternatively infected our dust or saline-pre-exposed mice to a lethal challenge of *S. pneumoniae* and found that dust pre-exposure protected from lethality of infection **(Figure 4.6A)**. Recoverable CFU from the BALF was not significantly altered between saline and dust pre-exposure **(Figure 4.6B)**. In contrast, the CFU recovered from lung and spleen were significantly reduced in dust pre-exposed animals compared to saline **(Figure 4.6B)**. We examined which cell populations within the BALF were therefore differentially found, as despite similar CFU, these populations are likely protective from this fatal challenge and induced by dust pre-exposure. CD8+ effector memory, ILC2, alveolar macrophage, and interstitial macrophage populations were all found significantly elevated in dust pre-exposed fatal challenge animals **(Figure 4.6C-F)**. Collectively, these findings demonstrate the reliance on macrophage populations and differential lymphoid

populations in a fatal challenge of *S. pneumoniae* compared to the more trained and effector memory (lymphocyte dependent) observed in a non-fatal infection.

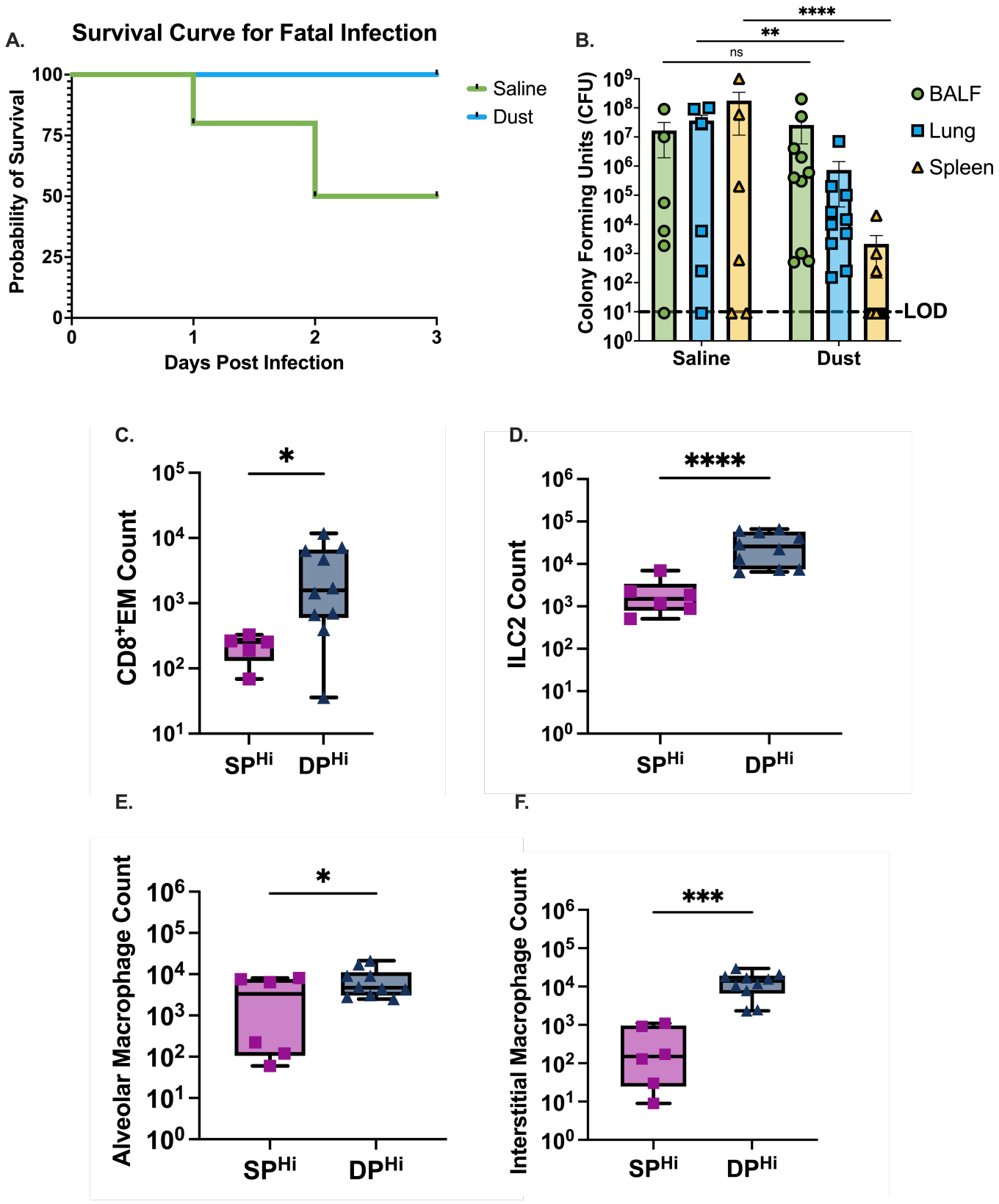
A.
Survival Curve for Fatal Infection
Probability of Survival
100
75
50
25
0
0
1
2
3
Days Post Infection
Saline
Dust
B.
****
**
ns
Colony Forming Units (CFU)
10^9
10^8
10^7
10^6
10^5
10^4
10^3
10^2
10^1
10^0
LOD
Saline
Dust
BALF
Lung
Spleen
C.
*
$CD8^+EM$ Count
10^5
10^4
10^3
10^2
10^1
SP^{Hi}
DP^{Hi}
D.
****
ILC2 Count
10^6
10^5
10^4
10^3
10^2
10^1
10^0
SP^{Hi}
DP^{Hi}
E.
*
Alveolar Macrophage Count
10^6
10^5
10^4
10^3
10^2
10^1
10^0
SP^{Hi}
DP^{Hi}
F.
***
Interstitial Macrophage Count
10^6
10^5
10^4
10^3
10^2
10^1
10^0
SP^{Hi}
DP^{Hi}

Figure 4.6. Kaplan-Meier survival curve of mice infected with a fatal challenge (1.2^8) CFU of *S. pneumoniae* strain D39 following 3 weeks of pre-exposure with saline or dust **(A.)**. Colony forming units recovered from BALF, lung, and spleen in saline and dust exposed animals at 3 DPI **(B.)**. CD8+ effector memory **(C.)**, ILC2 **(D.)**, alveolar macrophage **(E.)**, and interstitial macrophage **(F.)** cell counts. Box and whisker plots depict minimum to maximum values with all data points shown and the midline at the median value. SP=saline-*S. pneumoniae*, DP=dust-*S. pneumoniae*. Mann-Whitney U test. *p<0.05, **p<0.01, ***p<0.001, ****p<0.0001.

Discussion

Our findings in this model of repetitive ODE followed by infection with *S. pneumoniae* demonstrated a previously undescribed protective role of ODE in preventing *S. pneumoniae* growth. A consistent lack of recoverable CFU across BALF, lung, and spleen suggested complete clearance and a lack of dissemination in dust-exposed mice infected with *S. pneumoniae.* Pathologically, dust pre-exposure induces immune cell aggregate formation, the primary pathologic feature significantly increased in DP vs. SP groups. Within the lung tissue, DP groups have decreased total $CD4^+$, $CD8^+$, and T-regulatory cell populations, enhanced ILC1 counts, and increased proportions of $CD4^+$ effector memory and $CD8^+$ TEMRA populations. Correlation analysis revealed that dust exposure was independently associated with immune population differences observed in the DP group. Within the airways, only $CD4^+$ TEMRA populations were elevated in DP vs SP groups. Mice challenged with a fatal dose of *S. pneumoniae* were protected from mortality and exhibited reduced recoverable CFU, with subsequent increases in $CD8^+$ effector memory, ILC2, and macrophage populations. Collectively, our results demonstrate a dust-based increase in effector memory lymphocytes, while protection against fatal infection is also seemingly reliant on macrophage defense.

Our finding of complete clearance of *S. pneumoniae* from the airway, lung tissue, and spleen by 3 DPI in dust pre-exposed mice suggests the completion of a successful response resulting in clearance of infection **(Figure 4.1C)**. The immune response to repetitive (3-week) ODE is neutrophilic, but this increase in neutrophils self-resolved within 3 days of recovery (3,4,34–36). As such, our 3-day recovery period before *S. pneumoniae* infection was intentionally chosen to reduce the impact of the ODE-induced neutrophilic response, and BALF analysis corroborates

this timing **(Figure 4.5A)**. Neutrophil requirement for *S. pneumoniae* defense is well described and typically occurs within hours to 2 days of infection (37–39).

Via gross histopathologic analysis, our finding of increased scores of goblet cell metaplasia in DP vs SP groups suggests a role for goblet-cell mediated immunity **(Figure 4.2C)**. Goblet cell-secreted mucus is well documented to trap and enable killing of non-capsulated *S. pneumoniae*, but this mechanism is easily avoided if the bacterium is encapsulated (which the D39 strain used in these studies is) (40,41). Mucociliary clearance is an additional mechanism of anti-*S. pneumoniae* defense and would be a plausible explanation for our pathologic finding, however, dust exposure alone has been demonstrated to impair ciliary beating and thus homeostatic clearance (26,42–44). The other pathologic parameter increased in DP compared to SP was immune cell aggregate score **(Figure 4.2F)**. Intriguingly, these aggregations have previously been reported to be lymphoid cell dominant and reminiscent of induced bronchus associated lymphoid tissue (iBALTs) (5,11,45,46). Within the DP group, the number of these iBALT structures far surpassed the normal scoring metrics utilized for repetitive ODE, potentially suggesting that dust-induced recruitment and generation, followed by *S. pneumoniae* infection spurred on development of iBALTs, albeit not statistically significantly between DS and DP groups (47).

The lymphoid cell requirement for *S. pneumoniae* clearance within the lung is well documented, with $CD8^+$ T cells required for *S. pneumoniae* defense, and depletion of $CD4^+$ T cells enhancing this response (48). This study demonstrated a requirement for perforin and IFN-y, but these findings were in a pan-knockout model, not $CD8^+$ T cell specific depletion. Interestingly,

adoptive transfer of Naive CD8+ T cells was sufficient to reduce CFU burden within the lungs of infected animals in both $CD8^{-/-}$ and $CD4^{-/-}$ animals. Our findings suggest that naive lymphocyte populations are reduced with ODE **(Figure 4.3E, G)**. Instead, we demonstrated an increase in $CD4^{+}$ effector memory T cell proportions, specifically in response to ODE **(Figure 4.3I)**. $CD4^{+}$ effector memory populations are well documented in individuals carrying *S. pneumoniae* populations asymptomatically, and generation of these "memory" subset of T cells has been demonstrated to enhance host secondary infection response, decrease allergic response, and increase the resolution and repair processes associated with inflammation (49,50). In addition, increases in $CD4^{+}$ EMs correlate with reduction of T-regs, as demonstrated in our findings (51).

The other population of lymphocytes found proportionally increased in DP vs SP groups in the lung were that of CD8+ terminally differentiated effector memory reactivated (TEMRA) cells **(Figure 4.3L)**. These cells exhibit highly cytotoxic phenotypes and pro-inflammatory cytokine secretion (52). Within the context of COPD development, $CD8^{+}$ TEMRA populations are increasingly recognized as a clinical biomarker for mild to moderate COPD incidence (53). Given the propensity for ODE to contribute to COPD development, this incidental finding of increased proportions of $CD8^{+}$ TEMRAs following ODE has implications within the field of ODE-induced inflammation and disease risk.

Via correlation analysis, we found that reduced proportions of naive $CD4^{+}$ and $CD8^{+}$ populations inversely correlated with all lung pathologic parameters assessed **(Figure 4.4)**. CFUs were similarly inversely correlated with these naive lymphocyte populations, but most importantly, so was exposure. Repetitive ODE has been demonstrated to increase the populations of total $CD4^{+}$,

but not $CD8^+$ T cells, within the lung (54). Interestingly, these cells were demonstrated, following isolation and restimulation, to be primarily IL-17-producing populations. IL-17 production is implicated in polarizing the immune response towards a Th1/Th17 skew for *S. pneumoniae* protection and clearance (55–57). Within the airway, the site of complete bacterial clearance at 10^7 infectious dose, there were observed ODE-induced increases only in the $CD4^+$EMRA population **(Figure 4.5Q)**, but no other immune population that was differentially increase in DP compared to SP groups. Reductions in several immune cell populations, such as Tregs and Naive $CD8^+$ T cells in DP vs SP groups were also noted **(Figure 4.5H, S)**, suggesting that reduced naive populations and Tregs meant to dampen inflammatory resposnes are crucial to protecting from *S.pneumoniae* infection.

Within the DS group, it was important to note that this timeline, with recovery and infection, places these animals at a repetitive ODE timepoint of 3 weeks with a recovery period of no dust exposure or infection of 6 days **(Figure 4.1A)**. This timepoint grants a unique look into cell populations required for recovery of ODE-induced inflammation, and our current work expands on previous observations of reductions in neutrophils, not observed in our current BALF data, as well as similar levels of macrophage and lymphocyte populations (11). One major immune cell population not included in our analysis is B cells, which have previously been demonstrated as a requirement for iBALT formation following repetitive ODE (45). This lymphocyte signature was completely abolished when fatal *S. pneumoniae* challenge was conducted with the reliance shifting towards a macrophage-biased signature in dust-exposed and infected mice **(Figure 4.6)**. Increases in $CD8^+$ effector memory and ILC2 populations within the airway as a result of fatal challenge were also observed **(Figure 4.6C, D)**. Collectively, this observation suggests that

mitigating fatal challenge of *S. pneumoniae* is more reliant on macrophage populations than a non-fatal challenge, and that pre-exposure to dust enhances these macrophage populations. In a murine model of fatal *S. pneumoniae* infection, a link between IL-33 signaling, ILC2-produced IL-4 and IL-13, and *S. pneumoniae* clearance has been demonstrated (58,59). Intriguingly, their findings primarily revealed the requirement of reduced IL-33 and increased IL-22 as the primary causative factor in *S. pneumoniae* defense. Previous work from our lab has demonstrated that repetitive ODE induces increased IL-22 induction within the airways, polarizing macrophage populations towards a more M2-like phenotype. IL-22 production has profound downstream impacts, increasing the production of epithelial-produced antimicrobial peptides (AMPs), which exhibit varied success dependent on capsular makeup of the bacterium (60–62).

Our study faces several limitations and therefore provides ample opportunity for improving upon these initial findings. First and foremost, among these, is the necessity for understanding at what timepoint non-fatal doses of *S. pneumoniae* are cleared from the airway completely in dust-exposed mice. We reveal incomplete clearance in fatally challenged mice by 3 D.P.I., but an alternative strategy to increasing the dose would be better understanding at what timepoint complete clearance is obtained. Furthermore, our data do not include signaling molecules or biomarkers of cellular activation or phenotype, the inclusion of which would allow for a greater understanding of the cohesive immune response induced by dust-pre-exposure before *S. pneumoniae* infection. Curiously, there is a growing body of literature identifying “innate immune training” markers that confer susceptibility or protection against secondary insults or exposure (63–65). These findings are as of yet unexplored in the field of repetitive ODE but offer intriguing and exciting avenues to understand how a pre-exposure to environmental stimuli

alters an individual's ability to respond to "second hits". Future investigations should also aim to understand the epitopes of TCRs induced by repetitive ODE that may correlate with infection response to *S. pneumoniae*. Additionally, demonstrating a specific response versus a generalized inflammatory/innate immune response to ODE that decreases the response time needed for the immune system to secondary infectious challenges is also warranted.

References

1. Wyatt TA, Nemecek M, Chandra D, DeVasure JM, Nelson AJ, Romberger DJ, Poole JA. Organic dust-induced lung injury and repair: Bi-directional regulation by TNFα and IL-10. *J Immunotoxicol* (2020) 17:153–162. doi: 10.1080/1547691X.2020.1776428
2. Christiani DC. Organic dust exposure and chronic airway disease. *Am J Respir Crit Care Med* (1996) 154:833–4. doi: 10.1164/ajrccm.154.4.8887570
3. Poole JA, Zamora-Sifuentes JL, De las Vecillas L, Quirce S. Respiratory Diseases Associated With Organic Dust Exposure. *J Allergy Clin Immunol Pract* (2024) 12:1960–1971. doi: 10.1016/j.jaip.2024.02.022
4. Poole JA, Romberger DJ. Immunological and inflammatory responses to organic dust in agriculture. *Curr Opin Allergy Clin Immunol* (2012) 12:126–132. doi: 10.1097/ACI.0b013e3283511d0e
5. Poole JA, Wyatt TA, Oldenburg PJ, Elliott MK, West WW, Sisson JH, Von Essen SG, Romberger DJ. Intranasal organic dust exposure-induced airway adaptation response marked by persistent lung inflammation and pathology in mice. *American Journal of Physiology-Lung Cellular and Molecular Physiology* (2009) 296:L1085–L1095. doi: 10.1152/ajplung.90622.2008
6. Yang J, Kim EK, Park HJ, McDowell A, Kim Y-K. The impact of bacteria-derived ultrafine dust particles on pulmonary diseases. *Exp Mol Med* (2020) 52:338–347. doi: 10.1038/s12276-019-0367-3
7. Nordgren TM, Charavaryamath C. Agriculture Occupational Exposures and Factors Affecting Health Effects. *Curr Allergy Asthma Rep* (2018) 18:65. doi: 10.1007/s11882-018-0820-8
8. Nordgren TM, Bailey KL. Pulmonary health effects of agriculture. *Curr Opin Pulm Med* (2016) 22:144–149. doi: 10.1097/MCP.0000000000000247
9. Serhan CN, Savill J. Resolution of inflammation: the beginning programs the end. *Nat Immunol* (2005) 6:1191–1197. doi: 10.1038/ni1276
10. Levy BD, Serhan CN. Resolution of Acute Inflammation in the Lung. *Annu Rev Physiol* (2014) 76:467–492. doi: 10.1146/annurev-physiol-021113-170408
11. Warren K, Wyatt T, Romberger D, Ailts I, West W, Nelson A, Nordgren T, Staab E, Heires A, Poole J. Post-Injury and Resolution Response to Repetitive Inhalation Exposure to Agricultural Organic Dust in Mice. *Safety* (2017) 3:10. doi: 10.3390/safety3010010
12. Crawford MS, Nordgren TM, McCole DF. Every breath you take: Impacts of environmental dust exposure on intestinal barrier function–from the gut-lung axis to COVID-19. *American Journal of Physiology-Gastrointestinal and Liver Physiology* (2021) 320:G586–G600. doi: 10.1152/ajpgi.00423.2020
13. Isaak M, Ulu A, Osunde A, Nordgren TM, Hanson C. Nutritional Factors in Occupational Lung Disease. *Curr Allergy Asthma Rep* (2021) 21:24. doi: 10.1007/s11882-021-01003-0
14. Dominguez EC, Phandthong R, Nguyen M, Ulu A, Guardado S, Sveiven S, Talbot P, Nordgren TM. Aspirin-Triggered Resolvin D1 Reduces Chronic Dust-Induced Lung Pathology without Altering Susceptibility to Dust-Enhanced Carcinogenesis. *Cancers (Basel)* (2022) 14:1900. doi: 10.3390/cancers14081900
15. Weiser JN, Ferreira DM, Paton JC. Streptococcus pneumoniae: transmission, colonization and invasion. *Nat Rev Microbiol* (2018) 16:355–367. doi: 10.1038/s41579-018-0001-8
16. Tonkin-Hill G, Ling C, Chaguza C, Salter SJ, Hinfonthong P, Nikolaou E, Tate N, Pastusiak A, Turner C, Chewapreecha C, et al. Pneumococcal within-host diversity during colonization,

transmission and treatment. *Nat Microbiol* (2022) 7:1791–1804. doi: 10.1038/s41564-022-01238-1
17. Clark SE. Commensal bacteria in the upper respiratory tract regulate susceptibility to infection. *Curr Opin Immunol* (2020) 66:42–49. doi: 10.1016/j.coi.2020.03.010
18. Sigsgaard T, Basinas I, Doekes G, de Blay F, Folletti I, Heederik D, Lipinska-Ojrzanowska A, Nowak D, Olivieri M, Quirce S, et al. Respiratory diseases and allergy in farmers working with livestock: a EAACI position paper. *Clin Transl Allergy* (2020) 10:29. doi: 10.1186/s13601-020-00334-x
19. Freidl GS, Spruijt IT, Borlée F, Smit LAM, van Gageldonk-Lafeber AB, Heederik DJJ, Yzermans J, van Dijk CE, Maassen CBM, van der Hoek W. Livestock-associated risk factors for pneumonia in an area of intensive animal farming in the Netherlands. *PLoS One* (2017) 12:e0174796. doi: 10.1371/journal.pone.0174796
20. von Mutius E. The "Hygiene Hypothesis" and the Lessons Learnt From Farm Studies. *Front Immunol* (2021) 12:635522. doi: 10.3389/fimmu.2021.635522
21. Lotterman A, Baliatsas C, de Rooij MMT, Huss A, Jacobs J, Dückers M, Boender GJ, McCarthy C, Heederik D, Hagenaars TJ, et al. Increased risk of pneumonia amongst residents living near goat farms in different livestock-dense regions in the Netherlands. *PLoS One* (2023) 18:e0286972. doi: 10.1371/journal.pone.0286972
22. Yzermans CJ, Moleman YP, Spreeuwenberg P, Nielen MMJ, Dückers MLA, Smit LAM, Baliatsas C. Risk of pneumonia in the vicinity of goat farms: a comparative assessment of temporal variation based on longitudinal health data. *Pneumonia* (2023) 15:13. doi: 10.1186/s41479-023-00115-7
23. Romberger DJ, Bodlak V, Von Essen SG, Mathisen T, Wyatt TA. Hog barn dust extract stimulates IL-8 and IL-6 release in human bronchial epithelial cells via PKC activation. *J Appl Physiol* (2002) 93:289–296. doi: 10.1152/japplphysiol.00815.2001
24. Warren K, Wyatt T, Romberger D, Ailts I, West W, Nelson A, Nordgren T, Staab E, Heires A, Poole J. Post-Injury and Resolution Response to Repetitive Inhalation Exposure to Agricultural Organic Dust in Mice. *Safety* (2017) 3:10. doi: 10.3390/safety3010010
25. Nordgren TM, Bauer CD, Heires AJ, Poole JA, Wyatt TA, West WW, Romberger DJ. Maresin-1 reduces airway inflammation associated with acute and repetitive exposures to organic dust. *Translational Research* (2015) 166:57–69. doi: 10.1016/j.trsl.2015.01.001
26. Nordgren TM, Wyatt TA, Sweeter J, Bailey KL, Poole JA, Heires AJ, Sisson JH, Romberger DJ. Motile cilia harbor serum response factor as a mechanism of environment sensing and injury response in the airway. *American Journal of Physiology-Lung Cellular and Molecular Physiology* (2014) 306:L829–L839. doi: 10.1152/ajplung.00364.2013
27. Romberger DJ, Heires AJ, Nordgren TM, Souder CP, West W, Liu X, Poole JA, Toews ML, Wyatt TA. Proteases in agricultural dust induce lung inflammation through PAR-1 and PAR-2 activation. *American Journal of Physiology-Lung Cellular and Molecular Physiology* (2015) 309:L388–L399. doi: 10.1152/ajplung.00025.2015
28. Ulu A, Burr A, Heires AJ, Pavlik J, Larsen T, Perez PA, Bravo C, DiPatrizio N V., Baack M, Romberger DJ, et al. A high docosahexaenoic acid diet alters lung inflammation and recovery following repetitive exposure to aqueous organic dust extracts. *Journal of Nutritional Biochemistry* (2021) 97: doi: 10.1016/j.jnutbio.2021.108797
29. Poole JA, Nordgren TM, Heires AJ, Nelson AJ, Katafiasz D, Bailey KL, Romberger DJ. Amphiregulin modulates murine lung recovery and fibroblast function following exposure to

agriculture organic dust. *American Journal of Physiology-Lung Cellular and Molecular Physiology* (2020) 318:L180–L191. doi: 10.1152/ajplung.00039.2019
30. Bankhead P, Loughrey MB, Fernández JA, Dombrowski Y, McArt DG, Dunne PD, McQuaid S, Gray RT, Murray LJ, Coleman HG, et al. QuPath: Open source software for digital pathology image analysis. *Sci Rep* (2017) 7:16878. doi: 10.1038/s41598-017-17204-5
31. Burr AC, Velazquez J V, Ulu A, Kamath R, Kim SY, Bilg AK, Najera A, Sultan I, Botthoff JK, Aronson E, et al. Lung Inflammatory Response to Environmental Dust Exposure in Mice Suggests a Link to Regional Respiratory Disease Risk. *J Inflamm Res* (2021) Volume 14:4035–4052. doi: 10.2147/JIR.S320096
32. Threatt AN, White J, Klepper N, Brier Z, Dean LS, Ibarra A, Harris M, Jones K, Wahl MJL, Barahona M, et al. Aspirin-triggered resolvin D1 modulates pulmonary and neurological inflammation in an IL-22 knock-out organic dust exposure mouse model. *Front Immunol* (2024) 15: doi: 10.3389/fimmu.2024.1495581
33. Natalini A, Simonetti S, Favaretto G, Peruzzi G, Antonangeli F, Santoni A, Muñoz-Ruiz M, Hayday A, Di Rosa F. <scp>OMIP</scp> -079: Cell cycle of <scp>CD4</scp> $^{+}$ and <scp>CD8</scp> $^{+}$ naïve/memory T cell subsets, and of Treg cells from mouse spleen. *Cytometry Part A* (2021) 99:1171–1175. doi: 10.1002/cyto.a.24509
34. Threatt AN, White J, Klepper N, Brier Z, Dean LS, Ibarra A, Harris M, Jones K, Wahl MJL, Barahona M, et al. Aspirin-triggered resolvin D1 modulates pulmonary and neurological inflammation in an IL-22 knock-out organic dust exposure mouse model. *Front Immunol* (2024) 15: doi: 10.3389/fimmu.2024.1495581
35. Nordgren T, Friemel T, Heires A, Poole J, Wyatt T, Romberger D. The Omega-3 Fatty Acid Docosahexaenoic Acid Attenuates Organic Dust-Induced Airway Inflammation. *Nutrients* (2014) 6:5434–5452. doi: 10.3390/nu6125434
36. Poole JA, Thiele GM, Alexis NE, Burrell AM, Parks C, Romberger DJ. Organic dust exposure alters monocyte-derived dendritic cell differentiation and maturation. *American Journal of Physiology-Lung Cellular and Molecular Physiology* (2009) 297:L767–L776. doi: 10.1152/ajplung.00107.2009
37. Palmer CS, Kimmey JM. Neutrophil Recruitment in Pneumococcal Pneumonia. *Front Cell Infect Microbiol* (2022) 12: doi: 10.3389/fcimb.2022.894644
38. Horn KJ, Fulte S, Yang M, Lorenz BP, Clark SE. Neutrophil responsiveness to IL-10 impairs clearance of *Streptococcus pneumoniae* from the lungs. *J Leukoc Biol* (2024) 115:4–15. doi: 10.1093/jleuko/qiad070
39. Moldoveanu B, Otmishi P, Jani P, Walker J, Sarmiento X, Guardiola J, Saad M, Yu J. Inflammatory mechanisms in the lung. *J Inflamm Res* (2009) 2:1–11.
40. Antunes MB, Cohen NA. Mucociliary clearance – a critical upper airway host defense mechanism and methods of assessment. *Curr Opin Allergy Clin Immunol* (2007) 7:5–10. doi: 10.1097/ACI.0b013e3280114eef
41. Weiser JN, Ferreira DM, Paton JC. Streptococcus pneumoniae: transmission, colonization and invasion. *Nat Rev Microbiol* (2018) 16:355–367. doi: 10.1038/s41579-018-0001-8
42. Wyatt TA, Poole JA, Nordgren TM, DeVasure JM, Heires AJ, Bailey KL, Romberger DJ. cAMP-dependent protein kinase activation decreases cytokine release in bronchial epithelial cells. *Am J Physiol Lung Cell Mol Physiol* (2014) 307:L643-51. doi: 10.1152/ajplung.00373.2013

43. Nordgren TM, Heires AJ, Wyatt TA, Poole JA, LeVan TD, Cerutis DR, Romberger DJ. Maresin-1 reduces the pro-inflammatory response of bronchial epithelial cells to organic dust. *Respir Res* (2013) 14:51. doi: 10.1186/1465-9921-14-51
44. Wyatt TA, Sisson JH, Von Essen SG, Poole JA, Romberger DJ. Exposure to hog barn dust alters airway epithelial ciliary beating. *Eur Respir J* (2008) 31:1249–55. doi: 10.1183/09031936.00015007
45. Poole JA, Mikuls TR, Duryee MJ, Warren KJ, Wyatt TA, Nelson AJ, Romberger DJ, West WW, Thiele GM. A role for B cells in organic dust induced lung inflammation. *Respir Res* (2017) 18:214. doi: 10.1186/s12931-017-0703-x
46. Silva-Sanchez A, Randall TD. Role of iBALT in Respiratory Immunity. *Curr Top Microbiol Immunol* (2020) 426:21–43. doi: 10.1007/82_2019_191
47. Ulu A, Velazquez J V., Burr A, Sveiven SN, Yang J, Bravo C, Hammock BD, Nordgren TM. Sex-Specific Differences in Resolution of Airway Inflammation in Fat-1 Transgenic Mice Following Repetitive Agricultural Dust Exposure. *Front Pharmacol* (2022) 12: doi: 10.3389/fphar.2021.785193
48. Weber SE, Tian H, Pirofski L. CD8+ Cells Enhance Resistance to Pulmonary Serotype 3 *Streptococcus pneumoniae* Infection in Mice. *The Journal of Immunology* (2011) 186:432–442. doi: 10.4049/jimmunol.1001963
49. Masopust D, Vezys V, Marzo AL, Lefrançois L. Preferential Localization of Effector Memory Cells in Nonlymphoid Tissue. *Science (1979)* (2001) 291:2413–2417. doi: 10.1126/science.1058867
50. Smith NM, Wasserman GA, Coleman FT, Hilliard KL, Yamamoto K, Lipsitz E, Malley R, Dooms H, Jones MR, Quinton LJ, et al. Regionally compartmentalized resident memory T cells mediate naturally acquired protection against pneumococcal pneumonia. *Mucosal Immunol* (2018) 11:220–235. doi: 10.1038/mi.2017.43
51. He SWJ, van de Garde MDB, Pieren DKJ, Poelen MCM, Voß F, Abdullah MR, Hammerschmidt S, van Els CACM. Diminished Pneumococcal-Specific CD4+ T-Cell Response is Associated With Increased Regulatory T Cells at Older Age. *Frontiers in Aging* (2021) 2: doi: 10.3389/fragi.2021.746295
52. Jacquemont L, Tilly G, Yap M, Doan-Ngoc T-M, Danger R, Guérif P, Delbos F, Martinet B, Giral M, Foucher Y, et al. Terminally Differentiated Effector Memory CD8+ T Cells Identify Kidney Transplant Recipients at High Risk of Graft Failure. *Journal of the American Society of Nephrology* (2020) 31:876–891. doi: 10.1681/ASN.2019080847
53. Villaseñor-Altamirano AB, Jain D, Jeong Y, Menon JA, Kamiya M, Haider H, Manandhar R, Sheikh MDA, Athar H, Merriam LT, et al. Activation of CD8+ T Cells in Chronic Obstructive Pulmonary Disease Lung. *Am J Respir Crit Care Med* (2023) 208:1177–1195. doi: 10.1164/rccm.202305-0924OC
54. Poole JA, Gleason AM, Bauer C, West WW, Alexis N, Reynolds SJ, Romberger DJ, Kielian T. αβ T cells and a mixed Th1/Th17 response are important in organic dust-induced airway disease. *Annals of Allergy, Asthma & Immunology* (2012) 109:266-273.e2. doi: 10.1016/j.anai.2012.06.015
55.McAleer JP, Kolls JK. Directing traffic: IL-17 and IL-22 coordinate pulmonary immune defense. *Immunol Rev* (2014) 260:129–44. doi: 10.1111/imr.12183
56. Narciso AR, Dookie R, Nannapaneni P, Normark S, Henriques-Normark B. Streptococcus pneumoniae epidemiology, pathogenesis and control. *Nat Rev Microbiol* (2024) doi: 10.1038/s41579-024-01116-z

57. Gil E, Noursadeghi M, Brown JS. Streptococcus pneumoniae interactions with the complement system. *Front Cell Infect Microbiol* (2022) 12: doi: 10.3389/fcimb.2022.929483
58. Ulu A, Sveiven S, Bilg A, Velazquez J V., Diaz M, Mukherjee M, Yuil-Valdes AG, Kota S, Burr A, Najera A, et al. IL-22 regulates inflammatory responses to agricultural dust-induced airway inflammation. *Toxicol Appl Pharmacol* (2022) 446:116044. doi: 10.1016/j.taap.2022.116044
59. Röwekamp I, Maschirow L, Rabes A, Fiocca Vernengo F, Hamann L, Heinz GA, Mashreghi M-F, Caesar S, Milek M, Fagundes Fonseca AC, et al. IL-33 controls IL-22-dependent antibacterial defense by modulating the microbiota. *Proceedings of the National Academy of Sciences* (2024) 121: doi: 10.1073/pnas.2310864121
60. Le C-F, Gudimella R, Razali R, Manikam R, Sekaran SD. Transcriptome analysis of Streptococcus pneumoniae treated with the designed antimicrobial peptides, DM3. *Sci Rep* (2016) 6:26828. doi: 10.1038/srep26828
61. Waz NT, Oliveira S, Girardello R, Lincopan N, Barazzone G, Parisotto T, Hakansson AP, Converso TR, Darrieux M. Influence of the Polysaccharide Capsule on the Bactericidal Activity of Indolicidin on Streptococcus pneumoniae. *Front Microbiol* (2022) 13: doi: 10.3389/fmicb.2022.898815
62. Dean LS, Threatt AN, Jones K, Oyewole EO, Pauly M, Wahl M, Barahona M, Reiter RW, Nordgren TM. I don't know about you, but I'm feeling IL-22. *Cytokine Growth Factor Rev* (2024) 80:1–11. doi: 10.1016/j.cytogfr.2024.11.001
63. Hajishengallis G, Netea MG, Chavakis T. Innate immune memory, trained immunity and nomenclature clarification. *Nat Immunol* (2023) 24:1393–1394. doi: 10.1038/s41590-023-01595-x
64. Hajishengallis G, Netea MG, Chavakis T. Trained immunity in chronic inflammatory diseases and cancer. *Nat Rev Immunol* (2025) doi: 10.1038/s41577-025-01132-x
65. Töpfer E, Boraschi D, Italiani P. Innate Immune Memory: The Latest Frontier of Adjuvanticity. *J Immunol Res* (2015) 2015:478408. doi: 10.1155/2015/478408

Chapter 5

The immune response to inhaled organic dusts, both acute and chronic, is complex. Despite many advances in our understanding of how this immune response presents through the utilization of murine modeling, an exact understanding of the contributors to clinical disease development are under continued investigation. The aims of these studies were to 1.) Develop a flow cytometry method for NET-forming neutrophil identification and tracking following acute dust exposure, 2.) Deeply phenotype the response and resolution promoted by increased n-3 fatty acids following repetitive ODE. 3.) Determine the immune response induced by repetitive ODE followed by infection with *Streptococcus pneumoniae.* Collectively, these studies advance the fields understanding of immune-response alterations induced by organic dust exposure, providing key insights into how this exposure response can be altered in response to omega-3 fatty acid availability or infection with the common respiratory pathogen, *S. pneumoniae*.

Acute ODE increases neutrophils in the lung and airway, but only mature neutrophils in the lung exhibit increased NET formation.

Acute ODE is characterized by a prominent neutrophilic response. In what manner this neutrophilia contributes to the inflammatory environment within the airway and lung is less well understood. Herien, we developed a flow cytometry panel that profiled neutrophils, their precursors, and their NET-forming capacity from the bone marrow, through the blood, into the lung tissue and airways following an acute exposure to dust extract. Our findings revealed that 5 hours post ODE, both band and mature neutrophils significantly increased in the lung tissue and airway (via bronchoalveolar lavage fluid collection). Intriguingly, when examined for NET

formation, only mature neutrophils within the lung tissue were demonstrated to show an ODE-induced increase in NET formation. Furthermore, differential patterns of NET formation (lytic vs vital) were locationally dependent, with lung tissue demonstrating a more lytic pattern and airway NET-forming neutrophils exhibiting a vital-like pattern. Given these differential patterns of NET-formation in mature and band neutrophils, further studies should focus on the targeting of mature neutrophils as inducers of NET-driven inflammation. Additionally, observing NET formation patterns in repetitive ODE, to delineate if this process is a driver of repetitive ODE is warranted.

Monocytes are sex-dependently recruited to lung tissue and airways in a mouse model of balanced omega-3 fatty acids during repetitive ODE.

Repetitive ODE creates a chronic inflammatory environment, without normal resolution processes, ultimately contributing to development of chronic respiratory diseases such as asthma and COPD. Potent promoters of inflammation resolution processes, n-3 FA and their metabolites, termed SPM, have garnered attention for their efficacy in reducing ODE-induced inflammation. What cellular players and soluble mediators contribute to the resolution-promoting characteristics of n-3 FA remains relatively underreported. Our findings reveal that monocytes, specifically classical and intermediate monocytes, are preferentially recruited to the lung and airway in response to repetitive ODE in a balanced n-3 FA model, the *Fat-1* mouse. Within the airways, monocytes were increased in *Fat-1* males, coinciding with increased levels of CX_3CL1, while female *Fat-1* mice exhibited increased monocyte populations within the lung tissue. These findings highlight the importance of sex-difference considerations when combating ODE-induced inflammation via n-3 FAs, while providing a previously undescribed role for

monocytes in promoting resolution processes within the lung following ODE. Future experiments should delineate if the observed sex differences are hormonal or chromosomal in nature, thereby informing translational measures for agricultural and livestock laborers. Furthermore, investigations into how the monocytes, either through macrophage or dendritic cell renewal, or through phagocytosis and cytokine release, promote resolution in the *Fat-1* mouse following repetitive ODE.

Repetitive ODE protects from secondary *S. pneumoniae* infection and mortality through induction of effector memory lymphocyte populations.

The bacterium *S. pneumonia*e requires a dysregulated or altered immune response to move from upper respiratory tract mucosal colonization to lower respiratory tract infection. Clinical and epidemiologic data provide mixed consensuses on the impact of organic dust exposures and *S. pneumoniae* infection, so we leveraged our existing model of repetitive ODE to provide experimental insight into this phenomenon. Our model revealed that repetitive ODE protected from *S. pneumoniae* infection, dissemination, and mortality via the induction of effector memory lymphocyte populations in the airway and lung tissue. Based on our findings of these increased populations, further inquiries as to the necessity and functionality of these ODE-induced populations is warranted. Furthermore, our findings of increased iBALT formation suggests a potential role for antibody-mediated defense and is an apt direction to identify the specific antigen(s) potentially induced via repetitive ODE.

Concluding Remarks

Understanding the immune response to ODE remains a pivotal challenge in unravelling the major contributors to asthma and COPD development of workers in the livestock and agricultural industries. While additional work is very much so warranted, the studies presented in this dissertation have collectively served to advance the understanding of the immune response to acute and repetitive inhalational organic dust exposure. Identification of mature neutrophils within the lung tissue as the prominent source of NET-forming cells in acute ODE enables therapeutic efforts to be targeted. Revelations that balanced n-3 FA promotes a monocytic signature with potent sex-dependent differences enhances our understanding of translational implications of dietary based interventions for ODE-induced inflammatory mitigation. Finally, our murine ODE system revealed that repetitive ODE induces potent effector memory lymphocyte populations that may aid in the clearance of infection with *S. pneumoniae*. These advances in our understanding of the immune response to acute and repetitive ODE demonstrate forward progress towards therapeutic avenues that can combat end-stage respiratory disease development associated with ODE and additional PM exposures.

Appendix 1: Supplementary Material for Spectral Flow Cytometry Method for Immunophenotyping Neutrophil Activation and NET-forming Capabilities in an Acute Dust Exposure Model

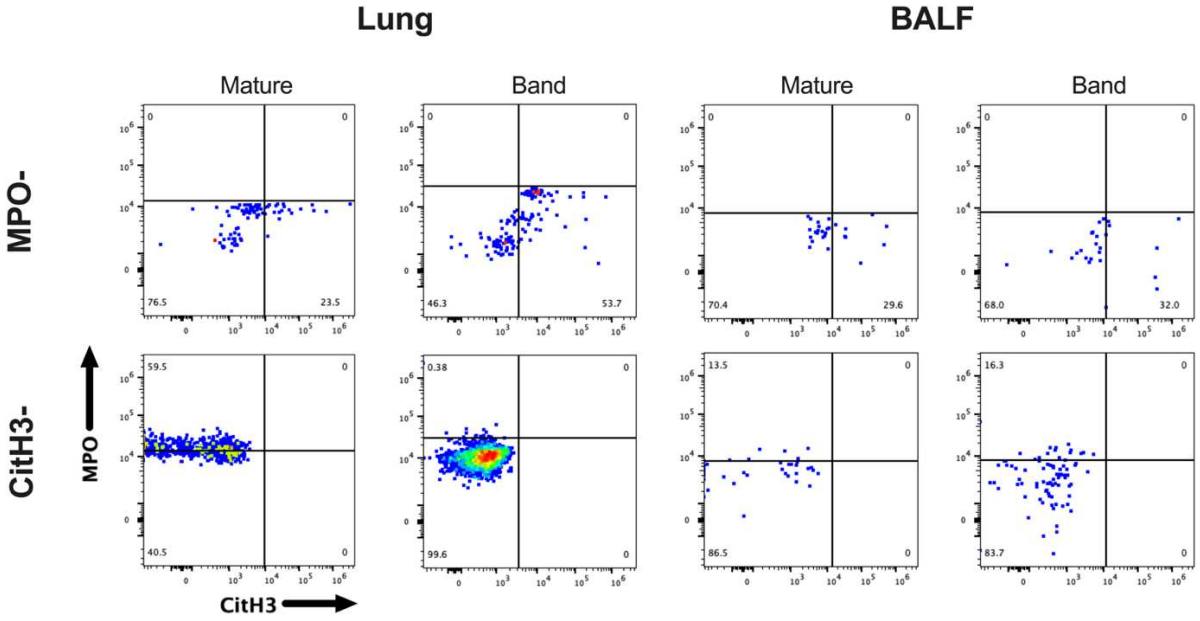

Supplementary Figure 2.1: Representative gating strategy for fluorescent minus one (FMO) sample utilized for gating placement for NET formation markers MPO and CitH3 in the lung and BALF in mature and band neutrophil populations.

Supplementary Table 2.1: Fluorescently conjugated antibodies used for flow cytometry. Panel denotes extracellular (ex) and intracellular (in) location of markers.

Marker	Fluor	Manufacturer	Dilution	Panel
Ly6G	PE-Dazzle 594	Biolegend, Cat# 127648, Clone:1A8	1:400	ex
CD34	BV605	Biolegend, Cat# 341642, Clone RAM34	1:800	ex
CD117	BV650	Biolegend, Cat# 563399, Clone:2B8	1:400	ex
CD62L	BV711	Biolegend, Cat# 104445, Clone: MEL-14	1:800	ex
CXCR2	BV786	Biolegend, Cat# 747811, Clone: V48-2310	1:400	ex
CXCR4	PerCP-eFlour 710	Thermofisher Scientific Cat# 46-9991-82, Clone: 2B11	1:400	ex
MPO	PE	Abcam, Cat# AF3667, Thermofisher Scientific Cat# PA1-29953	1:100 1°, 1:400 2°	in
CitH3	APC	Abcam, Cat# ab281584, Thermofisher Scientific Cat# A10931	1:100 1°, 1:400 2°	in
CD11b	AF700	Biolegend, Cat# 101222, Clone: M1/70	1:800	ex
NK1.1	FITC	Biolegend, San Diego, CA. Cat# 156507, Clone: 156507	1:1600	ex
CD3		Biolegend, San Diego, CA. Cat# 100305, Clone: 145-2C11		ex
B220		Biolegend, San Diego, CA. Cat# 103205, Clone: RA3-6B2		ex
CD19		Biolegend, San Diego, CA. Cat# 152403, Clone: 1D3/CD19		ex
Ter119	AF488	Biolegend, San Diego, CA. Cat# 116215, Clone: TER119	1:1600	ex
DNA	Hoechst 33342	Thermofisher Scientific, Cat# R37165	2 drops/mL	ex
Viability	Ghost Red 780	Tonbo Biosciences, Cat#13-0865-T100	1:5000	ex

Appendix 2: Supplementary Material for Spectral Immune Cell Profiling Reveals Modulations in Immune Cell Response to Repetitive Inhaled Organic Dust Exposure in a High Omega-3 Fatty Acid Mouse Model

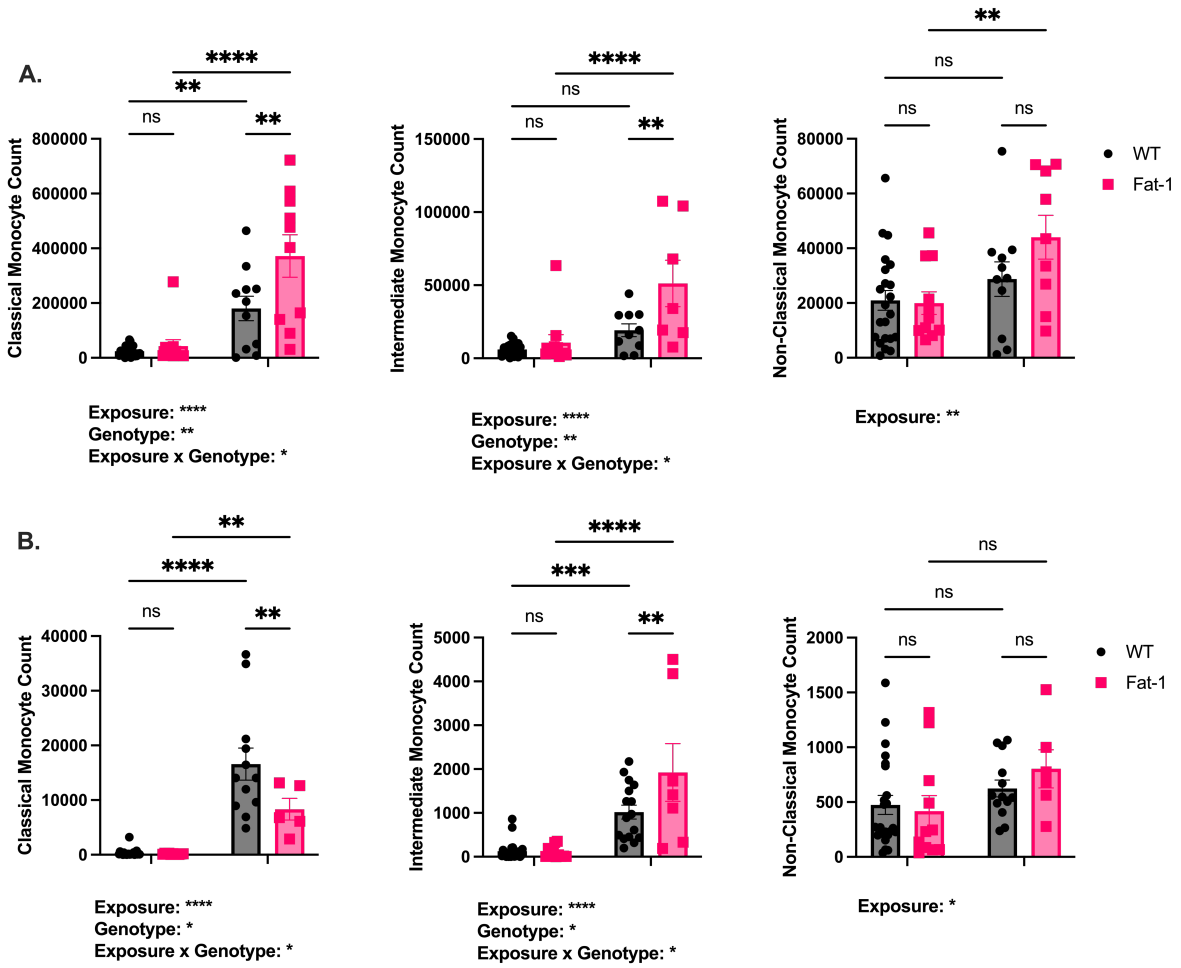

Supplementary Figure 3.1. Monocyte populations in the lung tissue (**A.**) and airway (**B.**) in WT and Fat-1 mice exposed to saline or dust. Main effects are shown below the graphs. 2-Way ANOVA with Tukey's Multiple Comparisons Test **p<0.01, ***p<0.001****p<0.0001, ns-non-significant.

Supplementary Table 3.1: Antibody-fluorophore conjugations and manufacturers.

Marker	Fluor	Manufacturer
CD45	**BV650**	Biolegend, San Diego, CA Cat#: 103151
CD11B	**AF700**	Biolegend, San Diego, CA Cat#: 103515
CD19	**FITC**	Biolegend, San Diego, CA Cat#: 152404
B220	**FITC**	Biolegend, San Diego, CA Cat#: 103205
CD27	**FITC**	Biolegend, San Diego, CA Cat#: 124207
LY6G	**BV510**	Biolegend, San Diego, CA Cat#: 127633
LY6C	**PE-Dazzle**	Biolegend, San Diego, CA Cat#: 128043
MERTk	**PE-Cy7**	Biolegend, San Diego, CA Cat#: 151521
CD11C	**PE-Cy5**	Biolegend, San Diego, CA Cat#: 117316
ST2	**PE**	Thermofisher, Waltham, MA Cat#: 12-9335-80
NKp46	**BV421**	Biolegend, San Diego, CA Cat#:137612
CD49a	**BV605**	BD Biosciences, Franklin Lakes, NJ Cat#: 740375
CD49b	**APC**	Biolegend, San Diego, CA Cat#: 103515
CD3	**PerCP-Cy5.5**	Biolegend, San Diego, CA Cat#: 100327
CD4	**BV711**	Biolegend, San Diego, CA Cat#:100447
CD8	**BV785**	Biolegend, San Diego, CA Cat#: 100750
Viability	**Ghost Dye Red 780**	Tonbo Biosciences, San Diego, CA Cat#: 13-0865-T100

Supplementary Table 3.2. Histopathologic scoring guidelines and pathologic characteristics on a scale of 0-5. An immune cell aggregate was defined as a clustering of greater than 30 immune cells.

Pathological Parameter	Score	Defining Characteristic(s)
Immune Cell Aggregates	**0**	No aggregates
	1	1-5 aggregates
	2	6-10 aggregates
	3	11-15 aggregates
	4	16-20 aggregates
	5	21+ aggregates
Perivascular/bronchiolar Inflammation	**0**	No inflammation
	1	Minimal inflammation around airway/vasculature
	2	Increased immune cells around airway/vasculature
	3	Moderate inflammation and smooth muscle around airway/vasculature
	4	Excessive amounts of epithelial cell proliferation around airway/vasculature, airways beginning to close
	5	Severe inflammation around airway/vasculature with airways 50% or more closed
Alveolar Cellularity	**0**	No inflammation or depleted alveolar space
	1	Some RBC and immune cell infiltration
	2	Increased RBC and immune cell infiltration with alveolar space thickening (25-50%)
	3	Moderate amount of alveolar inflammation with RBC infiltrate and alveolar wall thickening (50-60%)
	4	Excessive alveolar wall thickening with 65-75% of alveolar space occupied by RBC and/or immune cell infiltration
	5	Severe RBC and immune cell infiltration with 90%+ alveolar space filled with cells
Goblet Cell Metaplasia	**0**	No goblet cells present
	1	20% of airway is occupied by goblet cells
	2	25-40% of airway is occupied by goblet cells
	3	50-60% of airway occupied by goblet cells
	4	65-75% of airway occupied by goblet cells
	5	Airway fully occupied by goblet cells with airway closure

\

Supplementary Table 3.3. Differentially expressed genes from Myeloid NanoString Panel.

	Comparison	Explanation	# DEG Up	# DEG Down
Myeloid Panel	WT, S vs D	Exposure in WT	**230**	**36**
	Fat-1, S vs D	Exposure in Fat-1	**148**	**8**
	S, WT vs Fat-1	Genotype at Base	**0**	**6**
	D ,WT vs Fat-1	Genotype after Exposure	**3**	**2**
	WT S, M v F	Sex Difference at Base in WT	**20**	**1**
	WT D, M v F	Sex Difference after Exposure in WT	**6**	**4**
	Fat-1 S, M v F	Sex Difference at base in Fat-1	**7**	**0**
	Fat-1 D, M v F	Sex Difference after Exposure in Fat-1	**3**	**4**

Appendix 3: Supplementary Material for Repetitive Inhaled Dust Exposure Protects from *S. pneumoniae* Infection and Mortality

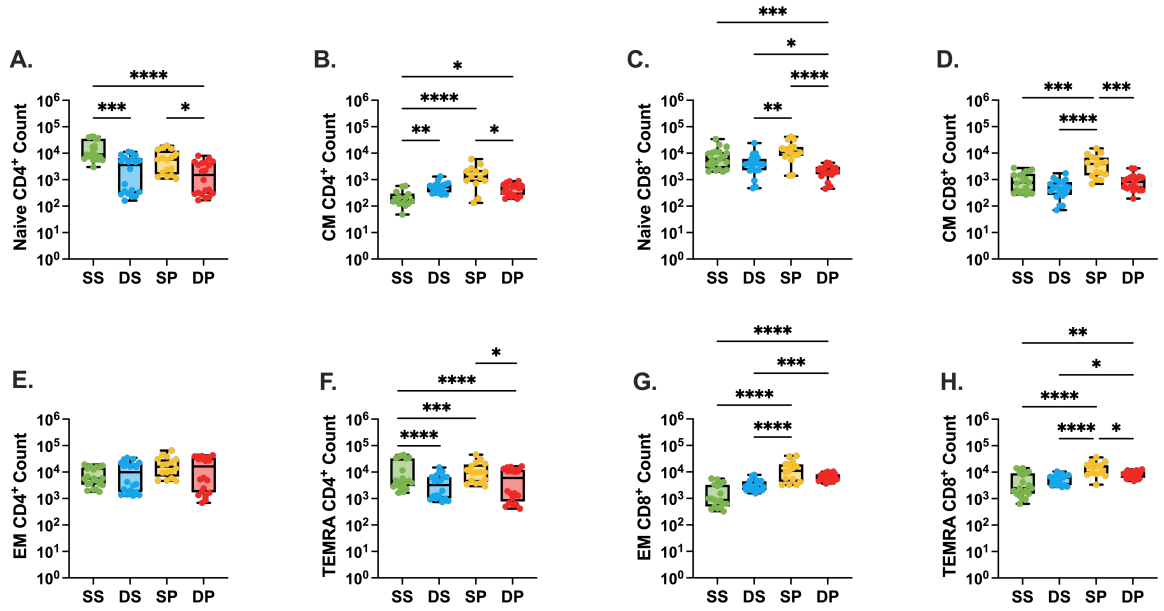

Supplemental Figure 4.1. Lung T cell subset counts. Naïve $CD4^+$T cell (**A.**), $CD4^+$ central memory (**B.**), naïve $CD8^+$ T cell (**C.**), $CD8^+$central memory (**D.**), $CD4^+$ effector memory (E.), $CD4^+$ EMRA (**F.**), $CD8^+$effector memory (**G.**), and $CD8^+$EMRA (**H.**) counts. Box and whisker plots depict minimum to maximum values with all data points shown and the midline at the median value. SS= saline-saline, DS=dust-pneumo, SP=saline-pneumo, DP=dust-pneumo. Kruskal Wallis test with Dunn's Multiple comparisons for post-hoc analysis. *p<0.05, **p<0.01, ***p<0.001, ****p<0.0001.

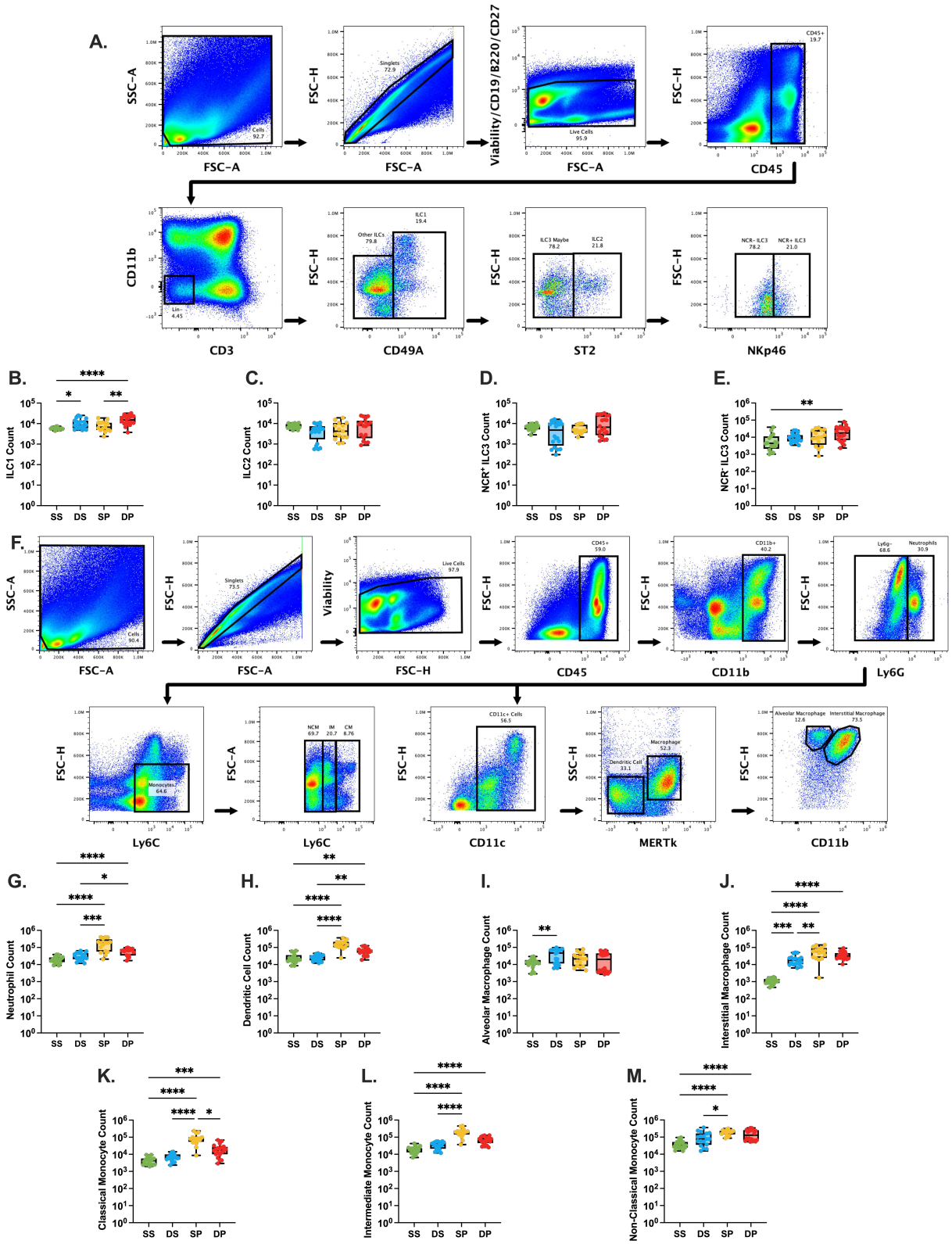

Supplemental Figure 4.2. ILC and Myeloid cell subset counts in the lung. Representative flow cytometry gating strategy for identifying ILC populations in the lung tissue (**A.**). ILC1 (**B.**), ILC2 (**C.**), NCR+ ILC3 (**D.**), NCR- ILC3 (**E.**) cell counts. Representative flow cytometry gating

strategy for identifying myeloid lineage cells in the lung tissue (**F.**). Neutrophil (**G.**), dendritic cell (**H.**), alveolar macrophage (**I.**), interstitial macrophage (**J.**), classical monocyte (**K.**), intermediate monocyte (**L.**), and non-classical monocyte (**M.**) counts. Box and whisker plots depict minimum to maximum values with all data points shown and the midline at the median value. SS= saline-saline, DS=dust-pneumo, SP=saline-pneumo, DP=dust-pneumo. Kruskal Wallis test with Dunn's Multiple comparisons for post-hoc analysis. *$p<0.05$, **$p<0.01$, ***$p<0.001$, ****$p<0.0001$.

Supplementary Table 4.1. Histopathologic scoring guidelines and pathologic characteristics on a scale of 0-5. An immune cell aggregate was defined as a clustering of greater than 30 immune cells.

Pathological Parameter	Score	Defining Characteristic(s)
Immune Cell Aggregates	**0**	No aggregates
	1	1-14 aggregates
	2	15-29 aggregates
	3	30-44 aggregates
	4	45-59 aggregates
	5	60+ aggregates
Perivascular/bronchiolar Inflammation	**0**	No inflammation
	1	Minimal inflammation around airway/vasculature
	2	Increased immune cells around airway/vasculature
	3	Moderate inflammation and smooth muscle around airway/vasculature
	4	Excessive amounts of epithelial cell proliferation around airway/vasculature, airways beginning to close
	5	Severe inflammation around airway/vasculature with airways 50% or more closed
Alveolar Cellularity	**0**	No inflammation or depleted alveolar space
	1	Some RBC and immune cell infiltration
	2	Increased RBC and immune cell infiltration with alveolar space thickening (25-50%)
	3	Moderate amount of alveolar inflammation with RBC infiltrate and alveolar wall thickening (50-60%)
	4	Excessive alveolar wall thickening with 65-75% of alveolar space occupied by RBC and/or immune cell infiltration
	5	Severe RBC and immune cell infiltration with 90%+ alveolar space filled with cells
Goblet Cell Metaplasia	**0**	No goblet cells present
	1	20% of airway is occupied by goblet cells
	2	25-40% of airway is occupied by goblet cells
	3	50-60% of airway occupied by goblet cells
	4	65-75% of airway occupied by goblet cells
	5	Airway fully occupied by goblet cells with airway closure

Supplementary Table 4.2: Marker-fluorophore conjugates, catalog numbers, and dilutions for flow cytometry. Markers are extracellular unless denoted as intracellular via an asterisk (*).

Panel	Marker	Fluorophore	Manufacturer	Dilution
T Cell	FoxP3*	BV421	Cat#404-5773-82, Thermofisher Scientific	1:400
	Viability	Live/Dead Fixable Aqua	Cat#L34965, Thermofisher Scientific	1:1000
	CD62L	BV605	Cat# 406-0621-82, Thermofisher Scientific	1:800
	CD3	BV650	Cat# 416-0031-82, Thermofisher Scientific	1:800
	CD8	BV711	Cat#407-0081-82, Thermofisher Scientific	1:800
	CD4	AF488	Cat#53-0041-82, Thermofisher Scientific	1:800
	CD44	APC-eFluor 780	Cat#47-0441-82, Thermofisher Scientific	1:800
	Ly6G	BV510	Cat#127633, Biolegend	1:800
	CD11c	BV605	Cat#117333, Biolegend	1:800
	MERTk	BV711	Cat#151515, Biolegend	1:800
	Viability	Ghost Dye Blue 516	Cat#13-0867-T100, Tonbo Biosciences	1:1000
	CD19	FITC	Cat#152404, Biolegend	1:800
	B220	FITC	Cat#103206, Biolegend	1:800
	CD27	FITC	Cat# MA5-17904, Thermofisher Scientific	1:800
	Ly6C	PerCP-Cy-5	Cat#45-5932-82, Thermofisher Scientific	1:800
	CD11b	AF700	Cat#101222, Biolegend	1:800
	CD45	APC-eFluor 780	Cat#47-0451-82, Thermofisher Scientific	1:800
ILCs	ST2	BV421	Cat#145309, Biolegend	1:800
	NKp46	BV510	Cat#137623, Biolegend	1:800
	CD49a	BV605	Cat#740375, BD Biosciences	1:800
	CD3	BV650	Cat#416-0031-82, Thermofisher Scientific	1:800
	Viability	Ghost Dye Blue 516	Cat#13-0867-T100, Tonbo Biosciences	1:1000
	B220	FITC	Cat#103206, Biolegend	1:800
	CD19	FITC	Cat#152404, Biolegend	1:800
	CD27	FITC	Cat# MA5-17904, Thermofisher Scientific	1:800
	CD11b	AF700	Cat#101222, Biolegend	1:800
	CD45	APC-eFluor 780	Cat#47-0451-82, Thermofisher Scientific	1:800

List of Abbreviations

AA – Arachidonic Acid

AF – Alexa Fluor

ALA – Alpha-Linolenic Acid

ALI – Acute Lung Injury

ALOX – Arachidonate Lipoxygenase

AM – Alveolar Macrophage

RTM – Resident Tissue Macrophage

MCP-1 – Monocyte Chemoattractant Protein-1

AMP – Anti-Microbial Peptide

ANOVA – Analysis of Variance

APC – Allophycocyanin

AT-RvD1 – Aspirin-Triggered Resolvin D-1

TSB – Tryptic Soy Broth

AT1 – Alveolar Type 1 cell

AT2 – Alveolar Type 2 cell

BALF – Broncho Alveolar Lavage Fluid

BLD – Blood

BLT – Leukotriene B4 (LTB4) Receptor 1

BM – Bone Marrow

BV – Brilliant Violet

cAMP – cyclic Adenosine Monophosphate

CD – Cluster of Differentiation

CFU – Colony Forming Units

cGMP – cyclic Guanosine Monophosphate

ChemR – Chemerin receptor 1

CitH3 – Citrullination of Histone H3

CMB – Cell and Molecular Biology

CMP – Common Myeloid Progenitor

COPD – Chronic Obstructive Pulmonary Disease

COX –Cyclooxygenase

CPS – Capsular Polysaccharide

D – Dust

DAMPs – Damage Associated Molecular Patterns

DAPI – 4',6-diamidino-2-phenylindole

DE – Dust Extract

DHA – Docosahexaenoic Acid

DNA – Deoxyribonucleic Acid

DP – Dust-*S. pneumoniae*

DS – Dust-Saline

EPA – Eicosapentaenoic Acid

EPA – Environmental Protection Agency

F – Female

FITC – Fluorescein Isothiocyanate

FPR – Formyl Peptide Receptor

FSC-A – Forward Scatter Area

FSC-H – Forward Scatter Height

G-CSF – Granulocyte-Colony Stimulating Factor

GEO – Gene Expression Omnibus

GM-CSF – Granulocyte Monocyte-Colony Stimulating Factor

GM-CSFR – Granulocyte Monocyte-Colony Stimulating Factor Receptor

GMP – Granulocyte-Monocyte Progenitor

GO – Gene Ontology

GOLD – Global Imitative for Obstructive Lung Disease

GPR – G Protein-Coupled Receptor

H&E – Hematoxylin and Eosin

HBSS – Hanks Balanced Salt Solution

PBS – Phosphate Buffered Solution

HLA-DR – Human Leukocyte Antigen DR isotype

IAV – Influenza A Virus

iBALT – inducible Bronchus Associated lymphoid Tissue

IFN – Interferon

IgA – Immunoglobulin A

IgE – Immunoglobulin E

IgG – Immunoglobulin G

ILC – Innate Lymphoid Cell

kEDTA – Potassium ethylenediaminetetraacetic acid

LGR – Leucine-Rich Repeat-Containing G Protein-Coupled Receptor

LNG – Lung

LPS – Lipopolysaccharide

LTB4 – Leukotriene B 4

LXA4 – Lipoxin A4

LXB4 – Lipoxin B4

M – Male

MAIT – Mucosal Associated Invariant T cell

Mb – Megabases

MDS – Multi-Dimensional Scaling

MERTk – MER proto-oncogene tyrosine kinase

MFI – Median Fluorescent Intensity

MHC-2 – Major Histocompatibility Complex 2

MMP – Matrix Metalloproteinase

MPO – Myeloperoxidase

n-3 FA – omega-3 Fatty Acids

NALT – Nasal Associated Lymphoid Tissue

NaN3 – Sodium Azide

NBF – Neutral Buffered Formalin

NCR – Natural Killer Cytotoxicity Receptor

NE – Neutrophil Elastase

NET – Neutrophil Extracellular Trap

NIH – National Institute of Health

NIMHD – National Institute on Minority Health and Health Disparities

NHLBI – National Heart, Lung, and Blood Institute

NK – Natural Killer cell

OD – Optical Density

ODE – Organic Dust Exposure

ODTS – Organic Dust Toxic Syndrome

PAM – Partitioning Around Medoids

PE – Phycoerythrin

PhD – Doctor of Philosophy

PKC – Protein Kinase C

PM – Particulate Matter

PMA – Phorbol Myristate Acetate

PUFA – Poly-Unsaturated Fatty Acid

QC – Quality Control

RBC – Red Blood Cell

RNA – Ribonucleic Acid

ROS – Reactive Oxygen Species

RSV – Respiratory Syncytial Virus

RvD – Resolvin D

RvE – Resolvin E

S – Saline

SARS-CoV-2 – Severe Acute Respiratory Syndrome Coronavirus 2

SCS – Single Cell Suspension

FCS – Flow Cytometry Standard

sIgA – soluble Immunoglobulin A

SP – Saline-*S. pneumoniae*

SPM – Specialized Pro-resolving Lipid Mediators

SS – Saline-Saline

SSC-A – Side Scatter Area

SSC-H – Side Scatter Height

ST2 – Suppressor of Tumorgenicity 2

TEMRA – Terminally differentiated Effector Memory Re-Expressing CD45R Cell

TGF-β – Transforming Growth Factor Beta

TLR – Toll-Like Receptor

Treg – T Regulatory Cell

WT – Wild Type (in reference to C57BL/6 mouse strain)